Journal of Research

of the

National Bureau of Standards

JANUARY 1958

VOLUME 60 NUMBER 1

DEPARTMENT OF COMMERCE
[illegible], Secretary
NATIONAL BUREAU OF STANDARDS
[illegible], Director

JANUARY 1
VOLUME
NUMBER

JOURNAL OF RESEARCH

of the

NATIONAL BUREAU OF STANDARDS

The National Bureau of Standards

Functions and Activities

The functions of the National Bureau of Standards are set forth in the Act of Congress, March 3, 1901, as amended by Congress in Public Law 619, 1950. These include the development and maintenance of the national standards of measurement and the provision of means and methods for making measurements consistent with these standards; the determination of physical constants and properties of materials; the development of methods and instruments for testing materials, devices, and structures; advisory services to Government Agencies on scientific and technical problems; invention and development of devices to serve special needs of the Government; and the development of standard practices, codes, and specifications. The work includes basic and applied research, development, engineering, instrumentation, testing, evaluation, calibration services, and various consultation and information services. A major portion of the Bureau's work is performed for other Government Agencies, particularly the Department of Defense and the Atomic Energy Commission. The scope of activities is suggested by the listing of divisions and sections on the inside of the back cover.

Publications

The results of the Bureau's work take the form of either actual equipment and devices or published papers. These papers appear either in the Bureau's own series of publications or in the journals of professional and scientific societies. The Bureau itself publishes three monthly periodicals, available from the Government Printing Office: The Journal of Research, which presents complete papers reporting technical investigations; the Technical News Bulletin, which presents summary and preliminary reports on work in progress; and Basic Radio Propagation Predictions, which provides data for determining the best frequencies to use for radio communications throughout the world. There are also five series of nonperiodical publications: The Applied Mathematics Series, Circulars, Handbooks, Building Materials and Structures Reports, and Miscellaneous Publications.

Information on the Bureau's publications can be found in NBS Circular 460, Publications of the National Bureau of Standards ($1.25) and its Supplement ($0.75), available from the Superintendent of Documents, Government Printing Office, Washington 25, D. C.

Order all publications from the Superintendent of Documents
U. S. Government Printing Office, Washington 25, D. C.

Use of funds for printing this publication approved by the Director of the Bureau of the Budget (May 4, 1956).

Journal of Research of the National Bureau of Standards Vol. 60, No. 1, January 1958 Research Paper 2815

The Condition of Certain Matrices, III[1]

John Todd[2]

The condition-numbers of certain matrices associated with various discretizations of the two-dimensional Laplacian operator are estimated. The condition-number gives an estimate of the error obtained by solving the corresponding systems of simultaneous linear equations.

1. *Introduction.* In a previous paper [Todd, 8a][3] the condition of a matrix associated with a particular method of solving a simple partial differential equation was discussed. Certain experimental computations of D. M. Young and his collaborators [Young, 13] suggested the discussion of other methods of handling the same equation. The P-condition number of a matrix M is defined as λ/μ where λ is the maximum and μ is the minimum of the absolute values of the eigenvalues of M; it gives a measure of the difficulty in the numerical inversion of M, or, more precisely, of an error in the inverse computed by an elimination method [von Neumann and Goldstine, 11; Todd, 8a, 9].

In [8a] we considered the solution of the Laplace equation in a unit square, with given boundary values. We then used the following five-point approximation to the Laplace operator:

$$z_{xx}+z_{yy}\doteq h^{-2}[z(r-1,s)+z(r,s-1)-4z(r,s)+z(r,s+1)+z(r+1,s)], \tag{1.1}$$

where $z(r,s)=z(rh,sh)$ and $h=1/(n+1)$, n a positive integer. Following Milne [4, p. 131] we indicate this approximation by the "stencil"

$$\begin{Bmatrix} 0 & 1 & 0 \\ 1 & -4 & 1 \\ 0 & 1 & 0 \end{Bmatrix}.$$

(This has been called a "computational molecule" by Bickley [2]). The $n^2\times n^2$ matrix which corresponds to the equations for the $z(r,s)$ can be indicated as

$$Z_1=\begin{pmatrix} & \cdots & \\ \cdots, & I, X, I, & \cdots \\ & \cdots & \end{pmatrix} \quad \text{where} \quad X=\begin{pmatrix} & \cdots & \\ \cdots, & 1, -4, 1, & \cdots \\ & \cdots & \end{pmatrix}.$$

is an $n\times n$ matrix and I is the $n\times n$ unit matrix. Here, and elsewhere, for brevity, we have indicated only the general row in the triple diagonal matrices. For clarity we describe Z_1 and X in words. The matrix Z_1 is an $n^2\times n^2$ matrix partitioned into $n\times n$ blocks; of these the diagonal blocks are all X and the blocks adjacent to the diagonal are unit matrices. The matrix X is an $n\times n$ matrix with diagonal elements all -4 and the elements adjacent to the diagonal all 1: In symbols $X=(x_{ij})$ where $x_{ii}=-4$, $i=1,2,\ldots n$, and for $i\neq j$, $x_{ij}=0$ unless $|i-j|=1$, when $x_{ij}=1$.

The equations corresponding to the problem

$$z_{xx}+z_{yy}=0 \text{ in interior}, \qquad z=f \text{ on boundary}$$

can be written as

$$Z_1\mathbf{z}=\mathbf{f}$$

[1] The problems considered here were suggested by lectures of D. M. Young, Jr., in the National Bureau of Standards-National Science Foundation Training Program in Numerical Analysis held in 1957.

[2] Present address, California Institute of Technology, Pasadena 4, Calif.

[3] Figures in brackets indicate the literature references at the end of this paper.

where the variables $z(r,s)$ are combined as the n^2-dimensional vector:

$$\mathbf{z}=(z(1,n),\ z(2,n),\ \ldots,\ z(n,n);\ z(1,n-1),\ z(2,n-1),\ \ldots,\ z(n,n-1);\ \ldots;\ z(1,1),\ z(2,1),\ \ldots,\ z(n,1))$$

and where

$$-\mathbf{f}=(f(0,n)+f(1,n+1),\ f(2,n+1),\ \ldots,\ f(n,n+1)+f(n+1,n);\ f(0,n-1),\ 0,\ \ldots,\ f(n+1,n-1);\ \ldots;\ f(0,1)+f(1,0),\ f(2,0),\ \ldots,\ f(n,0)+f(n+1,1)).$$

The essential result established in [8] was that

$$P(Z_1)\doteq 4\pi^{-2}n^2.$$

We shall now obtain the corresponding results for other discretizations of the Laplacian [Panow 5, Bickley 2].

2. *Auxiliary results.* We require the following results:

(2.1) *The characteristic values of the triple diagonal matrix of order n:*

$$C=\begin{pmatrix} & \ldots & \\ \ldots, & c,\ a,\ b, & \ldots \\ & \ldots & \end{pmatrix}$$

are

$$\lambda_k=a-2\sqrt{(bc)}\cos k\theta,\qquad k=1,2,\ \ldots,n$$

where

$$\theta=\pi/(n+1).$$

This is well known; it is easily proved by solving the difference equation

$$\Delta_n(\lambda)=(a-\lambda)\Delta_{n-1}(\lambda)-bc\Delta_{n-2}(\lambda)$$

for the characteristic polynomial $\Delta_n(\lambda)=|C-\lambda I|$.

We shall use the notation $\theta=\pi/(n+1)$ throughout this paper.

(2.2) *The characteristic roots of the quintuple diagonal matrix of order n:*

$$A=\begin{pmatrix} z-\beta, & 2\alpha, & \beta & & & & & \\ 2\alpha, & z, & 2\alpha, & \beta & & & & \\ \beta, & 2\alpha, & z, & 2\alpha, & \beta & & & \\ & \beta, & 2\alpha, & z, & 2\alpha, & \beta & & \\ & & & \cdot & & & & \\ & & & & \cdot & & & \\ & & & & & \cdot & & \\ & & & & \beta, & 2\alpha, & z, & 2\alpha, & \beta \\ & & & & & \beta, & 2\alpha, & z, & 2\alpha \\ & & & & & & \beta, & 2\alpha, & z-\beta \end{pmatrix}$$

are

$$\lambda_k=z-2\beta-\beta^{-1}\{\alpha^2-(\alpha-2\beta\cos k\theta)^2\},\qquad k=1,2,\ \ldots,n.$$

This result has been given by Rutherford [6, 7]. It can be verified as follows: If in the matrix C we put $c=b$ and square we obtain essentially the matrix A. In fact if we choose $b=\sqrt{\beta}$, $a=\alpha/\sqrt{\beta}$, then

$$A=C^2+(z-\alpha^2\beta^{-1}-2\beta)I.$$

(2.3) *Let F be a matrix of order n^2, partitioned into an array of n^2 submatrices f_{ij}, each of order n, such that each f_{ij} is a rational function $f_{ij}(\mathbf{a})$ of a fixed matrix $\mathbf{a}_2$ of order n. If the characteristic values of $\mathbf{a}$ are $\alpha_1, \alpha_2, \ldots, \alpha_n$ then those of F are given by the characteristic values of the n matrices*

$$(f_{ij}(\alpha_k)), \qquad k=1,2,\ldots,n,$$

each of order n.

This has been established by Williamson [12]; for extensions see Afriat [1].

3. We begin by discussing another five-point approximation which is represented by the stencil

$$\frac{1}{2}\begin{Bmatrix} 1 & 0 & 1 \\ 0 & -4 & 0 \\ 1 & 0 & 1 \end{Bmatrix}.$$

Omitting the factor $\frac{1}{2}$, we see that the corresponding $n^2\times n^2$ matrix is

$$Z_2=\begin{pmatrix} & \cdots & \\ \ldots, & X, & -4I, & X, & \ldots \\ & \cdots & \end{pmatrix},$$

where

$$X=\begin{pmatrix} & \cdots & \\ \ldots, & 1, & 0, & 1, & \ldots \\ & \cdots & \end{pmatrix}$$

is an $n\times n$ matrix and I the $n\times n$ unit matrix. The characteristic values of X are, from (2.1),

$$-2\cos k\theta, \qquad k=1,2,\ldots,n.$$

It follows that those of Z_2 are those of the n triple diagonal matrices

$$Z_2^{(k)}=\begin{pmatrix} & \cdots & \\ \ldots, & -2\cos k\theta, & -4, & -2\cos k\theta, & \ldots \\ & \cdots & \end{pmatrix}, \qquad k=1,2,\ldots,n,$$

which are, from (2.1),

$$\nu_{k,l}=-4[1+\cos k\theta\cos l\theta], \qquad k=1,2,\ldots,n, \qquad l=1,2,\ldots,n.$$

We have

$$\lambda(Z_2)=4[1+\cos^2\theta]$$

$$\mu(Z_2)=4\sin^2\theta$$

so that

$$P(Z_2)\doteq 2\pi^{-2}n^2.$$

4. We next discuss the nine-point approximation represented by the stencil

$$\begin{Bmatrix} 1 & 4 & 1 \\ 4 & -20 & 4 \\ 1 & 4 & 1 \end{Bmatrix}.$$

Omitting the factor $\frac{1}{6}$, we see that the corresponding $n^2 \times n^2$ matrix is

$$Z_3 = \begin{pmatrix} & \cdot\ \cdot\ \cdot & \\ \cdot\ \cdot\ \cdot, & Y,\ X,\ Y, & \cdot\ \cdot\ \cdot \\ & \cdot\ \cdot\ \cdot & \end{pmatrix}$$

where

$$X = \begin{pmatrix} & \cdot\ \cdot\ \cdot & \\ \cdot\ \cdot\ \cdot, & 4,\ -20,\ 4, & \cdot\ \cdot\ \cdot \\ & \cdot\ \cdot\ \cdot & \end{pmatrix} \quad \text{and} \quad Y = \begin{pmatrix} & \cdot\ \cdot\ \cdot & \\ \cdot\ \cdot\ \cdot, & 1,\ 4,\ 1, & \cdot\ \cdot\ \cdot \\ & \cdot\ \cdot\ \cdot & \end{pmatrix}.$$

We note that (2.3) will apply since

$$Y = \frac{1}{4}X + 9I.$$

The characteristic values of X are

$$-20 - 8\cos k\theta, \qquad k = 1,2, \ldots, n.$$

It follows that the characteristic values of Z_3 are those of the n matrices

$$Z_3^{(k)} = \begin{pmatrix} & \cdot\ \cdot\ \cdot & \\ \cdot\ \cdot\ \cdot, & 4 - 2\cos k\theta,\ -20 - 8\cos k\theta,\ 4 - 2\cos k\theta, & \cdot\ \cdot\ \cdot \\ & \cdot\ \cdot\ \cdot & \end{pmatrix}$$

which are

$$\nu_{k,l} = -20 - 8\cos k\theta - 8\cos l\theta + 4\cos k\theta \cos l\theta, \qquad k = 1,2, \ldots, n, \qquad l = 1,2, \ldots, n.$$

Hence

$$\lambda(Z_3) = \nu_{1,1} \doteq 32$$
$$\mu(Z_3) = \nu_{n,n} \doteq 12\pi^2 n^{-2}$$

which gives

$$P(Z_3) \doteq \frac{8}{3}\pi^{-2}n^2.$$

5. We conclude by discussing the nine-point approximation represented by the stencil

$$\frac{1}{12}\begin{Bmatrix} 0 & 0 & -1 & 0 & 0 \\ 0 & 0 & 16 & 0 & 0 \\ -1 & 16 & -60 & 16 & -1 \\ 0 & 0 & 16 & 0 & 0 \\ 0 & 0 & -1 & 0 & 0 \end{Bmatrix}.$$

This stencil must be modified for points near the boundary. Thus, at the corner $(1,n)$, we use

$$\frac{1}{12}\begin{Bmatrix} 0 & 0 & 0 & 0 & 0 \\ 0 & 0 & 14 & 0 & 0 \\ 0 & 14 & -58 & 16 & -1 \\ 0 & 0 & 16 & 0 & 0 \\ 0 & 0 & -1 & 0 & 0 \end{Bmatrix};$$

this means that we have estimated the outside value by linear interpolation on the two nearest values on the same line. For points (r,s) at the edge, i. e., $r=1$ or $r=n$ or $s=1$, $s=n$ which are not corners, e. g., $r=1$, $s=n-1$, we have to use a stencil of the form:

$$\frac{1}{12}\begin{Bmatrix} 0 & 0 & 0 & 0 & 0 \\ 0 & 0 & 14 & 0 & 0 \\ -1 & 16 & -59 & 16 & -1 \\ 0 & 0 & 16 & 0 & 0 \\ 0 & 0 & -1 & 0 & 0 \end{Bmatrix}.$$

Omitting the factor $\frac{1}{12}$ we see that the corresponding $n^2 \times n^2$ matrix is

$$Z_4 = \begin{pmatrix} Z+I, & 16I, & -I & & & & & & \\ 16I, & Z, & 16I, & -I & & & & & \\ -I, & 16I, & Z, & 16I, & -I & & & & \\ & & & \cdot & & & & & \\ & & & & \cdot & & & & \\ & & & & & \cdot & & & \\ & & & & & -I, & 16I, & Z, & 16I, & -I \\ & & & & & & -I, & 16I, & Z, & 16I \\ & & & & & & & -I, & 16I, & Z+I \end{pmatrix}$$

where Z is the $n \times n$ matrix:

$$Z = \begin{pmatrix} -59, & 16, & -1 & & & & & & \\ 16, & -60, & 16, & -1 & & & & & \\ -1, & 16, & -60, & 16, & -1 & & & & \\ & & & \cdot & & & & & \\ & & & & \cdot & & & & \\ & & & & & \cdot & & & \\ & & & & & -1, & 16, & -60, & 16, & -1 \\ & & & & & & -1, & 16, & -60, & 16 \\ & & & & & & & -1, & 16, & -59 \end{pmatrix}.$$

From (2.2) the characteristic values of Z are

$$\lambda_k = -60 + 2 + \{64 - (8 + 2\cos k\theta)^2\}, \qquad k = 1, 2, \ldots, n,$$

and by (2.3) the characteristic roots of Z_4 are those of the n matrices

$$Z_4^{(k)} = \begin{bmatrix} \lambda_k+1, & 16, & -1 & & & & & \\ 16, & \lambda_k, & 16, & -1 & & & & \\ -1, & 16, & \lambda_k, & 16, & -1 & & & \\ & \cdot & & \cdot & & \cdot & & \\ & & & & -1, & 16, & \lambda_k, & 16, & -1 \\ & & & & & -1, & 16, & \lambda_k, & 16 \\ & & & & & & -1, & 16, & \lambda_k+1 \end{bmatrix}, \qquad k = 1, 2, \ldots, n,$$

which are, again using (2.2),

$$\begin{aligned} \nu_{k,l} &= \lambda_k + 2 + \{64 - (8 + 2\cos l\theta)^2\}, \qquad k = 1, 2, \ldots, n, \qquad l = 1, 2, \ldots, n, \\ &= \lambda_k + \lambda_l + 60. \end{aligned}$$

It follows that

$$\begin{aligned} \lambda(Z_4) &= \nu_{1,1} \doteq 128 \\ \mu(Z_4) &= \nu_{n,n} \doteq 24\pi^2 n^{-2} \end{aligned}$$

so that

$$P(Z_4) = \frac{16}{3}\,\pi^{2-}n^2.$$

6. An evaluation of the various methods could now be made. In addition to the inversion error, which is given in terms of the P-condition number by von Neumann and Goldstine, the truncation error must be considered. The local truncation errors for the various stencils have been given by Bickley [2]; however, it seems that the global truncation errors have been studied only in the case of the approximation (1.1) by S. A. Gerschgorin, P. C. Rosenbloom, J. L. Walsh, W. Wasow, and others. We shall not, however, carry out an evaluation, for it seems clear that the elimination method is not the most suitable one for problems involving sparse matrices; numerical experience, nevertheless, does show that the P-condition number of a matrix is a good indication of the intrinsic difficulty of the inversion problem.

7. *Remarks.*

(1) Dr. Young pointed out that our results could be obtained by solving the difference equations by separating the variables (cf., e. g., B. Friedman [3]).

(2) As in [8] the estimates of the N-condition of Turing [10] can be obtained, since we know *all* the eigenvalues of the matrices in question.

(3) Similar results can be obtained for the biharmonic equation (cf. [9]).

(4) I take this opportunity to correct slips in two papers in this series.

In p. 117 of [8] the expression for γ_{kj} for $j \leq k \leq n$ should read $(n+1)\gamma_{kj} = -k(n-j+1) + (n+1)(k-j)$. This was pointed out by D. E. Rutherford [7].

In p. 471 of [8a], line 3, the adjective "symmetric" (or "normal") should be inserted to qualify "matrix". This was pointed out in conversation by Martin Pearl.

References

[1] S. N. Afriat, Composite matrices, Quart. J. Math., Oxford 2d Ser. **5,** 81–98 (1954).

[2] W. G. Bickley, Finite difference formulae for the square lattice, Quart. J. Mech. Appl. Math. **1,** 35–42 (1948).

[3] B. Friedman, Eigenvalues of compound matrices, New York Univ. Rept. TW–16 (1951).

[4] W. E. Milne, Numerical solution of differential equations (John Wiley & Sons, Inc., New York, N. Y., 1953).

[5] D. J. Panow, Formelsammlung zur numerische Behandlung partieller Differentialgleichungen nach dem Differenzenverfahren (translated from 5th Russian ed.) (Akad. Verlag, Berlin, 1955).

[6] D. E. Rutherford, Some continuant determinants arising in physics and chemistry, Proc. Roy. Soc. Edinburgh **62A,** 229–236 (1947).

[7] D. E. Rutherford, Some continuant determinants arising in physics and chemistry, II, Proc. Roy. Soc. Edinburgh **63A,** 232–241 (1952).

[8] J. Todd, The condition of a certain matrix, Proc. Cambridge Phil. Soc. **46,** 116–118 (1949).

[8a] J. Todd, The condition of certain matrices, I, Quart. J. Mech. Appl. Math. **2,** 469–472 (1949).

[9] J. Todd, The condition of certain matrices, II, Arch. Math. **5,** 249–257 (1954).

[10] A. M. Turing, Rounding-off errors in matrix processes, Quart J. Mech. Appl. Math. **1,** 287–308 (1948).

[11] H. H. Goldstine and J. von Neumann, Numerical inverting of matrices of high order, Bul. Am. Math. Soc. **53,** 1021–1097 (1947); Proc. Am. Math. Soc. **2,** 188–202 (1951).

[12] J. Williamson, The latent roots of a matrix of special type, Bul. Am. Math. Soc. **37,** 585–590 (1931).

[13] D. M. Young, Jr., Ordvac solutions of the Dirichlet problem, J. Assoc. Computing Mach. **2,** 137–161 (1955).

[14] H. I. Meyer and B. J. Hollingsworth, A method of inverting large matrices of special form, Math. Tables and Other Aids to Computation **11,** 94–97 (1957).

[15] P. Stein and J. E. L. Peck, On the numerical solution of Poisson's equation over a rectangle, Pacific J. Math. **5,** 999–1011 (1955).

WASHINGTON, June 17, 1957.

Journal of Research of the National Bureau of Standards Vol. 60, No. 1, January 1958 Research Paper 2816

Infrared Study of Some Structural Changes in Natural Rubber During Vulcanization*

Frederic J. Linnig and James E. Stewart [1]

A knowledge of the structure of vulcanized rubber is essential to the interpretation of vulcanization and oxidation studies and the physical properties of the material.

In the present work an infrared study has been made of structures resulting from a number of different methods of vulcanization. Sulfur vulcanizates show the presence of a shifted double bond, originally observed by Sheppard and Sutherland. The presence of conjugated double bonds is also indicated. Accelerators such as tetramethylthiuram disulfide and zinc dibutyl dithiocarbamate increase the rate of the double-bond shift and reduce the amount of conjugated double bonds. Neither the double-bond shift nor conjugation is observed as a result of vulcanization with tetramethylthiuram disulfide alone, hydrogen sulfide and sulfur dioxide (Peachey process), a peroxide, or gamma rays. These result in a possible decrease in carbonyl structures, and in the case of the last three, possible increased absorption due to OH and ionized carboxyl groups.

Apparently, the double-bond shift and conjugation are primarily phenomena related to the use of elemental sulfur. The other vulcanization systems studied evidently involve different mechanisms. An implication of the present work is that there may be a relationship between the reported ease of oxidation of sulfur vulcanizates, accelerated vulcanizates, and sulfurless vulcanizates (tetramethylthiuram disulfide alone), which decreases in the order named, and the probable amount of conjugation in the compound, which decreases in the same order.

1. Introduction

In order to elucidate structural changes occurring during vulcanization, Sheppard and Sutherland [35, 36] [2] studied the infrared spectra, between 2 and 18 μ, of accelerated and unaccelerated sulfur vulcanizates. In the 6.0 μ region they found little evidence of changes in absorption due to double bonds. A band at 10.4 μ was attributed to *trans* hydrogens adjacent to a carbon-to-carbon double bond resulting from a shift of the double bond normally present in unvulcanized rubber. This band had been discovered earlier by Sears [31]. Salomon and Van der Schee [28] have confirmed, essentially, the findings of Sheppard and Sutherland [35, 36]. The results of infrared studies of vulcanization through 1949 are summarized by Mann [25].

The earlier studies had been made using single-beam instruments. The double-beam instruments now available are, of course, capable of greater definition in the critical double-bond region near 6.0 μ and in other regions where there occurs intense atmospheric absorption. For these reasons, some of the studies of these workers were repeated using a double-beam instrument. Since the work on accelerated and unaccelerated sulfur vulcanizates proved fruitful, additional studies were made of other vulcanization systems including those involving tetramethylthiuram disulfide (TMTD) alone, a peroxide, gamma rays, and sulfur dioxide and hydrogen sulfide (Peachey process).

Some spectra were also obtained in the region between 15 and 40 μ using a cesium bromide prism to determine the existence of bands in this region, which might be due to C—S and S—S linkages.

In order to support the work on sulfur vulcanization a study was made of the squalene-sulfur system, and chemical evidence was obtained for one of the infrared interpretations.

2. Experimental Procedure

Most of the infrared spectra were obtained with a Perkin-Elmer model 21 double-beam spectrophotometer equipped with a sodium chloride prism for the range between 2 and 15μ, and a cesium bromide prism for the range between 15 and 40μ. An attachment ordinarily used to hold small KBr disks was employed in most of this work. With this attachment, the specium is inserted through the opening in the instrument cover to a position of minimum beam size, thus making possible the use of specimens as small as 3/8 in. in diameter, which in some cases were all that could be obtained.

Additional measurements at higher resolution were made on certain bands using a Beckman IR–4 spectrophotometer equipped with two sodium chloride prisms. Some of the complete spectra were also obtained with this instrument.

Specimens of unvulcanized rubber were prepared by evaporating to dryness natural rubber latex which had been diluted with water sufficiently to give a film of satisfactory thickness. In addition, specimens of unvulcanized smoked sheet, crepe rubber, or purified rubber were prepared by hot-pressing the material between sheets of aluminum foil with the aid of a Carver press. It was found that a pressure of about 1,000 to 4,000 lb/in.^{2} was sufficient to produce a specimen of suitable thickness, i. e., somewhere between 0.05 and 0.12

*This work was presented at the 70th meeting of the Division of Rubber Chemistry of the American Chemical Society, Atlantic City, N. J., September 1956. A portion of this work was performed as part of a research project sponsored by the National Science Foundation in connection with the Government Synthetic Rubber Program.

[1] Present address: Beckman Instruments, Inc., Fullerton, Calif.

[2] Figures in brackets indicate the literature references at the end of this paper.

447210—58——2

mm. The samples vulcanized by the Peachey process or by treatment with gamma rays were first pressed between sheets of aluminum foil for a short time at elevated temperature to obtain a thin sheet, and then subjected to the vulcanization treatment. All the other samples were vulcanized under pressure in a Carver press.

Compounding was done on a laboratory rubber mill equipped with rolls 3 in. by 8 in.

3. Results

The results of this study are presented in typical spectra given in figures 1 to 9, which are discussed in detail along with related spectra, in the sections that follow. The arrows in the figures indicate the pertinent bands in this study. The results are summarized in table 1. This table indicates changes in bands and in band intensities as a result of the various vulcanization processes, and is included for convenient reference in reading the discussions.

In this table and in the following discussions, it is to be emphasized that conclusions involving changes in band intensities are to be viewed with caution. In general, the intensities of absorptions in films, in addition to thickness, are influenced by factors such as scatter, inhomogeneity, surface reflection, and the effect of neighboring bands. These factors are important in rubber and especially so when the added solids used in vulcanization are present.

Consequently, in a number of cases it was not possible to come to a definite decision regarding changes in band intensities. However, in cases where a change in intensity appeared to occur, the change has been noted as a possible or apparent change, with the intention of indicating to the reader that the intensity change is at least a possible result of the treatment discussed.

3.1. Unvulcanized Natural Rubber

Figure 1 shows the spectrum between 2 and 15 μ of a film of natural rubber obtained by the evaporation of water from latex. This spectrum is essentially the same as that obtained by previous investigators. Sheppard and Sutherland [35] suggest that the band at 3.05 μ may be due to the C—H stretching vibration of the "lone" hydrogen on the ethylene bond in rubber. If, on the other hand, this band is due to NH groups in proteins perhaps, or to OH groups, its position indicates that these groups are strongly hydrogen bonded. No interpretation of the weak absorption near 4.9 μ is possible beyond the fact that it occurs in the region where acetylenes, nitriles, isocyanates, allenes, and amino acids absorb; it is probably the same band that Sheppard and Sutherland [35] found at 4.98 μ. The bands near 5.75 and 5.85 μ may indicate two types of carbonyls; they may be due to carbonyls already present in the hydrocarbon chain, or formed by oxidation of the chain, or else to carbonyls in the resinous portion. They are probably the small bands near 5.8 μ mentioned by Dinsmore and Smith [12], and Saunders and Smith [30].

It is interesting to note that purification of natural rubber by the method of McPherson [26] does not change markedly the intensity of any of these bands. The purified rubber used here contained 98.7-percent rubber hydrocarbon, 0.44-percent protein, and 0.18-percent ash. The sample also contained 1-percent phenyl-beta-naphthylamine added as an antioxidant, an amount that proved insufficient to affect the spectrum. This purified rubber had also been used by Roberts and Mandelkern [27] and was obtained from them. The fact that purification does not greatly reduce the intensity of these bands indicates that they are not related to the resin or protein content of the rubber, which is greatly reduced on

TABLE 1. *Spectral results and conclusions*

P, Present; A, absent; I, increases; D, decreases; —, not investigated.

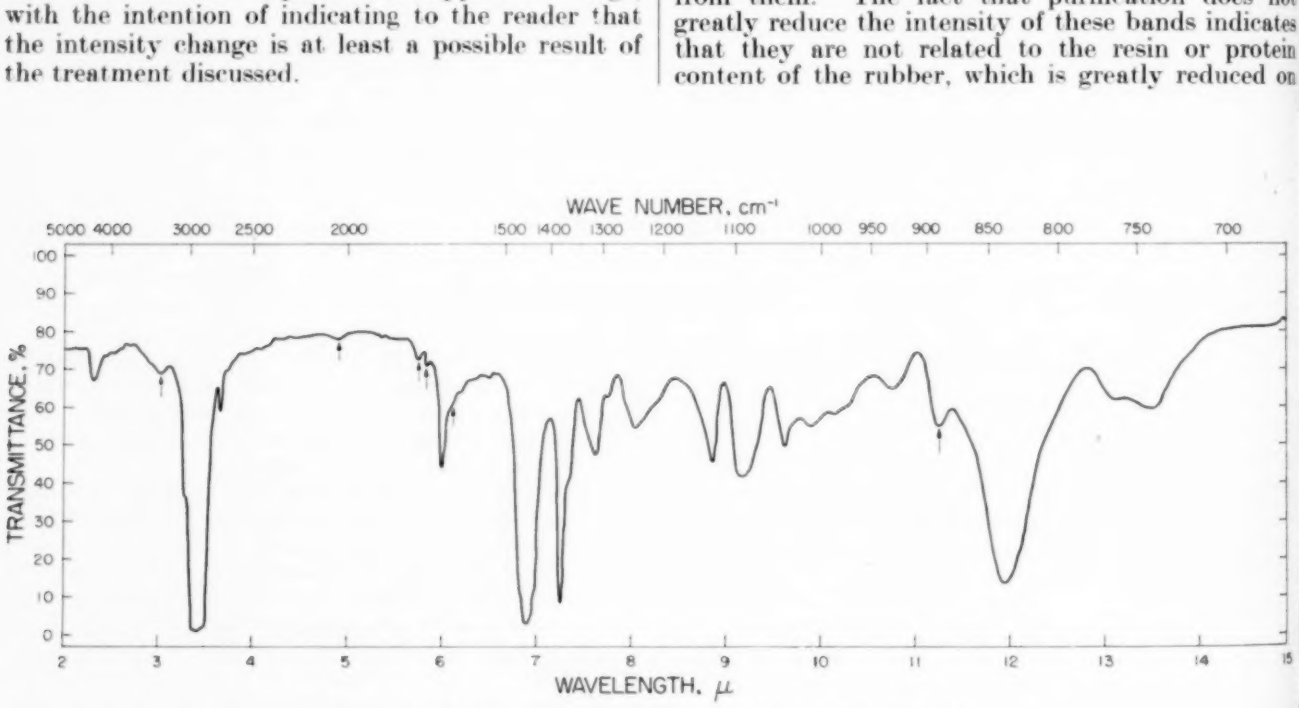

FIGURE 1. *Infrared spectrum of film of dried natural rubber latex.*

TABLE 1. *Spectral results and conclusions*

P, Present; A, absent; I, increases; D, decreases; —, not investigated.

Wavelength	Previous observations [1]	1	2	3	4	5	6	7	8	9	Remarks
		Unvulcanized			Sulfur alone	Sulfur and accelerators	TMTD alone	Peachey	Peroxide	Gamma rays	
		Purified	Dried latex	Coagulated							
μ											
2.9	12, 35	A	A	A	A	A	A	A	A	A	Probably oxidation band.
3.05	12, 30, 35	P	P	P	P	I	P	I	I	I	May be somewhat stronger in 3 than in 1 and 2. May increase in 5 with TMTD and BZ and in 7, 8, and 9 (on 9, see text). Not markedly changed by purification of rubber; therefore, not wholly characteristic of proteins or resins as such.
4.90	35 [2]	P	P	P	P	I	I	P	P	P	May increase in 5 with TMTD and in 6.
5.75	12, 30 [3]	P	P	P	P	D	P	D	D	D	Possible decrease in 7, 8, 9, may be related to increase of 6.5-μ band. Either one or both bands may be affected in 5.
5.85	12, 30 [3]	P	P	P	P	D	D	P	P	P	Possible decrease in 6.
6.02	12, 30, 35	P	P	P	P	P	P	P	P	P	Double bond in unvulcanized rubber. These bands indicate that considerable unsaturation of various types remains even after vulcanization with 25-percent sulfur.
6.10 {6.10 / 6.13}	12, 30	P	P	P	P	P	P	P	P	P	Band at 6.02μ unsymmetrical in purified rubber; inflection in dried latex; shoulder in coagulated rubber; resolved at least for sulfur vulcanizates; appears to become stronger relative to 6.02-μ band in vulcanizates containing more than 12-percent sulfur (see text).
6.25	None [4]	A	A	A	P	D	A	A	A	A	Conjugated double bonds; band appears in sulfur vulcanizates with over 5-percent sulfur.
6.5	12, 30, 35	A	A	P	P	P	A	I	I	I	Present in 5 with smaller quantity of TMTD, otherwise presence in 5 and 6 may be obscured by bands in TMTD and BZ; may be increased in 7, 8, and 9 (on 9, see text).
10.4	35, 36	A	A	A	P	P	A	A	A	A	Shifted double bond; confirmed for compounds containing more than 2-percent sulfur; rate of formation increased by accelerators.
11.95	12, 30, 36	P	P	P	D	D	P	P	P	P	Hydrogen on double bond in unvulcanized rubber.
14.3	None [4]	A	A	A	P	P	A	A	A	A	Appear in sulfur vulcanizates containing more than 12-percent sulfur; sometimes present with accelerators (15% sulfur).
14.8											
14.5	None [4]	A	A	A	P	P	P	A	A	A	Occurs in sulfur vulcanizates with less than 12-percent sulfur; usually present in 5 (15% sulfur) and in 6 (15% TMTD 4 hr and over at 125° C).
17.0	35	A	A	.....	P	.....	.....	.....	.....	.....	May be slight intensification of a shoulder on 17.5-μ band in unvulcanized rubber.
17.5	22, 30, 35 [5]	P	P	.....	D	.....	.....	.....	.....	.....	Band confirmed.
19.8	22, 30	P	P	.....	D	.....	.....	.....	.....	.....	Band confirmed.
23.5	None [4]	P	P	.....	A	.....	.....	.....	.....	.....	Broad swellings centered near these wavelengths.
28.0											
21.2	None [4]	A	A	.....	P	.....	.....	.....	.....	.....	These bands occur in region where S—S linkages absorb.
22.7											
24.4											
26.6											

[1] Numbers indicate references in literature cited.
[2] Probably 4.98-μ band of reference 35.
[3] Probably one of weak bands near 5.8μ in reference 12 and 30.
[4] Newly observed.
[5] Probably band at 16.6 to 17.7 μ of reference 35.

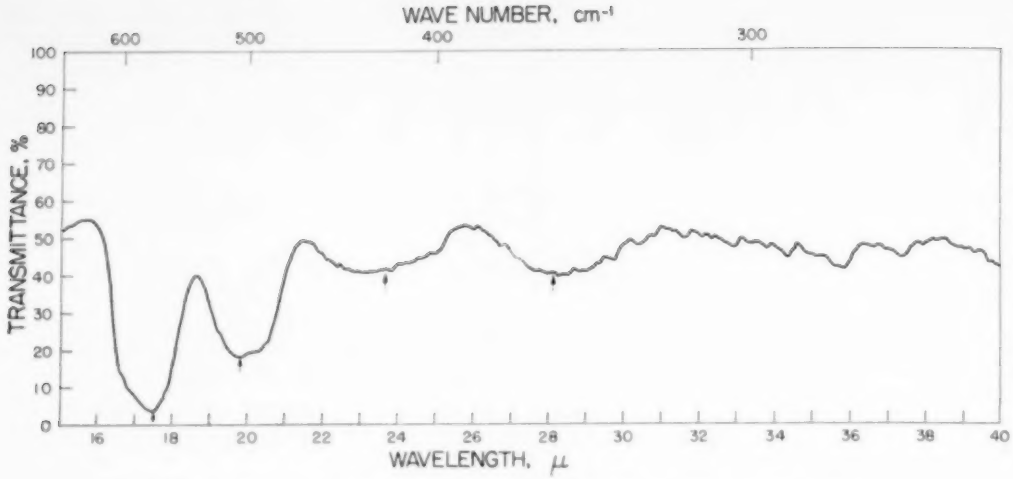

FIGURE 2. *Far infrared spectrum of film of dried natural rubber latex.*

purification, unless appreciable quantities of resin- or proteinlike units are in some way part of the polymer chain. Dinsmore and Smith [12B], and Saunders and Smith [30], however, did not find the 3.05 μ band in deproteinized rubber. It should be pointed out that it is possible to explain all four of these bands as either combinations or overtones of frequencies observed for absorptions in figures 1 and 2. These bands are of interest here since their intensities may be affected by certain vulcanization processes.

There is an inflection point at 6.1 μ in the spectrum of dried latex given in figure 1. This absorption is all but absent in the spectrum of purified rubber, the only evidence of its presence being the unsymmetrical nature of the band at 6.0 μ which is broader on the longer wavelength side. On the other hand, this absorption appears as a strong shoulder in spectra of coagulated rubber, i. e., Tensocrepe, pale crepe No. 1 thin, pale crepe No. 1 thick, smoked sheet and Tensosheet. Dinsmore and Smith [12] first attributed this shoulder to absorption by a terminal double bond. In a later article Saunders and Smith [30] concluded that the band at 6.1 μ was largely due to an impurity. The present work indicates that this impurity is probably introduced during coagulation. Apparently the strong shoulder at least is not, as suggested by Sheppard [34], an overtone of the 11.95 μ band. It may be, however, that the residual absorption in purified rubber is due to terminal double bonds or to an overtone of the 11.95 μ band. The slight difference between dried latex and purified rubber, if real, may be due to an impurity in dried latex.

The coagulated samples also showed what is probably a somewhat stronger absorption at 3.05 and a band at 6.5 μ. Again, these effects are apparently due to impurities introduced during coagulation and not removed by the washing process.

As a result of a comparison of spectra of smoked sheet and purified rubber, Saunders and Smith [30] seem to consider not only the band at 6.1, but also the bands at 3.05, 5.75, 5.85, and 6.5 μ to be due largely to impurities.

Figure 2 shows the spectrum of dried natural rubber latex in the region between 15 and 40 μ. The spectrum of purified rubber is essentially the same. There are two broad absorptions with peaks near 17.5 and 19.8 μ, respectively, in reasonable agreement with the findings of other workers [22, 30]. It is probably the former to which Sheppard and Sutherland [35] refer as extending from 16.6 to 17.7 μ. In addition, there are two very broad swellings between 21 and 30 μ which have not been reported previously. The smaller bands beyond 30 μ are due to uncompensated atmospheric water-vapor absorption.

3.2. Vulcanization With Sulfur Alone

In this work, some samples of natural rubber (pale crepe No. 1 thick) containing from 2- to 25-percent sulfur and no zinc oxide were vulcanized approximately to completion (about 20 hr) at 150° C while others containing 15-percent sulfur and no zinc oxide were vulcanized for periods of time ranging from 15 min to 4 days at 125° C and from 1 hr to 20 hr at 150° C.

Figure 3 gives the spectrum between 2 and 15 μ of natural rubber vulcanized with 15-percent sulfur for 96 hr at 125° C. In addition to the changes indicated in table 1, some other unexplained changes near 9.0 μ have taken place during vulcanization. These changes become noticeable with about 5- to 8-percent sulfur; they also occur in accelerated vulcanizates, but not in the other types of vulcanizates discussed here.

The band at 10.4 μ not present in unvulcanized rubber has been interpreted by Sheppard and Sutherland [36] to be due to the out-of-plane de-

formation vibration of the *trans* hydrogens on a double bond resulting from a shift of the following type:

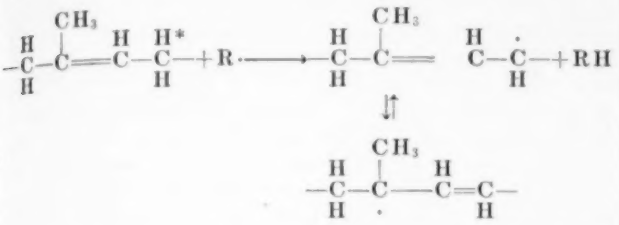

where $R\cdot$ is a free radical. These workers pointed out that this is consistent with the idea of α-methylenic initiation of the sulfuration reaction as advanced by Farmer and Shipley [16]. Sheppard and Sutherland found the intensity of this band to be correlated with the amount of combined sulfur. In this case the attack took place on the α-methylene group marked with an asterisk. This change in the spectrum would, of course, not occur if the attack had taken place on the α-methylene group on the other side of the double bond. In the present work, this band was observed in fully vulcanized compounds containing only 2-percent sulfur, the smallest quantity studied here, and it increased in intensity and shifted to slightly longer wavelengths (ca. 10.35 to 10.44 μ) as the sulfur content was increased from 2 percent to 25 percent. It will be referred to, however, as the band at 10.4 μ. As would be expected, the intensity of the band at 11.95 μ related to the hydrogen on the original double bond decreased with an increase in the intensity of the band at 10.4 μ.

The weak absorptions at 14.3 and 14.8 μ could be due to the hydrogens on the corresponding *cis* configuration. It is reasonable to expect both isomers to be formed during the double-bond shift. These bands could also be caused, however, by C—S linkages, or by skeletal vibrations not characteristic of any particular functional group. These bands appear as separate absorptions in fully vulcanized compounds containing more than 12-percent sulfur. With sulfur concentrations from 2 to 12 percent, only a broad general absorption appears that is centered near 14.5 μ. The newly discovered sharp band at 6.25 μ occurs in the region where conjugated double bonds absorb, and is treated separately in a later section. It occurs in all rubber-sulfur vulcanizates containing 5 percent or more of sulfur, and its intensity increases with increasing sulfur content.

The weak broad band near 6.5 μ is presumably the same band reported by Sheppard and Sutherland [35] as occurring at 6.52 μ in unvulcanized rubber mixes to which stearic acid and zinc oxide had been added. They attributed this band to the stearate ion and reported that it disappeared on vulcanization. However, Ellis and Pyszora [13] have shown that the intensity of the band increases again to approximately its original value when the specimen is allowed to remain at room temperature for 18 hr. They attribute the observed effects to an interaction between natural rubber and zinc sterate that is not related to the vulcanization process. The compound used to obtain figure 3 did not contain added zinc oxide or stearic acid, but the original rubber sample showed an absorption at 6.5 μ which, as suggested earlier, may result from impurities introduced during coagulation. The intensity of this band sometimes appeared to be reduced on vulcanization in this work.

The presence of zinc oxide in sulfur vulcanizates of Tensocrepe or pale crepe No. 1 thin, leads to no apparent change in the rate of the double-bond shift and the band at 6.25 μ appears about as soon as it does without zinc oxide. There usually seems to be some reduction in the intensity of either or both the carbonyl bands near 5.75 and 5.85 μ.

There is a change in the relative intensities of the bands at 6.0 and 6.1 μ as a result of vulcanization. The increase of the 6.1-μ band relative to the band at 6.0 μ is noticeable in compounds containing

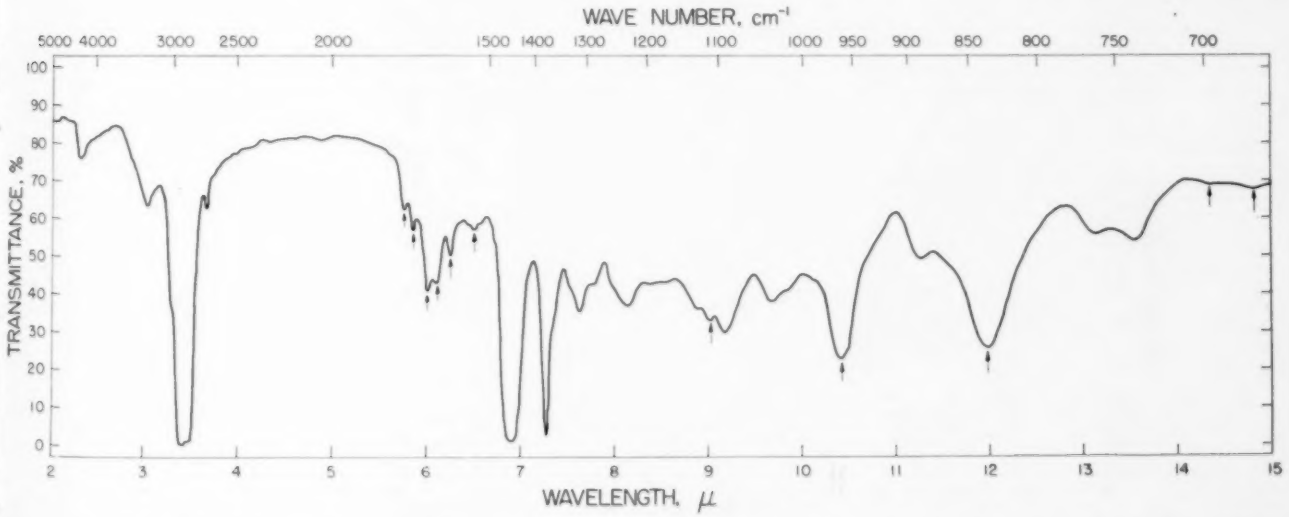

FIGURE 3. *Infrared spectrum of natural rubber (pale crepe No. 1 thick) vulcanized with 15-percent sulfur for 96 hr at 125° C.*

12-percent sulfur, and increases with increased sulfur content until with 25-percent sulfur it becomes the more prominent band, while the band at 6.0 μ appears only as a shoulder.

Under higher resolution, the band at 6.1 μ in vulcanized rubber may be resolved into two components at 6.10 and 6.13 μ with the main "6-μ" band appearing at 6.02 μ. The shoulder at 6.1 μ in unvulcanized rubber could also be due to two components, but this fact is not quite as apparent as in the case of vulcanized rubber.

At present it cannot be said with certainty whether there is an actual increase in the intensity of the 6.1-μ band on vulcanization or whether the observed relative change is due entirely to a decrease in the 6.0-μ band.

Because of the uncertainty of the nature of the band at 6.1 μ, and because the absorptivity of double-bond stretching vibrations is quite variable, no quantitative statement can be made about changes in unsaturation during vulcanization except that in accordance with the results of previous workers [28, 35, 36] even with 25-percent sulfur considerable unsaturation of various types including those absorbing at 6.1 μ remains. To this residual unsaturation should now be added that due to the conjugated double bonds absorbing at 6.25 μ.

The same structural changes take place when natural rubber is vulcanized at 150° C but at an accelerated rate. There is often some increase in carbonyl structure, which also results from heating rubber alone at this temperature.

It is interesting to note that in a spectrum of a vulcanizate of Coral rubber, a synthetic polyisoprene [37], the intensities of the band at 6.25 μ indicating conjugation and the band near 6.1 μ were considerably greater relative to the band at 6.0 μ than in the case of vulcanized natural rubber with the same amount of added sulfur (15%). The band at 6.0 μ was reduced to a slight shoulder on the band at 6.1 μ. The spectrum of the unvulcanized Coral rubber used here contained small bands near 6.1, 6.2, 6.3, and 6.65 μ.

Figure 4 shows the spectrum between 15 and 40 μ of natural rubber (pale crepe No. 1 thick) vulcanized with 13-percent sulfur for 20 hr at 150° C. It will be noted that: (1) There is some reduction in the intensity of the band at 17.5 μ, (2) the broad band at 19.8 μ is reduced, (3) the two consecutive swellings in the region between 21 and 30 μ have disappeared, and (4) these swellings have been replaced by weak bands at 21.2, 22.7, 24.4, and 26.6 μ. No interpretation of these bands is possible at the present time beyond the observation that S—S linkages absorb in this region.

The band at 17.0 μ, mentioned by Sheppard and Sutherland [35] appears possibly as a slight intensification of a shoulder on the original band at 17.5 μ.

Gehman [19], and Gehman and Osterhoff [20] have obtained Raman spectra of portions of acetone-extracted rubber soluble in petroleum ether or ethyl ether. Apparently, reported attempts to obtain Raman spectra of whole rubber have been unsuccessful because of difficulties due to Rayleigh scattering by rubber and by particles in the rubber as well as fluorescence of the nonrubber constituents of the whole sample. Attempts at the Bureau to obtain Raman spectra of whole rubber both unvulcanized and vulcanized have also been unsuccessful for the same reason. Raman spectra of vulcanized rubber, if obtained, would shed light on the existence of C—S and S—S linkages, which are generally known to produce stronger effects in the Raman spectrum than in the infrared, and should aid in establishing the identity of some of the infrared bands observed in this work.

3.3. Reaction Between Squalene and Sulfur

Squalene (a hexaisoprene), having a lower molecular weight and being a liquid, is more useful for certain experiments than rubber. It has been suggested

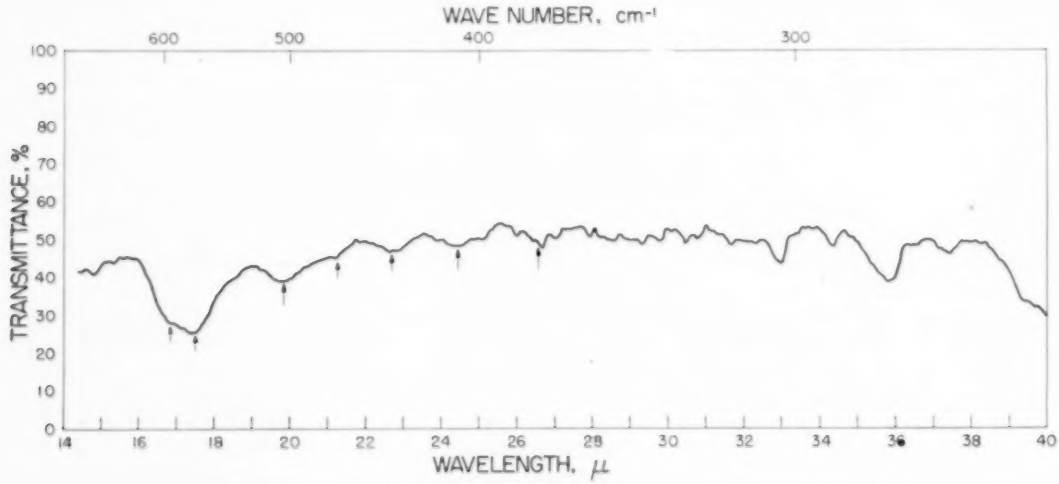

FIGURE 4. *Far infrared spectrum of natural rubber (pale crepe No. 1 thick) vulcanized with 13-percent sulfur for 20 hr at 150° C.*

by Bloomfield [5] that squalene, because of its molecular complexity, is more similar to long chain polyisoprenes than smaller compounds that have been used as rubber substitutes. It should be well adapted for the study of the structural changes of the double-bond shift and conjugation discussed here. If we consider two adjacent isoprene units in the squalene molecule

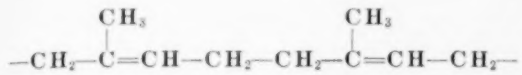

it will be seen that a conjugated system could appear as a result of either a shift of two double bonds toward each other or two successive shifts of one double bond. It could also result from the introduction of a new double bond between two original double bonds. Similar possibilities for conjugation of this type, of course, exist in natural rubber. The spectrum of Eastman practical grade (90%) squalene given in the upper part of figure 5 is essentially the same as that obtained by other workers [9,10,11,38]. It is similar in many respects to that of rubber as shown in figure 1, including the band at 6.0 μ and the strong absorption at 12.0 μ, probably due to the hydrogen on the carbon adjacent to the double bond. Furthermore, it has no absorption at 10.4 μ characteristic of *trans* hydrogens adjacent to a double bond, and there is no band at 6.25 μ indicating conjugation.

This material was reacted for 22 1/2 hr at 150° C with sulfur in a sealed tube under nitrogen. The squalene-sulfur reaction product was very dark and more viscous than the original squalene. The spectrum of the reaction product is given in the lower part of figure 5. This spectrum contains the bands at 10.4 and 6.25 μ. The new band near 6.1 μ is accompanied in this case by an increase in the absorption at 11.25 μ. Both effects have been [12A, 29] related to the formation of terminal double bonds. This situation is different from that observed with rubber vulcanizates for which an increased absorption at 11.25 μ was not observed (figs. 1 and 3). The migration of double bonds in squalene as a result of different treatments has been discussed by other authors [9,11]. In their study of double bond migrations in squalene during hydrogenation and dehydrogenation, Dale and Artun [9] found evidence of conjugation in the ultraviolet spectrum but no band at 6.25 μ in the infrared spectrum. There are also two bands near 14.5 and 14.9 μ which are reasonably close to the bands at 14.3 and 14.8 μ which in sulfur vulcanizates were attributed to the C—S linkage, to hydrogens *cis* to a double bond, or to skeletal vibrations.

3.4. Chemical Evidence of Conjugated Double Bonds

Farmer and Shipley [16] have discussed the possibility of conjugated systems in vulcanization. Other authors [2, 4, 6, 15] have mentioned apparently conjugated reaction products formed in the study of vulcanization using small molecules.

The band observed in these studies at 6.25 μ, if not due to conjugation, could be the result of combinations or overtones of absorptions occuring at other frequencies. None of the bands or combinations of bands observed to increase on vulcanization could account for the 6.25-μ band in this manner. However, in view of the apparent importance of this band, which is discussed later, it was deemed desirable to attempt to verify the presence of conjugated systems by chemical means.

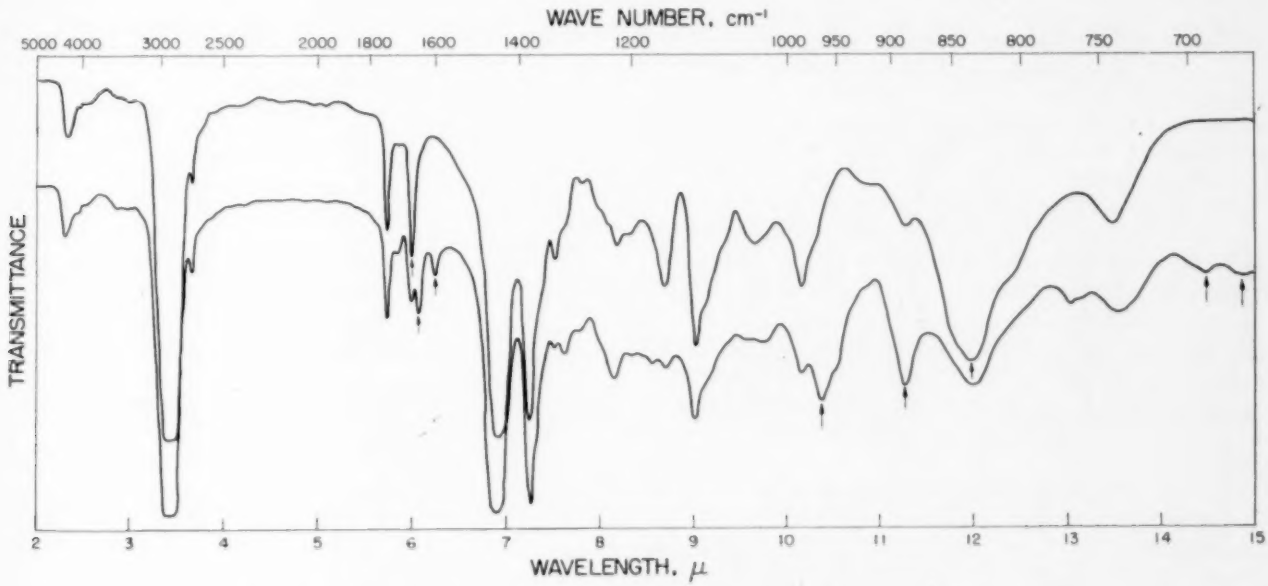

FIGURE 5. *Infrared spectra of squalene and squalene-sulfur reaction product.*

Upper curve: Eastman practical grade (90%) squalene Lower curve: Eastman (90%) squalene after reaction with 15-percent sulfur for 22 ½ hr at 150° C under nitrogen.

This was accomplished by demonstrating that a reaction takes place between the squalene-sulfur reaction product and maleic anhydride and that, as a result of this reaction, the band at 6.25 μ is removed.

Compounds containing conjugated double bonds normally react with maleic anhydride to form adducts in which the conjugation is removed not only from the compound in question but also from the anhydride. Examples of this Diels-Adler type of reaction are described by Kloetzel [24].

A portion of the squalene-sulfur reaction product (0.17 g) was mixed with 0.04 g of maleic anhydride, Fisher reagent. The mixture was agitated and heated for about 15 min to produce good mixing and a spectrum was obtained using a heated cell to keep the mixture molten. This spectrum is given in the upper half of figure 6. Absorptions near 5.05, 5.2, 5.4, 5.6, 7.8, 7.9, 8.1, 9.5, 11.25, 11.55, 11.9, and 14.35 are at least in part due to the presence of maleic anhydride. It will also be noted that the bands near 6.0 and 6.1 due to the squalene-sulfur reaction product are quite apparent. The broadening of the band at 6.25 μ is probably due to the absorption of the maleic anhydride that occurs at 6.27 μ. Though there is no evidence of complete removal of conjugation, the extension of the band at 10.4 μ to 10.55 μ indicates that some reaction has already taken place.

This mixture was then reacted for 70 hr at 100° C in a sealed tube under nitrogen. The tube was cooled, broken open, and the reaction mixture heated until completely melted. After mixing with a spatula, a spectrum was obtained in a heated cell to maintain the liquid state of the sample.

The spectrum of the final reaction mixture is given in the lower part of figure 6. Increased absorption near 5.8 μ and just beyond 8.0 and 9.0 μ as well as the greatly increased absorption from about 10.5 to beyond 11.0 μ indicate that reaction has taken place. The continued absorption at 6.0 and 6.1 μ indicates that at least a portion of this part of the squalene-sulfur reaction product is still intact. It will be noticed that the band at 6.25 μ has been removed completely, leaving, in fact, a slightly increased transmittance. The fact that a reaction has taken place and the band at 6.25 μ has been removed is evidence of the presence of conjugated double bonds in the original reaction product. It is interesting to note that there is still absorption at 10.4 μ probably due in part, at least, to shifted double bonds which are not conjugated. This, of course, assumes that the double bond in the final reaction product is *cis* as in the case of the reaction product obtained with butadiene and maleic anhydride [17, 24].

A sample of unreacted squalene mixed with maleic anhydride and run as a control showed no change after heating, except for the production of a band at 10.9 μ and shoulders at 5.35 and 5.85 μ indicating that the other changes observed with the squalene-sulfur reaction product are probably due to the Diels-Adler type of reaction. The quantity of maleic anhydride used in the above experiment was sufficient to react completely with one conjugated system per squalene molecule. Doubling this quantity of anhydride led to the same spectral picture, but increasing it fivefold obscured all the bands of the squalene-sulfur reaction product.

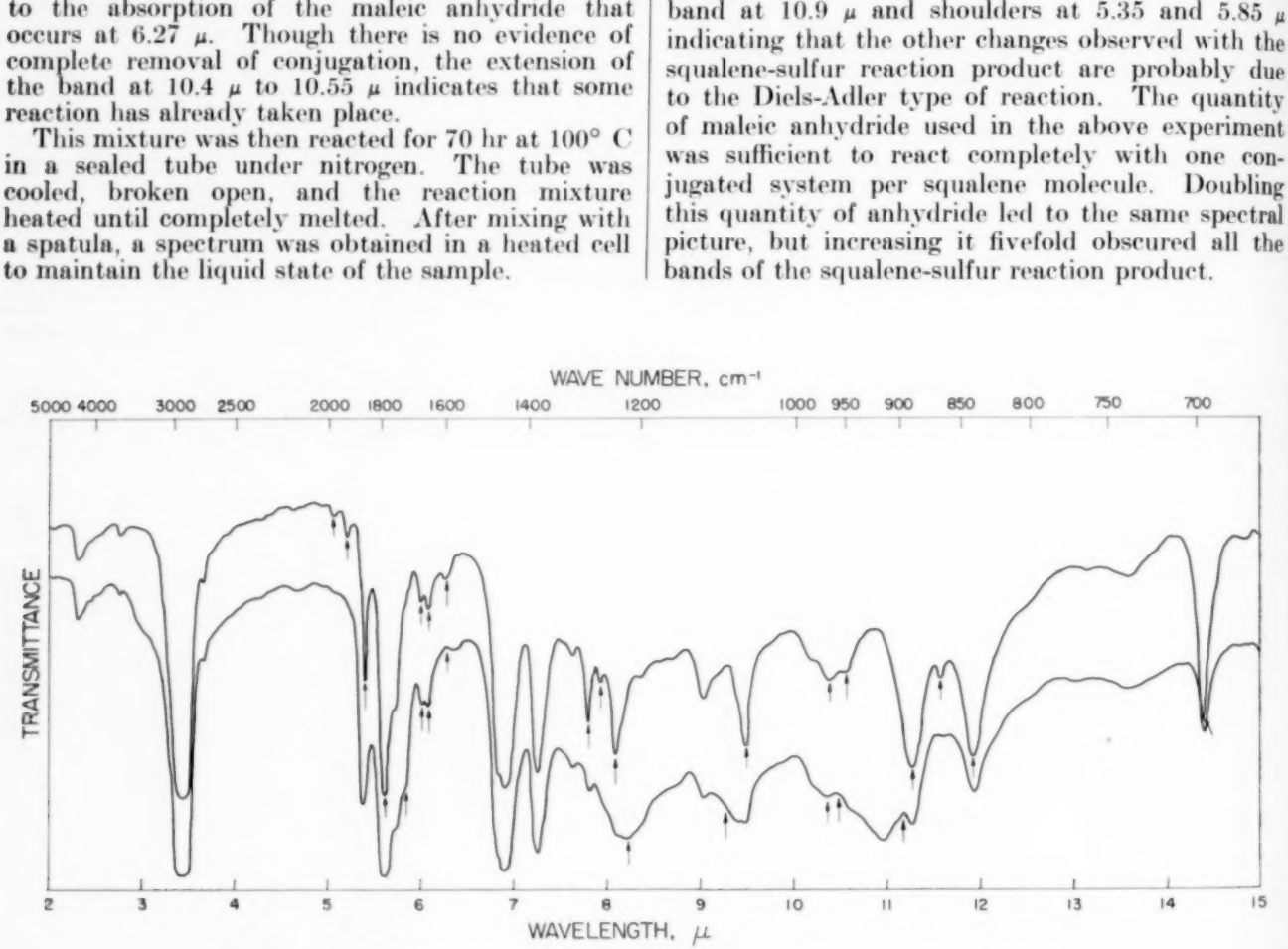

FIGURE 6. *Infrared spectra of squalene-sulfur reaction product and maleic anhydride.*

Upper curve: mixture of 0.17-g squalene-sulfur reaction product and 0.04-g maleic anhydride before reaction. Lower curve: above mixture after reaction for 70 hr at 100° C in a sealed tube under nitrogen.

Preliminary work had shown that the reaction between maleic anhydride and the squalene-sulfur reaction product does not take place in 8 days at room temperature. Backer and Blaas [1] have used temperatures between 150° and 165° C in reactions involving thioether compounds containing conjugated double bonds, molecular types which might be present in the squalene-sulfur reaction product. These higher temperatures were avoided here in an attempt to eliminate the non-Diels-Adler type reactions involving maleic anhydride and various hydrocarbons [17].

It is interesting to note that, since maleic anhydride does not react with the benzene nucleus, the conjugated systems in the squalene-sulfur reaction product are not phenyl rings. This conclusion is consistent with the spectrum in the lower half of figure 5 which shows no change in the 11- to 15-μ region where various aromatic compounds absorb. Similarly, this lack of new bands in the 11- to 15-μ range in the spectrum of vulcanized rubber indicates that the conjugation in vulcanized rubber is probably not caused by phenyl rings which might result from reversion during the vulcanization process.

Using purified squalene available only in small quantities, spectra were obtained on squalene and the squalene-sulfur reaction product in order to determine the effect of the impurities present in the practical grade. Except for the absence of carbonyl groups in the purified material, the spectra of the unreacted and reacted samples were qualitatively similar. Reaction of maleic anhydride with squalene-sulfur reaction product obtained from purified squalene also resulted in removal of the band at 6.25 μ. There was, however, a sharper band at 5.8 μ, and differences in the absorption pattern between 9 and 11 μ. These differences are not unexpected in view of the purified nature of the sample.

Following the work with squalene, attempts were made to remove the band at 6.25 μ in rubber-sulfur vulcanizates by adding various dienophiles to the compound before vulcanization. Of the reagents tried, maleic anhydride, diethyl fumarate, di(2-ethylhexyl) maleate and dicetyl maleate, only diethyl fumarate produced an apparent decrease in the intensity of the band at 6.25 μ. The larger quantity (13.5%) produced a greater apparent effect than the smaller quantity (5%), but did not completely remove the band.

TABLE 2. *Accelerated compounds*

Constituent	Amount in compound					
	A	B	C	D	E	F
	%	%	%	%	%	%
Pale crepe No. 1 thin	83	77	77			77
Tensocrepe				77.5	77.5	
Sulfur	15	15	15	15	15	15
Tetramethylthiuram disulfide (TMTD)	1.5	7.5		7.5		
Zinc dibutyl dithiocarbamate (BZ)			7.5		7.5	
Mercaptobenzothiazole (MBT)						7.5
Zinc oxide	0.5	0.5	0.5			0.5

3.5. Vulcanization With Sulfur and Accelerators

In order to determine the effect of accelerators on some of the structures found in unaccelerated samples, spectra were obtained on the vulcanizates of pale crepe rubber given in table 2. The quantities of sulfur and accelerator used in these studies were much larger than those used in conventional compounds in order to produce pronounced effects in the infrared spectra. Compounds A through E were vulcanized at 125° C for periods of time up to 48 hr. Compound F was vulcanized for from 7½ min to 8 hr at 150° C.

In samples accelerated with TMTD and BZ (compounds A through E) the rate of the double-bond shift was greater than in the unaccelerated samples. For example, about as much double-bond shift occurred in 2 hr in samples accelerated with BZ as occurred in 16 hr with samples accelerated with the larger quantity of TMTD. This same amount of double-bond shift occurs in about 48 to 70 hr in unaccelerated samples. The effect of the smaller quantity of TMTD on the double-bond shift may not have been as great as that of the larger quantity.

In comparison with unaccelerated compounds, however, conjugation, as determined by the presence of a band at 6.25 μ, was either virtually eliminated or its first appearance was delayed relative to a given amount of double-bond shift. Moreover, once slight conjugation had appeared, further vulcanization of these accelerated compounds did not cause as great an increase in the amount of conjugation as was observed in unaccelerated compounds.

In all cases the relative change in the intensities of the bands at 6.0 and 6.1 μ was observed as was in all but the shorter cures, a band or bands between 14 and 15 μ. The band at 6.5 μ was present in samples containing the smaller quantity of TMTD only; in the other samples it was probably partly obscured by bands from TMTD and BZ.

In samples accelerated with mercaptobenzothiazole (MBT) the rate of the double-bond shift was again more rapid than without the accelerator but nothing could be determined regarding the presence of conjugation since the benzene nucleus in the accelerator also has an absorption at 6.25 μ.

In some of the samples accelerated with TMTD and BZ, there may be an intensification of the band at 3.05 μ. There may also be an increase in the intensity of the small band at 4.9 μ in a few of the samples accelerated with TMTD. Accelerators also seem to reduce either or both of the carbonyl bands near 5.75 and 5.85 μ.

3.6. Vulcanization With TMTD

Compounds of pale crepe No. 1 thin containing 15-percent TMTD and 0.5-percent ZnO alone were vulcanized at 125° and 150° C for periods of time varying from 7½ min to 40 hr at the lower and 8 hr at the higher temperature. A spectrum of a sample

vulcanized for 2 hr at 125° C is typical and is given in figure 7. Unlike spectra of compounds in which TMTD serves as an accelerator in sulfur vulcanization, this spectrum shows no evidence of either conjugation or the double-bond shift indicated by bands at 6.25 and 10.4 μ, respectively. There is, however, an absorption near 10.3 μ. There also seems to be no appreciable change in the absorptions at 12.0 and near 6 μ as a result of different periods of vulcanization, indicating that the double bond in the polymer is not noticeaoly affected.

After curing there is sometimes an apparent in crease in the intensity of the weak band observed at 4.9 μ. As curing proceeds, there is a decrease in absorptions at 6.65, 8.1, 8.7, 9.6, and 10.3 μ, wavelengths at which TMTD itself absorbs. This indicates destruction of the TMTD during the curing process. The band at 5.85 attributed to carbonyl absorption in rubber seems to be reduced. The band at 14.5 μ appears in samples vulcanized over 4 hr. Again, the band at 6.5 μ may be obscured by a band in TMTD.

In some samples vulcanized for the longer periods of time, there is increased absorption near 10.4 μ which disappears after the sample has been allowed to stand in air at room temperature.

3.7. Vulcanization by the Peachey Process

In preparing samples for this type of vulcanization, one piece of aluminum was stripped off the pressed sample leaving the rubber film on the other piece of aluminum. The rubber film (pale crepe) on the aluminum was cut into small strips and these strips were attached to a wire rack in a tube and vulcanized by the Peachey process for from 1 to 24 cycles as described in the paper by Bekkedahl, Quinn, and Zimmerman [3]. A single cycle consisted of passing sulfur dioxide over the sample for 5 min, followed by a brisk 10-sec sweep of air to remove the sulfur dioxide gas not absorbed by the samples, and then passing hydrogen sulfide over the sample for 5 min, followed by another brisk 10-sec sweep of air.

Spectra were obtained on a number of these samples, of which the one given in figure 8 for the sample receiving an 8-cycle treatment is typical. It will be noted that there is no evidence of the double-bond shift, of conjugation or of bands between 14 and 15 μ. There is also little evidence of changes in absorption at 12.0 and near 6 μ.

The absorption at 3.05 μ appears stronger. The carbonyl absorption at 5.75 μ appears to be reduced, and the strong absorption at 6.5 due to ionized carboxyl or to nitro groups may be intensified. If the 6.5-μ band is actually due to ionized carboxyl groups, it would appear that the band at 5.75 μ is related to the carboxylic acids in the rubber. Since the band at 5.75 μ is not greatly affected by purification, some of these acids may be attached to the polymer chain. In addition, there are some slight changes in absorption near 9.8 μ.

The intensities of these various bands do not seem to change much from 2 to 24 cycles. For the more highly vulcanized samples there seemed to be a tendency for the other carbonyl absorption at 5.84 μ to be reduced. At 24 cycles there was some slight evidence of a band at 10.4 μ. However, the more highly vulcanized samples had thickened during the process and comparison of their spectra with others was rather difficult. It should be noted that only two cycles are required for an optimum cure and that a sample treated with 24 cycles might be expected to contain nearly 9.0 percent combined sulfur, while one treated with only 8 cycles might contain somewhat over 7 percent combined sulfur [3].

Salomon and Van der Schee [28] observed no changes in the infrared spectrum of rubber vulcanized by the Peachey process.

It is interesting to note that, while an active sulfur radical has been assumed to produce the double-bond shift in sulfur vulcanization [18], no double-

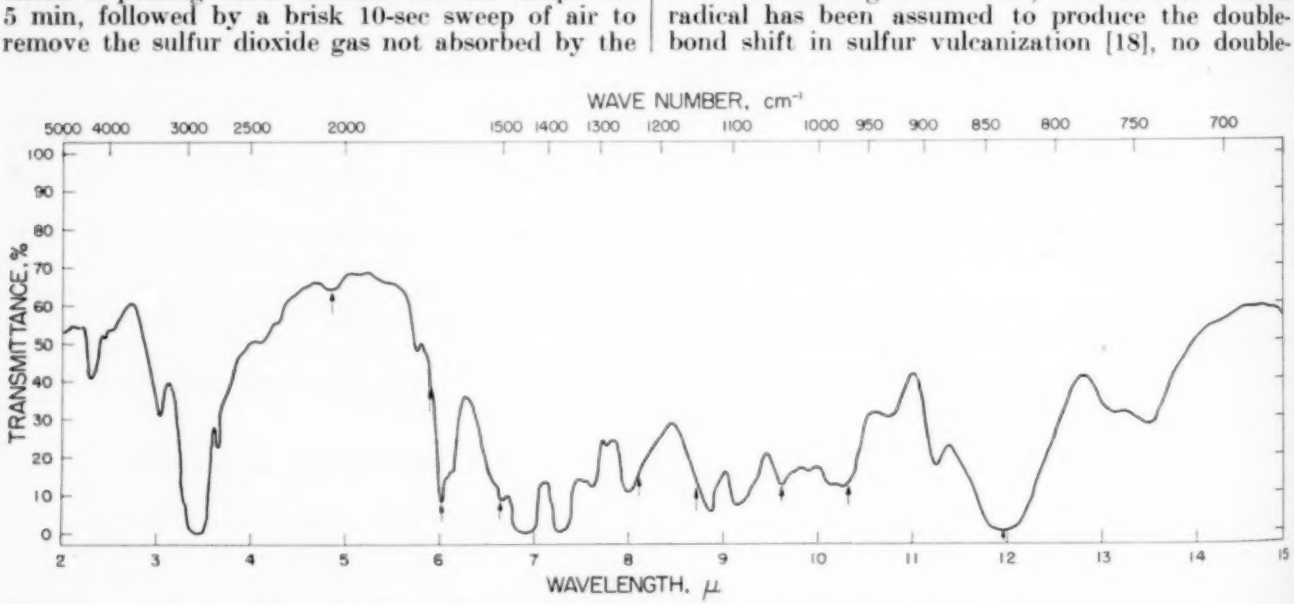

FIGURE 7. *Infrared spectrum of natural rubber (pale crepe No. 1 thin vulcanized with 15-percent tetramethylthiuram disulfide (TMTD) and 0.5-percent zinc oxide for 2 hr at 125° C.*

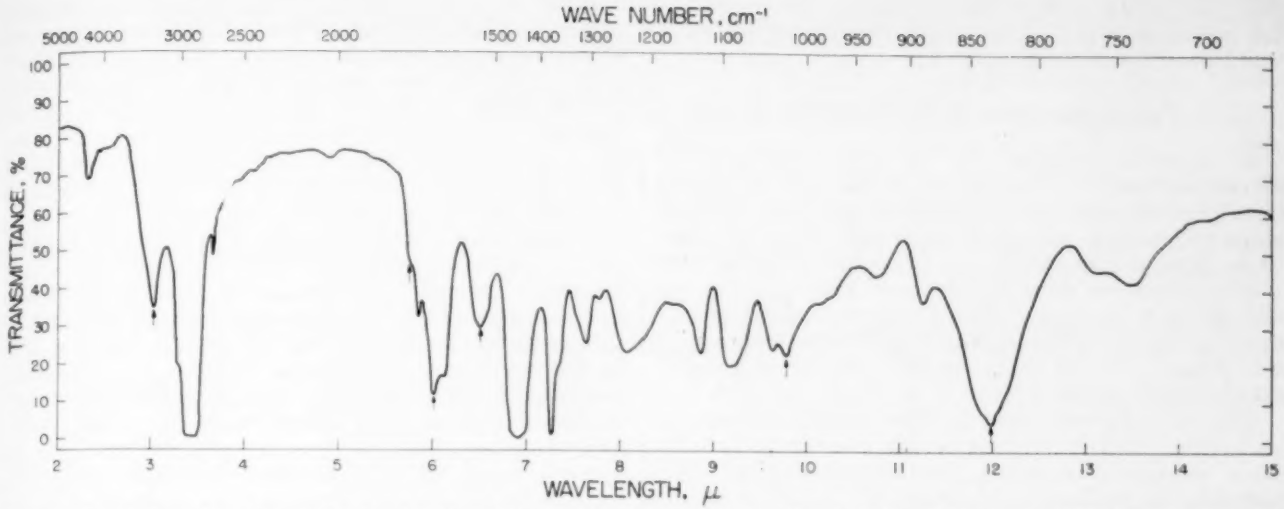

FIGURE 8. *Infrared spectrum of natural rubber (pale crepe) vulcanized with sulfur dioxide and hydrogen sulfide (Peachey process) using 8 cycles of both gases.*

bond shift occurs in the Peachey process which is also believed to involve an active form of sulfur [23].

3.8. Vulcanization With Di-Tertiary Butyl Peroxide

In comparing peroxide vulcanization with sulfur vulcanization it was necessary to choose a peroxide that did not contain conjugated double bonds. Di-tertiary butyl peroxide was satisfactory from this standpoint and has received some study [7, 14]. It is believed to act by a free radical mechanism, does not combine with the polymer, and forms only volatile decomposition products, tertiary-butanol and acetone [14]. Furthermore, the oxygen content of the vulcanizate is said to be not significantly higher than that of the raw rubber [14].

Samples of pale crepe natural rubber were prepared containing 1.5-, 4.0-, and 7.25-percent peroxide. These samples were vulcanized for different periods of time varying from 15 min to 24 hr at 125° and 135° C. The spectrum given in figure 9 was typical and was obtained on a sample containing 4.0-percent peroxide vulcanized for 2½ hr at 135° C. The apparent changes have been noted in Peachey vulcanization. There is a possible increase in the intensities of the bands at 3.05 and 6.5 μ, and a possible reduction in the carbonyl absorption at 5.75 μ.

It was found, however, that these apparent changes were present in a sample (containing 7.25% peroxide) which had not been vulcanized, i. e., heated above the temperature involved in milling. However, this sample exhibited none of the mechanical properties of the vulcanized materials, nor was it transparent and free from tackiness. Different times of vulcanization for the samples containing the different quantities of peroxide did not change the spectrum appreciably. Slight increases in absorption at 8.4 and 10.3 μ were noted when samples containing 7.25-percent peroxide were vulcanized for 24 hr at

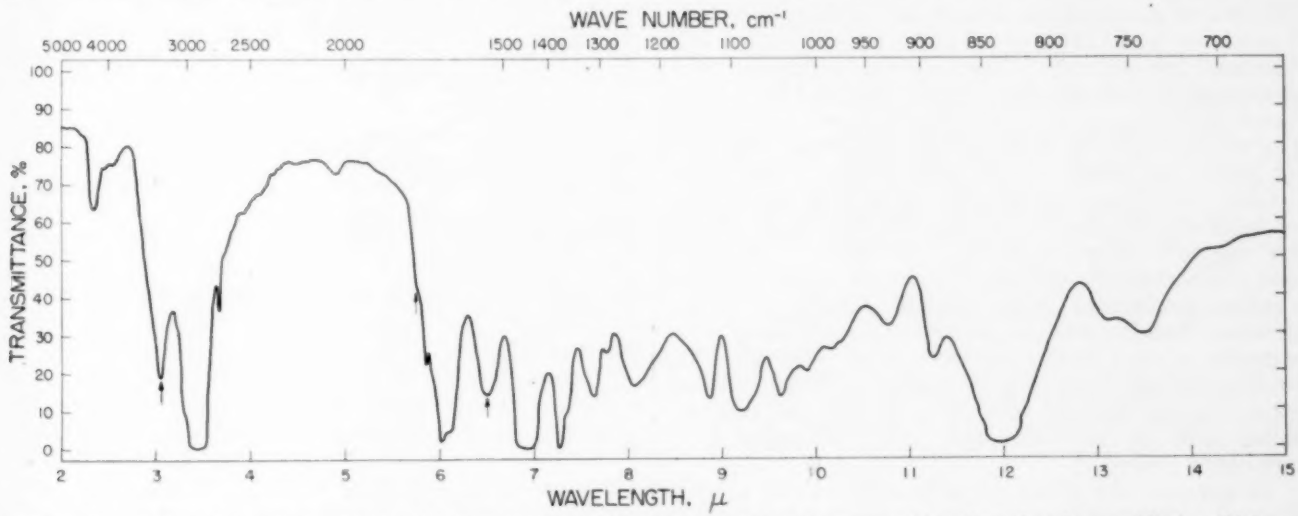

FIGURE 9. *Infrared spectrum of natural rubber (pale crepe) vulcanized with 4.0 percent di-tertiary butyl peroxide for 2½ hr at 135° C.*

135° C. Only a very slight change was noted at 8.4 μ and none at 10.3 μ when these samples were vulcanized for 24 hr at 125° C.

3.9. Vulcanization With Gamma Rays

In order to compare the structural changes observed for sulfur vulcanization with those resulting from gamma rays, pressed films of pale crepe rubber alone and with 8- and 15-percent sulfur were exposed to a gamma-ray source of 50-curies strength for 120 hr (exposure dose of 10^6 to 10^7 roentgens) in air and under a vacuum. This exposure is sufficient to cause gelation. The treated specimens were quite sticky and some of them became too thick to give satisfactory spectra.

The changes occurring in the sample containing no sulfur when irradiated in air appear to be the same as those resulting from compounding with peroxide as indicated in figure 9. For the specimens containing no sulfur and vulcanized in a vacuum and for the samples containing 8- and 15-percent sulfur vulcanized either in air or in a vacuum, the spectra were not sufficiently satisfactory to estimate the status of the bands at 3.05 and 6.5 μ; however, the band at 5.75 μ did not seem to be reduced. None of the specimens showed any evidence of conjugation. Because of an incomplete spectrum, the status of the band at 10.4 μ could not be determined for the specimen containing no sulfur and vulcanized in a vacuum, but in all other cases there was no evidence of a double-bond shift.

Sears and Parkinson [32] and Sears, Parkinson, Sisman, and Towns [33] have exposed Hevea presumably vulcanized and containing sulfur, zinc oxide, stearic acid, benzothiazyl disulfide, and phenyl β-naphthylamine to gamma radiation (absorption dose of 2.2×10^9 rads). They report a continuation of the double-bond shift already started during vulcanization.

4. Summary and Conclusions

Infrared studies have been made of natural rubber vulcanized with sulfur alone and also with sulfur and various accelerators. The spectral change (appearance of band at 10.4 μ) resulting from the double-bond shift observed by Sheppard and Sutherland [36] was verified for compounds containing 2 percent or more of sulfur. The presence of conjugated double bonds in compounds containing 5 percent or more of sulfur has been indicated spectroscopically for the first time (appearance of band at 6.25 μ) and supported by chemical evidence obtained from studies performed with squalene-sulfur reaction product and maleic anhydride. Conjugation presumably results from either two double-bond shifts, or the introduction of a new double bond. Sheppard and Sutherland [36] have shown the double-bond shift to be correlated with the amount of combined sulfur.

In general, the effect of such accelerators as zinc dibutyl dithiocarbamate (BZ) and tetramethylthiuram disulfide (TMTD) is to reduce at least the amount of conjugation occurring with a given amount of double-bond shift and hence with a given amount of combined sulfur. Apparently these accelerators either prevent the formation of the conjugated double bonds or react to remove them after they are formed. Accelerated compounds also show evidence of reduced absorption due to carbonyl groups and possible increased absorption due to OH groups as the most likely structures.

Compounds cured with TMTD alone, peroxides, gamma rays, or sulfur dioxide and hydrogen sulfide (Peachey process) do not show evidence of the double-bond shift or of conjugation. They do show a possible decrease in carbonyl structures, and in the case of the last three, possible increased absorption due to OH and ionized carboxyl groups. Again, the structures named seem to be the most likely ones involved.

Apparently, the double-bond shift and the resulting conjugation are primarily phenomena related to the use of elemental sulfur. The other vulcanization systems studied evidently involve different mechanisms.

There is, during sulfur vulcanization, an increase in the intensity of the band near 6.1 μ relative to that of the band at 6.0 μ. This change in relative intensity is noticeable with 12-percent sulfur and increases with increased sulfur content. In rubber-sulfur vulcanizates, at least, the band near 6.1 μ has been resolved into a doublet with one absorption at 6.10 μ and the other at 6.13 μ.

The fact that the double-bond shift, conjugation, etc., were observed spectroscopically in this work only with certain minimum quantities of sulfur or times of vulcanization, does not imply that they do not actually occur with less sulfur or shorter times of vulcanization. It is only reasonable to assume that they are a continuing part of the over-all vulcanization reaction and that the condition of occurrence of the bands results from their absorptivity and the particular method of spectroscopic study employed.

It is well-known that rubber-sulfur compounds, accelerated compounds, and compounds cured with TMTD alone (all containing the usual percentages of compounding ingredients) are increasingly resistant to aging in the order named. If the present studies can indeed be extrapolated to the smaller percentages of compounding ingredients usually employed, the concentration of conjugated double bonds should also decrease in the same order. Since conjugated double bonds are known to be highly reactive, it is reasonable to assume that there should be some relationship between the ease of oxidation and the concentration of conjugated double bonds in the compound.

Preliminary observations have revealed that, as a sulfur-vulcanized film of rubber oxidizes, the appearance of absorption bands of C=O, C—O, and OH groups in the infrared spectrum is accompanied, among other things, by a reduction in the conjugated double-bond absorption at 6.25 μ.

It should be noted that the interpretation of the

band at 10.4 μ, as discussed in this article is different from that proposed by Glazebrook and Saville [21], and Bateman, Glazebrook, Moore, and Saville [2]. These authors suggest that this band is due to substituted tetrahydrothiophenes which their studies with small molecules have indicated are formed during vulcanization. These tetrahydrothiophenes are reported to have bands near 10.5 to 10.6 μ and one of them also is reported to have a band at 10.44 μ. Ebonite containing 32-percent sulfur and squalene-polysulfide residue from distillation of the reaction product are also reported to have bands in this region in contrast to the results obtained under the conditions employed in the present work. It should be noted that the wavelength of the band observed at 10.4 μ in the present work is shifted to longer wavelengths with increased sulfur content and occurs at 10.45 μ with 25-percent sulfur. This general trend is in agreement with the findings of Sheppard and Sutherland [36]. Furthermore, the spectrum of the squalene-sulfur reaction product in figure 5 has a shoulder at 10.5 μ. It may be that the tetrahydrothiophenes produce the bands at the longer wavelengths and that the band at the shorter wavelengths near 10.4 μ is actually due to a shifted double bond. Perhaps the tetrahydrothiophenes form at a late stage of the reaction or under conditions of higher concentration of sulfur. In this connection Craig [8] has shown that tetrahydrothiophene itself does not react with maleic anhydride when the two are heated at 125° C for 90 min. Thus, the changes observed on reacting the squalene-sulfur reaction product with maleic anhydride, including removal of the band at 6.25 μ and a possible decrease in the intensity of the band at 10.4 μ, were probably not due to reaction with tetrahydrothiophenes. In the absence of some other interpretation, it is assumed that these changes are due to reaction with a conjugated hydrocarbon system.

The authors are indebted to F. H. Stross of the Shell Development Co., Emeryville, Calif., for supplying the purified squalene used in this work; and to Edmund J. Blau, formerly of the Bureau and now with the Applied Physics Laboratory, Johns Hopkins University, Silver Spring, Md., for his assistance in the Raman studies.

5. References

[1] H. J. Backer and Th. A. H. Blaas, Rec. trav. chim. **61,** 785 (1942).
[2] L. C. Bateman, R. W. Glazebrook, C. G. Moore, and R. W. Saville, Proceedings of the third rubber technology conference, p. 298 (W. Heffer & Sons, Ltd., Cambridge, London, 1954); Rubber Chem. and Technol. **30,** 397 (1957).
[3] N. Bekkedahl, F. A. Quinn, Jr., and E. W. Zimmerman, J. Research NBS **40,** 1 (1948); Rubber Chem. and Technol. **21,** 701 (1948).
[4] G. F. Bloomfield, J. Chem. Soc. 1547 (1947); Rubber Chem. and Technol. **22,** 348 (1949).
[5] G. F. Bloomfield, J. Polymer Sci. 1, 312 (1946); Rubber Chem. and Technol. **20,** 360 (1947).
[6] G. F. Bloomfield and R. F. Naylor, Proceedings of the XIth International congress of pure and applied chemistry, Vol. II, p. 7, Organic Chemistry, Biochemistry (London, 1947).
[7] M. Braden, W. P. Fletcher, and G. P. McSweeny, Transactions of the institution of the rubber industry **30,** 44 (1954); Rubber Chem. and Technol. **28,** 190 (1955).
[8] David Craig, B. F. Goodrich Research Center (private communication).
[9] J. Dale and T. Artun, Acta Chem. Scand. **10,** 439 (1956).
[10] W. G. Dauben and H. L. Bradlow, J. Am. Chem. Soc. **74,** 5205 (1952).
[11] W. G. Dauben, H. L. Bradlow, N. K. Freeman, D. Kritchevsky, and M. Kirk, J. Am. Chem. Soc. **74,** 4321 (1952).
[12] H. L. Dinsmore and D. C. Smith, A, Anal. Chem. **20,** 11 (1948); B, Rubber Chem. and Technol. **22,** 572 (1949).
[13] B. Ellis and H. Pyszora, J. Polymer Sci. **22,** 348 (1956).
[14] E. H. Farmer and C. G. Moore, J. Chem. Soc. 142, (1951); Rubber Chem. and Technol. **24,** 777 (1951).
[15] E. H. Farmer and F. W. Shipley, J. Chem. Soc. 1519 (1947).
[16] E. H. Farmer and F. W. Shipley, J. Polymer Sci. **1,** 293 (1946); Rubber Chem. and Technol. **20,** 341 (1947).
[17] L. H. Flett and W. H. Gardner, Maleic anhydride derivatives—Reactions of the double bond (John H. Wiley & Sons, Inc., New York, N. Y. 1952).
[18] P. J. Flory, Principles of polymer chemistry, p. 454 (Cornell University Press, Ithaca, New York, 1953).
[19] S. D. Gehman, J. Am. Chem. Soc. **57,** 1382 (1935); Rubber Chem. and Technol. **8,** 521 (1935).
[20] S. D. Gehman and H. J. Osterhoff, J. Am. Chem. Soc. **58,** 215 (1936); Rubber Chem. and Technol. **9,** 275 (1936).
[21] R. W. Glazebrook and R. W. Saville, J. Chem. Soc. 2094 (1954); Rubber Chem. and Technol. **28,** 109 (1955).
[22] S. E. Horne, et al., Ind. Eng. Chem. **48,** 784 (1956); Rubber Chem. and Technol. **29,** 687 (1956).
[23] E. Kindscher, The vulcanization of rubber, The science of rubber, edited by K. Memmler (Rheinhold Publishing Corp., New York, N. Y., 1934).
[24] M. C. Kloetzel, Diels-Adler reaction with maleic anhydride, Organic reactions Vol. IV, edited by R. Adams, et al. (John Wiley & Sons, Inc., New York, N. Y., 1948).
[25] J. Mann, J. Rubber Research **18,** 79 (1949).
[26] A. T. McPherson, BS J. Research **8,** 751 (1932); Rubber Chem. and Technol. **5,** 523 (1932).
[27] D. E. Roberts and L. Mandelkern, J. Am. Chem. Soc. **77,** 781 (1955); Rubber Chem. and Technol. **28,** 718 (1955).
[28] G. Salomon and A. Chr. van der Schee, J. Polymer Sci. **14,** 181 (1954); Rubber Chem. and Technol. **28,** 213 (1955).
[29] G. Salomon, A. Chr. van der Schee, J. A. A. Ketelaar, and B. J. van Eyk, Discussions Faraday Soc. **9,** 291 (1950); Rubber Chem. and Technol. **25,** 265 (1952).
[30] R. A. Saunders and D. C. Smith, J. Appl. Phys. **20,** 953 (1949).
[31] W. C. Sears, J. Appl. Phys. **12,** 35 (1941); Rubber Chem. and Technol. **14,** 572 (1941).
[32] W. C. Sears and W. W. Parkinson, Bull. Am. Phys. Soc. **1** (II), No. 4, 203 (1956).
[33] W. C. Sears, W. W. Parkinson, O. Sisman, and R. L. Towns, Oak Ridge National Laboratory, Solid state division semiannual progress report for period ending February 29, 1956, ORNL–2051 p. 16.
[34] N. Sheppard, Discussions Faraday Soc. **9,** 331 (1950).
[35] N. Sheppard and G. B. B. M. Sutherland, Trans. Faraday Soc. **41,** 261 (1945); Rubber Chem. and Technol. **19,** 66 (1946).
[36] N. Sheppard and G. B. B. M. Sutherland, J. Chem. Soc. 1699 (1947); Rubber Chem. and Technol. **21,** 799 (1948).
[37] F. W. Stavely and Coworkers, Ind. Eng. Chem. **48,** 778 (1956); Rubber Chem. and Technol. **29,** 673 (1956).
[38] H. W. Thompson and P. Torkington, Trans. Faraday Soc. **41,** 246 (1945); Rubber Chem. and Technol. **19,** 46 (1946).

WASHINGTON, June 7, 1957.

Journal of Research of the National Bureau of Standards Vol. 60, No. 1, January 1958 Research Paper 2817

Crystal Structure of Barium Hydrogen Orthophosphate

Gordon Burley

The structure of anhydrous $BaHPO_4$ was determined from three Fourier projections. The unit cell is orthorhombic with the space group $Pn2_1a$—No. 33. The cell dimensions are $a=14.12$, $b=17.15$, and $c=4.59$ A, and it contains twelve formula units. Each Ba atom has a coordination polyhedron of ten oxygen atoms, being bonded to four phosphate tetrahedra by edge sharing and to two more by corner sharing of oxygen atoms. The phosphate groups are in separate tetrahedra, linked by hydrogen bonding to form continuous chains.

1. Introduction

The crystal structure of anhydrous barium hydrogen phosphate, $BaHPO_4$, was investigated as part of a program of systematic study of orthophosphate structures. Recent publication of the results of a structure determination of $CaHPO_4$ (monetite) [*1*] [1] made it advisable to refine the $BaHPO_4$ structure to such an extent as to allow an examination of the relationship between the two.

2. Experimental Techniques

The crystals used in this investigation were grown at the interface of a solution of $Ba_3(PO_4)_2$ covered by a layer of dilute H_3PO_4. The morphology of the crystals is that of a horizontal prism on a, with average diagonal dimension of 0.35 mm and thickness of about 0.07 mm.

Oscillation and Weissenberg photographs were taken about the principal axes using Cu and Mo radiation. Additional data was also obtained from a precession photograph of the $0kl$ reflections, using Mo radiation. Intensity data was obtained with a Wiebenga-Nonius integrating Weissenberg camera and a densitometer adapted for the purpose. All reflections were corrected for Lorentz and polarization factors by the method of Lu [*2*].

3. Structure

3.1. Cell Dimensions and Space Group

According to Groth [*3*], De Shulten reported anhydrous $BaHPO_4$ as orthorhombic, in the form of short prisms, and with axial ratios of $a:b:c=0.7133:1:0.8117$.

In the present work the $BaHPO_4$ unit cell was found to be orthorhombic with space group $Pn2_1a$—No. 33 [*4*]. The observed reflection conditions were

$$0kl: k+l=2n,$$

$$hk0: \quad h=2n.$$

From single crystal photographs, the cell dimensions were obtained as

$$a=14.12 \pm 0.03 \text{ A},$$

$$b=17.15 \pm 0.03 \text{ A},$$

$$c=4.59 \pm 0.02 \text{ A}.$$

Relative intensities of the layer lines on oscillation photographs strongly suggested a pseudocell having dimensions $a/2$, $b/3$, c. This is somewhat more pronounced in the b direction than along a.

Cell dimensions similar to those obtained here, with the same indication of a smaller cell, were given by Bengtsson [*5*], but the space group Pccn suggested by him did not agree with our observed reflection conditions.

A preliminary AEC paper on this structure by R. C. L. Mooney [*6*] was recently declassified and made available for inspection. This previous work was based on the pseudocell derived from powder diffraction data and assigned oxygen parameters on the basis of space group symmetry alone. Only qualitative single crystal intensity data was used. The barium parameters are in excellent agreement with those obtained in this investigation, although oxygen positions are different. This is primarily due to the fact that all reflections contain a barium contribution, and the comparatively small variation in the calculated intensity, resulting from the assumption of a small oxygen shift could not be detected with the qualitative data used.

On the basis of the larger unit cell established in this investigation, there are 12 formula units in the cell and all atoms are in the fourfold general positions

$$x,y,z;\ \bar{x},\tfrac{1}{2}+y,\bar{z};\ \tfrac{1}{2}-x,\tfrac{1}{2}+y,\tfrac{1}{2}+z;\ \tfrac{1}{2}+x,y,\tfrac{1}{2}-z.$$

The space group is proposed on the basis of the observable scattering contribution of all atoms, but the almost negligible scattering of hydrogen atoms precludes their inclusion in the original selection of symmetry elements. The calculated density is 4.170 g/cm^3, compared with a reported value of 4.165 g/cm^3 [*3*].

3.2. Absorption Corrections

The $hk0$ reflections were obtained from Weissenberg photographs using Mo K_α radiation, since the largest dimension of the crystal was well below the optimum size calculated from linear absorption data

[1] Italicized figures in brackets indicate the literature references at the end of this paper.

for this wavelength. The $0kl$ pattern was obtained on a precession camera with the largest crystal face normal to the incident beam. Only the usual Lorentz-polarization correction was applied. For the $h0l$ zone of reflections, it was necessary to use an absorption correction because of the geometry of the crystal. This was done by setting up a graph of the correction factor as a function of $\sin\theta/\lambda$ and obtaining the appropriate interpolated value for each $h0l$ reflection. The graph was constructed from a comparison of the observed $h00$ reflections on the $h0l$ films with the calculated values, used as the standard, available from the $hk0$ projection. A separate straight line relationship held for each of three separate films and the agreement for the three films was within better than 5 percent for all observed reflections. This scaling assumed approximate circular cross section of a cylindrical specimen and is essentially an absorption correction approximation. In order to evaluate this approximation method, the absorption for eight reflections, widely differing in intensity and position, was separately calculated by the geometrical absorption correction method of Evans [7]. The agreement was within 8 percent, and deviated in both directions. Therefore, the values of the $h0l$ intensities, corrected for absorption and scaled by the above method, were used in the calculations, but substantially only as a secondary check to reject a grossly inaccurate structure.

3.3. Structure Determination

The presence of the short c axis suggested a preliminary trial projection on the 001 plane. Approximate Ba positions were found from line syntheses along [100] and [010] and a Patterson projection. A Fourier projection using only these Ba parameters showed the position of the P atoms. Rows of alternating Ba atoms and P atoms were alined parallel to the a axis with a separation of $b/6$ and with an interval between adjacent atoms of the same row of about $a/4$. The projection was then refined by four successive difference Fourier syntheses, where the coefficients are obtained by subtracting the calculated from the observed structure factor for each index. This indicated that the phosphate tetrahedra were turned approximately 20° about a rotation axis parallel to the a axis, and that successive tetrahedra in the same row were turned in opposite directions. Because the magnitude of the angle of rotation was of importance in fixing the position of the hydrogen bond, it was determined by calculating structure factors for increments of 10° rotation of the tetrahedra from 0° to 90°. A graph of R values versus angle of rotation, with additional calculations at intervals of 2 deg from 18° to 26°, showed a minimum at about 21° (fig. 1). The final value of R for the $hk0$ reflections was 14.4 percent, where R is defined as

$$\frac{\Sigma|(|F_{obs}|-|F_{calc}|)|}{\Sigma|F_{obs}|}.$$

Patterson syntheses, using $h0l$ and $0kl$ data, showed conclusively that all the Ba and P atoms on a row parallel to the a axis had almost identical z parameters, and that each row was separated from its neighbor by about $b/6$ and $c/2$. There was overlap of atoms in both the a and b directions and Fourier projections did not resolve individual atoms. For the three independent Ba atoms, refinement of the z parameters was accomplished by calculation of structure factors for various combinations of Ba positions. The approximate contribution from the other atoms was added to this partial structure factor, and the total matched with the observed data. Several combinations of the three independent parameters gave satisfactory agreement for the $h0l$ data, but only one set could also be reconciled with the $0kl$ data. A least-squares refinement was attempted, but there was no convergence because of the overlap. Simultaneous adjustment in small increments of all atomic z parameters resulted in final agreement factor (R) values of 17.2 percent for the $h0l$ reflections and 14.5 percent for the $0kl$ set. The P to O distance was assumed constant at 1.56 A for this purpose. The independent atomic parameters are listed in table 1.

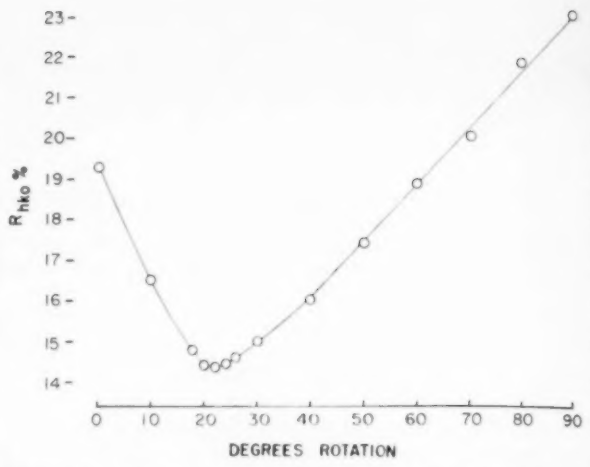

FIGURE 1. *Graph of R values for the hk0 zone of reflections versus angle of rotation of the phosphate tetrahedra.*

TABLE 1. *Coordinates of atoms in* $BaHPO_4$

	$BaHPO_4$, atomic parameters		
	x/a	y/b	z/c
Ba	0.103	0.083	0.325
	.103	.417	.276
	.397	.250	.648
P	.37	.08	.21
	.13	.25	.80
	.37	.42	.15
O	.43	.02	.12
	.43	.15	.30
	.31	.06	.47
	.31	.11	.95
	.19	.22	.06
	.19	.28	.54
	.07	.19	.71
	.07	.31	.89
	.43	.36	.06
	.43	.48	.24
	.31	.39	.41
	.31	.44	.89

A comparison of observed and calculated structure factors is given in table 2. All intensities were measured on a relative scale for each zone of reflection and scaled by comparison with the calculated structure factors. Since each zone of reflections was treated independently, all row lines appear twice in this table, for these reflections are observed separately on two films.

TABLE 2. *Comparison of calculated and observed structure factors for* $BaHPO_4$

h	k	l	F_o	F_c	h	k	l	F_o	F_c	h	k	l	F_o	F_c
00	00	02	76	84−	13	00	03	15	11−	00	00	02	105	84−
00	00	04	12	11	13	00	04	10	18−	00	00	04	13	11
01	00	01	0	13	14	00	00	54	50−	00	00	06	20	19
01	00	02	16	9−	14	00	01	30	29−	00	01	01	0	9
01	00	03	21	17	14	00	02	29	31					
										00	01	03	36	43−
01	00	04	24	20−	14	00	03	10	14	00	01	05	32	40
01	00	05	33	32−	15	00	01	0	2−	00	02	02	22	19
02	00	00	0	22	15	00	02	0	3−	00	02	04	40	46−
02	00	01	48	80−	16	00	00	46	45−	00	02	06	39	39
02	00	02	43	44−	16	00	02	67	78					
					16	00	02	20	23	00	03	01	vl	165−
02	00	03	0	5−						00	03	03	49	49
02	00	04	20	21−						00	03	05	10	12
02	00	05	27	28	00	06	00	130	156−	00	04	02	19	32−
03	00	01	0	1	00	12	00	136	134	00	04	04	33	42
03	00	02	0	2	00	18	00	119	93−					
					02	00	00	0	22	00	04	06	25	37−
03	00	03	21	12−	02	03	00	86	84−	00	05	01	0	7
03	00	04	48	36−						00	05	03	36	30−
03	00	05	24	20	02	06	00	0	0	00	05	05	27	30
04	00	00	112	156−	02	09	00	117	102−	00	06	00	123	158−
04	00	01	38	45−	02	12	00	47	35					
					02	15	00	81	65−	00	06	02	73	75
04	00	02	69	98	02	18	00	0	28−	00	06	04	17	24−
04	00	03	21	26						00	06	06	14	8−
04	00	04	0	8	02	21	00	83	74	00	07	01	0	5−
04	00	05	0	4	04	00	00	81	156−	00	07	03	33	40
05	00	01	0	2	04	03	00	92	108−					
					04	06	00	117	117	00	07	05	27	31−
05	00	02	0	0	04	09	00	108	86	00	08	02	16	20−
05	00	03	23	17−						00	08	04	35	40
05	00	04	0	5−	04	12	00	127	114−	00	08	06	26	29−
05	00	05	39	36	04	15	00	52	35−	00	09	01	105	116
06	00	00	108	103−	04	18	00	105	91					
					04	21	00	61	47	00	09	03	41	43−
06	00	01	39	52	06	00	00	78	103−	00	09	05	0	3−
06	00	02	41	42						00	10	02	29	20
06	00	03	0	0	06	03	00	70	90	00	10	04	34	34−
06	00	04	15	20	06	06	00	63	47	00	11	01	0	8−
06	00	05	20	20−	06	09	00	69	54−					
					06	12	00	88	70−	00	11	03	29	33
07	00	01	0	0	06	15	00	41	36	00	11	05	26	34−
07	00	02	0	5−						00	12	00	121	138
07	00	03	0	1	06	18	00	55	53	00	12	02	85	85−
07	00	04	34	30	08	00	00	44	43	00	12	04	14	10
07	00	05	0	1−	08	03	00	78	104					
					08	06	00	78	70−	00	12	06	13	8
08	00	00	44	43	08	09	00	114	114−	00	13	01	0	6
08	00	01	84	100						00	13	03	28	32−
08	00	02	38	53−	08	12	00	61	56	00	14	02	13	18
08	00	03	34	31−	08	15	00	94	86	00	14	04	26	36−
08	00	04	0	2	08	18	00	58	57−					
					10	00	00	83	105	00	15	01	98	114−
08	00	05	10	10−	10	03	00	0	10−	00	15	03	37	33
09	00	01	0	1						00	16	02	26	21−
09	00	02	0	6−	10	06	00	70	85−	00	16	04	28	32
09	00	03	0	10	10	09	00	0	4−	00	17	01	0	2
09	00	04	12	16−	10	12	00	72	67					
					10	15	00	0	15−	00	17	03	17	23−
09	00	05	25	32−	10	18	00	58	51−	00	18	00	85	96−
10	00	00	106	105						00	18	02	62	73
10	00	01	0	17−	12	00	00	0	1−	00	19	01	0	7−
10	00	02	36	30−	12	03	00	97	108−	00	19	03	18	30
10	00	03	0	11−	12	06	00	0	21					
					12	09	00	86	103	00	20	02	0	15−
10	00	04	20	19−	12	12	00	0	9	00	21	01	66	77
11	00	01	0	2						00	21	03	27	34−
11	00	02	0	6−	12	15	00	86	101−	00	22	02	0	5−
11	00	03	0	6	14	00	00	44	50−	00	23	01	0	4
11	00	04	19	16−	14	03	00	39	44−					
					14	06	00	54	68	00	24	00	76	80
12	00	00	0	1−	14	09	00	33	40					
12	00	01	101	106−										
12	00	02	0	13−	14	12	00	42	55−					
12	00	03	32	28−	16	00	00	50	45−					
12	00	04	22	20−	16	03	00	75	96					
13	00	01	0	2−	16	06	00	39	42					
13	00	02	0	6	16	09	00	58	73−					

3.4. Estimate of Accuracy

An estimation of the accuracy of the structure determination was made from the final difference map on the *hk*0 plane by Cruickshank's method [*8,9*]. Assuming isotropic variation, the standard deviations of atomic parameters are

$$\begin{aligned} \text{Ba} &= 0.018 \text{ A}, \\ \text{P} &= .055 \text{ A}, \\ \text{O} &= .065 \text{ A}. \end{aligned}$$

Because of the large uncertainty in the positions of the lighter atoms, no artificial temperature factor was used.

The standard deviations of bond lengths are

$$\begin{aligned} \text{Ba—O} &= 0.067 \text{ A}, \\ \text{P—O} &= .085 \text{ A}, \\ \text{O—O} &= .091 \text{ A}. \end{aligned}$$

4. Description of Structure

The unit cell contains 12 formula weights of $BaHPO_4$. All atoms are in general positions that are related by symmetry in sets of four. Consequently, there are only 3 Ba, 3 P, and 12 O atoms with independent parameters. The x and y coordinates of the Ba atoms are in excellent agreement with those given previously by Bengtsson [*5*]. The present investigation has contributed the z parameters for the Ba atoms and the placement of the lighter atoms.

A schematic projection of the structure on the *hk*0 plane is shown in figure 2. The height above the base plane where $z=0$ is indicated for each atom in units of $z/100$.

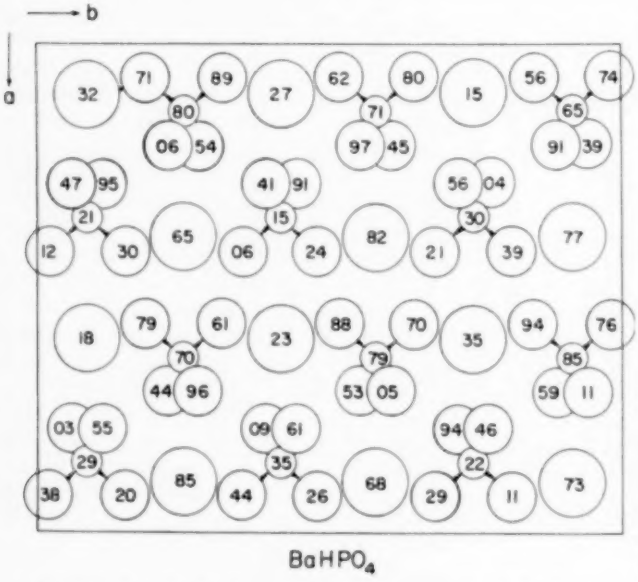

FIGURE 2. *Projection of the structure on the hk0 plane.*

(Circles in decreasing order of size represent Ba, O, and P, respectively.) Complete phosphate tetrahedra are shown, but the heights indicated refer to the position in the single unit cell.

At about $z=0.25$ and $z=0.75$ there are rows parallel to the a axis of alternating Ba and P atoms. The atoms within each row are not perfectly alined, but vary somewhat in their z parameters. Adjacent rows at a given c level are separated by $b/3$. The families of rows $c/2$ apart are displaced from each other by $b/6$. Thus the projection on the base plane shows six such rows, separated by $b/6$. All phosphate tetrahedra are rotated by roughly 21° about these row axes. The reference position of 0° rotation is taken as that in which a twofold axis of symmetry relates all the oxygens of the tetrahedron, and two of these oxygens are superimposed on each other in the projection on 001. Successive tetrahedra within the same row are rotated through an angle of the same magnitude but opposite sign. Figure 2 also shows that in rows adjacent in the projection on the base plane all the tetrahedra are oriented in opposite directions.

The P atoms are each surrounded by four oxygen atoms in apparently undistorted tetrahedral configuration and at distances of 1.56 A within the limits of experimental error. A summary of all other coordination distances is given in figure 3. Lines with two numbers indicate coordination with two separate tetrahedra at different heights. Each Ba atom is in sevenfold coordination with oxygen atoms at distances varying from 2.6 to 3.1 A. (The sum of the atomic radii is 2.75 A.) Three additional oxygen atoms are tied to each Ba atom if the coordination distance is extended to 3.5 A. Beyond this distance there is a considerable jump to the next nearest neighbor at 4.2 A. Because of the uncertainty in the oxygen positions, coordination distances are significant only to the nearest 0.1 A.

In the larger coordination sphere of barium, each Ba atom is linked to the oxygen atoms of four phosphate tetrahedra by edge sharing and to the oxygen atoms of two more by corner sharing. The coordi-

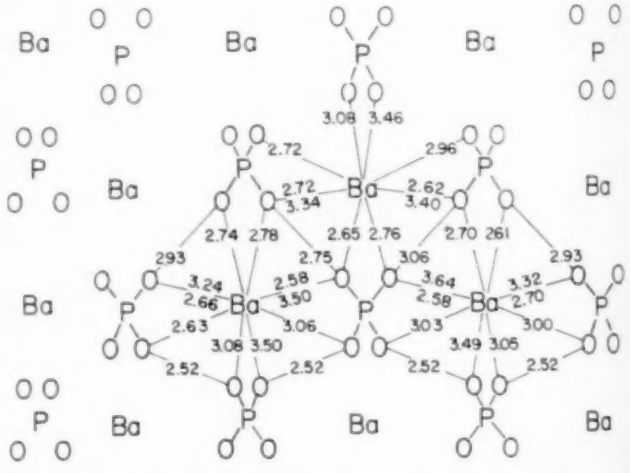

FIGURE 3. *Coordination distances in projection on the hk0 plane, indicating the three independent barium atoms.*

nation distances for each independent Ba atom are slightly different, but the general configuration around each is similar. This explains the presence of the pseudocell, because the pattern repeats at intervals of $a/2$ and $b/3$, and the contents of each pseudounit differ only in the relative displacements in the c direction of the component atoms. Each phosphate tetrahedron has 2 oxygen atoms each linked to 2 different Ba atoms and the other 2 each bonded to 3 Ba atoms.

The position of the hydrogen atom can be inferred from structural considerations. The experimentally observed O to O distances between adjacent tetrahedra are 3.1 and 3.2 A in one direction and two of 2.5 A in the opposite direction. It is generally assumed [*10*] that the extremely short bonds can be due only to an unusually large binding force, which must be ascribed to hydrogen bonding between these atoms. This would assign half the proton to each of the two O atoms bonded to only two barium atoms. No data could be obtained with X-rays on the symmetry of this hydrogen bond. This bonding would link phosphate tetrahedra in roughly a diagonal progression with translation of $c/2$ and $b/6$. The propagation direction is symmetrically opposed for tetrahedra separated by $a/2$.

Structurally, there is a marked resemblance between the projection on (001) of $BaHPO_4$ and the same projection of the triclinic $CaHPO_4$. However, the coordination numbers of the metal atoms differ due to variation in the relative positions of the phosphate groups and the compounds are not isostructural.

5. Summary

The structure of $BaHPO_4$ essentially consists of discrete phosphate tetrahedra, undistorted within the limits of measurement, held together by Ba ions and probably hydrogen bonding. The coordination sphere of the Ba atoms includes 10 oxygen atoms, 7 of which are bonded more firmly than the other 3.

The author is indebted to Rose C. L. Mooney for suggesting this problem and helpful advice during the course of the investigation. Alvin Perloff prepared the crystals.

6. References

[*1*] G. MacLennan and C. A. Beevers, Acta Cryst. **8,** 579 (1955).
[*2*] C. S. Lu, Rev. Sci. Instr. **14,** 331 (1943).
[*3*] P. Groth, Chemische Kristallographie **2,** 821 (Engelmann, Leipzig, 1908).
[*4*] Int. tables for X-ray crystallography, vol. I (The Kynoch Press, Birmingham, 1952).
[*5*] E. Bengtsson, Arkiv Kemi, Mineral. Geol., 15B, No. 7 (1941).
[*6*] R. C. L. Mooney, Atomic Energy Commission TID–5212, p. 165 (Technical Information Service, Oak Ridge, Tenn., Sept. 1955).
[*7*] H. T. Evans, Jr., J. Appl. Phys. **23,** 663 (1952).
[*8*] D. W. J. Cruickshank, Acta Cryst. **2,** 65 (1949).
[*9*] H. Lipson and W. Cochran, The determination of crystal structures (G. Bell & Sons, Ltd., London, 1953).
[*10*] M. Gorman, J. Chem. Educ. **33,** 468 (1956).

Washington, June 5, 1957.

Journal of Research of the National Bureau of Standards Vol. 60, No. 1, January 1958 Research Paper 2818

A Study of Sampling of Flame Gases [1]

C. Halpern and F. W. Ruegg

A study of sampling of hot combustion gases by means of water-cooled probes of internal diameter of 0.027 to 0.070 cm has been made. Effect of conditions of sampling on concentrations of CO, CO_2, H_2, and H_2O was the primary interest in this study. The probes were unable to quench reactions completely and were unable to preserve the original composition of the gas, but small probes were more effective than larger probes. Sample composition was unaffected by sampling velocity, except that at the higher rates of sampling it appears that gradients of composition and temperature caused the effectiveness of quenching to decrease. Probe material and configuration had little effect on sample composition.

1. Introduction

The current interest in high-temperature combustion as applied to the field of jet propulsion has led to a need for means to determine the state of the combustion gases in and near the region of chemical reaction. Knowledge of the pressure, temperature, and composition of the gases, among other quantities, is needed to understand the phenomena observed. The composition of the flame gas may be determined by chemical analysis, and temperature, concentration of fuel, and the extent of reaction can be derived. These quantities are determined, of course, for the point or small volume of the engine from which the sample is drawn, and this is one advantage of using chemical analysis.

Samples are commonly taken by drawing the hot gas through tubes that are cooled with water both to protect the tube and to help preserve the composition of the gases being sampled. Chemical analysis will be of value only if the composition of the sample remains unchanged, and this investigation is concerned with the determination of the effectiveness of this method of sampling in preserving the composition of the gas at the point of sampling. The primary interest here is in samples from streams of gas whose compositions are constant at the point of sampling. One requirement of this investigation, therefore, is a source of hot gas whose composition will be constant during the sampling period; a flame burning under controlled steady conditions and of sufficient size relative to the probe and rate of sampling will satisfy this need.

Considerable work which involved sampling and analysis of flame gas was reported during the early years of this century [1 to 16].[2] Most of this work was done with flames of comparatively low temperature, 1,800° C or less, and the main interest was to determine if chemical equilibrium existed in the flame. Generally, there was no interest in or even recognition of the problems of sampling. Only Haber and Le Rossignol [6] and Haber and Hodsman [7] did any work that involved changing the conditions of sampling. Their method of sampling was to attach an evacuated container to a water-cooled probe and let gas flow in through a stopcock until the pressure reached 0.5 atm. Haber and Le Rossignol used a probe, i.d.=0.015 cm, to sample a carbon monoxide-oxygen flame with a temperature of about 2,900° K. Results of 7 tests, 5 at one rate of sampling and 2 at lower rates, showed some variation of sample composition with rate, but were interpreted to be only a negligible change. The position of the stopcock probably was changed to change the rate of sampling. The speed of the hot gas sample entering the probe at the largest rate of sampling is estimated to be sonic and thus the pressure for this rate is about 0.5 atm at the entrance of the probe. For the lower rates of sampling, the speed and corresponding pressure drop is less. Since the composition of a gas sample in equilibrium is affected by pressure, the composition of the gas sample obtained at the highest rate may have changed more than the others. Haber and Le Rossignol compared the temperature derived from the equilibrium constant for the dissociation of carbon dioxide calculated from the composition of their sample with a calculated adiabatic flame temperature, and concluded that their probe was capable of freezing the dissociation of carbon dioxide and thus of preserving the sample unchanged. But since their method of sampling involves a large pressure change, the effect of the change of pressure on the composition of the sample may have obscured the effect of the probe alone.

Haber and Hodsman used flames of carbon monoxide and oxygen, acetylene and oxygen, and hydrogen and oxygen. Using the hydrogen and oxygen flame, two out of three tests showed a 0.01-cm probe to be more effective than a 0.015-cm probe in freezing the water dissociation, since the temperature based on the water dissociation found in samples taken by the smaller probe was higher than in those taken by the larger probe. As even this higher temperature was about 300° C lower than their calculated flame temperature, they concluded that even the smaller probe could not freeze the water dissociation. Considering the samples drawn from the acetylene-oxygen flames, they concluded that their probes could freeze the carbon dioxide dissociation but not the water dissociation.

[1] This work was sponsored by the Power Plants Division, Bureau of Aeronautics, Department of the Navy.

[2] Figures in brackets indicate the literature references at the end of this paper.

Erbe, Grey, and Beal [17] sampled a natural gas-oxygen flame, and temperatures derived from the values of the equilibrium constants of the products of dissociation of carbon dioxide and water were 2,589° and 2,644° K, respectively. They concluded that since these two temperatures were in good agreement their water-cooled probe (internal diameter=0.051 cm) was able to preserve the composition of the flame gas. The given composition of the gas sample can be used to compute the ratio of natural gas to oxygen, and from this ratio, the flame temperature was calculated to be about 2,850° K. On this basis, their probe did not preserve the composition of the gas in the flame.

It is well known that the composition of a gaseous system in equilibrium can be changed by changing the pressure or by diluting the system with an inert ingredient, provided that the number of molecules of products and reactants are unequal. Hough, Valle-Riestra, and Sage [18] have employed a sampling system in which combustion gas is expanded to a low pressure and simultaneously diluted with helium. Their analytical data indicate the possibility that the reduction of the partial pressure of the components of the sample caused dissociation to overcome the association that would be normal with reduction of temperature only. In this event, apparent quenched temperatures (based on an equilibrium constant derived from the original partial pressures) of the sample would be higher than flame temperature. If a plain water-cooled sampling probe proves inefficient, this procedure of reducing the pressure of the sample may be necessary.

Since previous investigators had paid so little attention to the techniques of sampling, and water-cooled sampling probes continued to be widely used, it was decided that a study of sampling hot gases by means of water-cooled probes to determine the effectiveness of this method might prove useful.

The composition of a gas in chemical equilibrium can be determined from a knowledge of the equilibrium constants of the reactions that are taking place. As temperature changes, values of equilibrium constants change, and a sample of gas that is cooled slowly will change in composition down to a temperature T_q where the reaction rates are too slow to make any further noticeable change in composition. If gas at temperature T were cooled instantaneously to T_q, then the composition of the gas at T_q would be the same as at T, and the reaction is said to be quenched. In a real case of rapid cooling, as in a sampling probe, equilibrium probably is not maintained and there must be some reaction occurring during the time of cooling down to about temperature T_q. Therefore the gas has a final composition between the initial composition and the composition corresponding to the case of equilibrium cooling. An equilibrium constant based on the final composition and its associated temperature, T_{aq}, may approximate a temperature to which the gas is cooled slowly along an equilibrium path, followed by infinite rate of cooling to stop further reaction. T_{aq}, which may be called an apparent quenched temperature, will approach T only when the degree of conversion of reactants to products is made small by rapid cooling.

Hottel, Williams, and Satterfield [19] have calculated the theoretical composition of flame gas at various temperatures for various burning mixtures based on the assumption that chemical equilibrium exists. Table 1 presents some of their calculated compositions. If a mixture is burned whose theoretical burnt composition is known, and if samples are drawn from the flame and analyzed, we may, by comparing the composition determined by experiment with the theoretical composition, determine T_{aq} for the cooled gas. It is realized that the assumption of chemical equilibrium in flames is questionable, but for the lack of any other data, the values of table 1 are made the basis for comparison. Hottel et al. present the theoretical composition in terms of the molecules H_2, H_2O, N_2, CO, CO_2, and NO, the atoms H and O, and the free radical OH. Of these, H, O, and OH do not exist in the cooled gas, and of

TABLE 1. *Equilibrium composition of flame gas according to Hottel, et al.*

Compound	Percentage present at—						
	1,800°K	2,000°K	2,200°K	2,400°K	2,600°K	2,800°K	3,000°K
CH_4+2O_2, calculated flame temperature=3,050°K							
H_2O	0.66440	0.65920	0.6467	0.6216	0.5775	0.5103	0.4192
H_2	.00096	.00284	.0069	.0144	.0266	.0443	.0662
O	.00001	.00005	.0003	.0014	.0051	.0144	.0338
H	.00001	.00009	.0005	.0019	.0063	.0172	.0406
O_2	.00130	.00426	.0110	.0233	.0413	.0620	.0796
OH	.00051	.00201	.0061	.0152	.0316	.0561	.0862
CO	.00190	.00669	.0182	.0402	.0737	.1136	.1496
CO_2	.33091	.32486	.3103	.2820	.2379	.1821	.1248
$CH_4+2O_2+2N_2$, calculated flame temperature=2,800°K							
H_2O	0.39866	0.39559	0.38827	0.37340	0.34719	0.30636	
H_2	.00070	.00210	.00510	.01071	.01992	.03332	
O	.00000	.00004	.00025	.00115	.00407	.01148	
H	.00001	.00007	.00040	.00164	.00542	.01495	
O_2	.00086	.00282	.00725	.01525	.02670	.03946	
OH	.00035	.00141	.00428	.01059	.02196	.03887	
NO	.00021	.00068	.00177	.00384	.00709	.01135	
N_2	.39944	.39808	.39482	.38831	.37725	.36091	
CO	.00140	.00493	.01336	.02925	.05291	.08040	
CO_2	.19837	.19428	.18450	.16586	.13749	.10290	
$CH_4+2O_2+4N_2$, calculated flame temperature=2,600°K							
H_2O	0.28473	0.28251	0.27723	0.26645	0.24728		
H_2	.00057	.00170	.00413	.00869	.01621		
O	.00000	.00003	.00022	.00101	.00356		
H	.00001	.00007	.00036	.00148	.00489		
O_2	.00067	.00220	.00563	.01178	.02046		
OH	.00028	.00122	.00340	.00839	.01734		
NO	.00022	.00072	.00187	.00405	.00746		
N_2	.57079	.56925	.56554	.55811	.54549		
CO	.00113	.00398	.01074	.02339	.04195		
CO_2	.14160	.13842	.13088	.11665	.09536		
$CH_4+2O_2+7.52N_2$, calculated flame temperature=2,250°K							
H_2O	0.18942	0.18789	0.18420				
H_2	.00044	.00131	.00320				
O	.00000	.00003	.00019				
H	.00001	.00006	.00032				
O_2	.00050	.00163	.00416				
OH	.00021	.00084	.00257				
NO	.00021	.00070	.00180				
N_2	.71421	.71272	.70914				
CO	.00088	.00307	.00824				
CO_2	.09412	.09175	.08618				

the molecules. H_2, CO, and CO_2 are most easily determined analytically. In the experimental work to be presented, T_{aq} is determined by comparison of theoretical and experimental mole ratios of CO/CO_2 and H_2/H_2O. By comparing the apparent quenched temperature with the calculated adiabatic flame temperature T, the effectiveness of probes in quenching reactions can be determined qualitatively at least.

Sodium line reversal temperatures for some combustible mixtures are listed in reference [20a]. The calculated adiabatic flame temperatures for some acetylene mixtures are within 100° of the measured temperatures of 2,500° and 3,200° K. The measured temperature of a natural gas flame was 2,200° K, and the calculated temperature was 2,230° K. Some measurements of temperatures of methane flames at the Bureau show similar results. At a sodium line reversal temperature of 2,600° K, the calculated temperature was about 75° higher, whereas at 2,100° K, the measured and calculated temperatures corresponded. Since measured temperatures are close to the calculated equilibrium temperatures, it seems likely that the composition of the flame gas should be close to the calculated equilibrium composition.

2. Apparatus and Analytical Method

Exhaust gas was provided by burning mixtures of methane, air, and oxygen in Bunsen cones at the discharge port of a nozzle. Three different nozzles with port diameters of 1.27, 0.475, and 0.318 cm, respectively, were used in order to keep within the blowoff and flashback limits of the burning mixtures. The burner was mounted horizontally to prevent water condensing on the probe from falling into the fire.

The rates of flow of methane, oxygen, and air to the burner were controlled and measured in separate systems; each consisted of a pressure-reducing valve, a flow controller, a rotameter, and a manometer. The gases were first dried by passing through activated alumina.

Water-cooled probes, illustrated in figure 1, were used to sample the hot flame gas. Probes of design 1 were constructed of stainless-steel hypodermic needles or of tubing of other metals mounted transversely in a piece of flattened copper tubing. Dimensions of these probes are listed in table 2. Probes of design 2 were made of stainless steel hypodermic needles with a right-angle bend or with a 90° turn, with a radius of 1/16 in., mounted in thin-walled copper tubing. The bend or turn was set as close as possible to the copper wall and the projecting tip was made less than 1 diameter of the gas passage in length. Probes were mounted with the entrance to the gas passage coaxial with the cone of the flame, and the distance from the cone could be changed by a rack and pinion.

TABLE 2. *Probe design 1, dimensions*

D/A	Material	Probe				
		A	B	C	D	E
		cm	cm	cm	cm	cm
31	Stainless steel	0.027	0.051	0.04	0.83	0.38
33	do	.057	.089	.08	1.86	.56
25	do	.070	.094	.11	1.70	.65
35	Platinum	.037	.135	.08	1.30	.43
39	do	[a].035	.135	.08	1.35	.36
75	do	.035	.135	.10	2.62	.75
39	Silver	.035	.135	.08	1.38	.46

[a] Nozzle inlet diameter 0.060 cm, outlet diameter 0.035 cm, formed at entrance

Gas samples were analyzed either gravimetrically, using a combustion train, or volumetrically, using a Shepherd gas-analysis apparatus. The rate of flow of gas through the train was controlled and measured by the exhaust-metering system. The combustion train and exhaust-metering system are illustrated in figure 2, in which A represents a cold trap; B, a

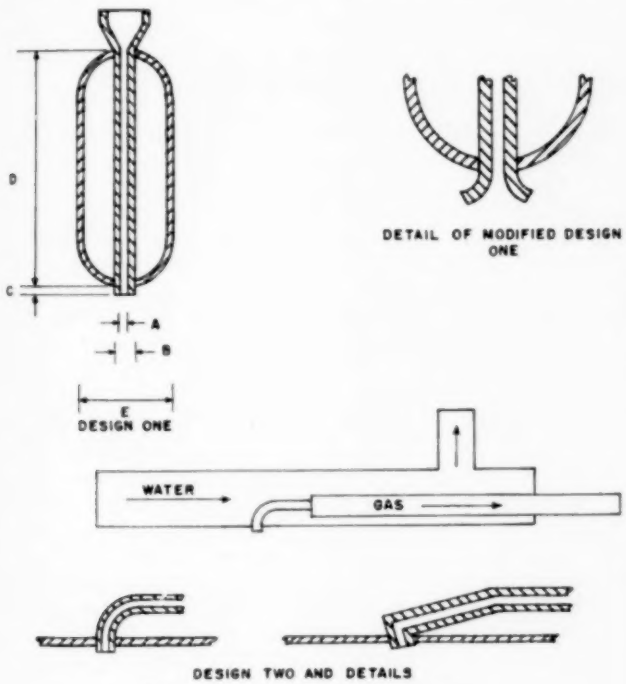

FIGURE 1. *Gas sampling probes.*

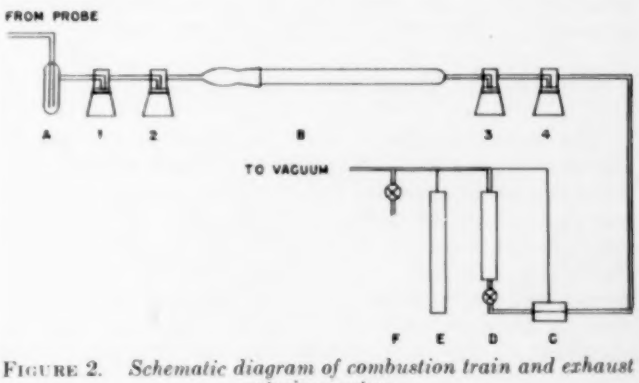

FIGURE 2. *Schematic diagram of combustion train and exhaust metering system.*

quartz combustion tube packed with copper oxide; C, a flow controller; D, a rotameter and control valve; E, a manometer to measure the pressure in the metering part of the system; F, a bleed valve to control the pressure in the system; 1, a Turner absorption bottle containing in order Drierite and phosphorus pentoxide separated by asbestos; 2 and 4, Turner absorption bottles containing in order Ascarite and phosphorus pentoxide separated by asbestos; and 3, a Turner absorption bottle containing in order Anhydrone and phosphorus pentoxide separated by asbestos. The Turner absorption bottles were modified by fusing male spherical joints to the arms of the caps.

Temperature of the combustion tube was measured by a Chromel-Alumel thermocouple, placed alongside it and shielded from the coils of the furnace by platinum foil.

For gravimetric analysis, gas samples were drawn continuously from the flame through a water-cooled probe and into the combustion train at a constant specified rate. The pressure in the exhaust-metering system was kept at 20 in. of mercury absolute. The combustion tube was kept at 270° to 295° C, the range in which carbon monoxide and hydrogen are oxidized to carbon dioxide and water respectively, while hydrocarbons are unaffected. Water in the sample was condensed in the cold trap and the remaining traces were removed by the Drierite. Carbon dioxide in the sample was determined by change in weight of the first Ascarite bottle, while carbon monoxide and hydrogen were determined by change in weight of the Ascarite and the Anhydrone bottles, respectively, both after the furnace. Water in the sample was approximated from the total weight of carbon dioxide collected and the carbon-hydrogen ratio of methane.

Samples for volumetric analysis were collected by two different methods: (1) By drawing exhaust gas at a measured rate through a sample container and displacing the air, and (2) by the outflow of mercury from the sampling container into a leveling container which was lowered at a constant rate. Method 1 was used only when it was desired to collect a sample for volumetric analysis simultaneously with the operation of the train. The sample container was inserted between the cold trap and the first absorption bottle. Method 2 was used to collect samples for volumetric analysis when the sampling rate was too low to be measured in the exhaust-metering system.

3. Experimental Results

The factors studied in the investigation of quenching of reactions were the velocity of the hot gas in the entrance of the probe, the internal diameter of the gas passage in the probe, the materials of which the gas passage was constructed, and the probe design. Sampling velocity is calculated as follows: It is considered that, since fuel and oxygen are always used in stoichiometric proportions, only the nitrogen supplied in the combustible mixture remains to be metered in the gas after passing through the combustion train. The theoretical nitrogen content of the burnt gas for a given combustible mixture and given flame temperature is obtained from table 1. The volume of gas entering the probe is calculated from the volume of gas passing through the rotameter of the exhaust-metering system corrected to atmospheric pressure, the theoretical nitrogen content, the ratio of the calculated flame temperature to room temperature, and the measured diameter of the probe.

3.1. Effect of Sampling Velocity and Probe Size

In all of the experiments reported in this section, the burning mixture used had mole proportions $CH_4:O_2:N_2=1:2:2$, and the calculated adiabatic flame temperature of this mixture was 2,800° K. The mixture was burned on the port of a 0.475-cm nozzle and the probe was set 0.36 cm from the tip of the inner cone of the flame. Lewis and Von Elbe [20b] report that the maximum temperature is some distance from the tip of the inner cone. Some tests were made of the variation of apparent quenched temperature with distance from the flame tip, and these showed that the distance chosen, 0.36 cm, was at or near the zone of maximum temperature. A series of experiments was made to discover if the composition of the sample varied with velocity of sampling. Four probes were used in these experiments: A 0.027-cm steel probe, a 0.035-cm platinum probe, a 0.057-cm steel probe, and a 0.070-cm steel probe. Effect of sampling velocity on the composition of the sample, as measured by the mole ratios of carbon monoxide to carbon dioxide and of hydrogen to water, is shown in figures 3 and 4. Table 3 presents some data that was derived from these experiments. The experimental ratio H_2/H_2O is compared with the calculated ratio $H_2/H_2O+\frac{1}{2}H+\frac{1}{2}OH$ because it is considered that H and OH appear as H_2O in the cooled sample.

For all four probes, the ratio CO/CO_2 appears to be constant for a limited range of sampling velocities and then decreases as the velocity of sampling increases. The ratio H_2/H_2O exhibits a similar behavior for three out of four probes, only the curve for the 0.035-cm platinum probe does not show a point of inflection. If the amount of flame gas drawn into the probe is expressed as a fraction of the total mass of the burnt gas, it is found that this fraction is always between 1 and 2 percent at the point of inflection. This suggests that as the rate of sampling is increased beyond this point, gas from cooler regions of the flame is drawn into the probe, causing the values of the ratios to decrease. The sampling velocities at the point of inflection listed in the previous table represent the limit beyond which our samples are no longer representative of the central region being sampled. Under different circumstances, if the gas being sampled contained no fixed temperature and concentration gradients, these points of inflection would not be expected to occur.

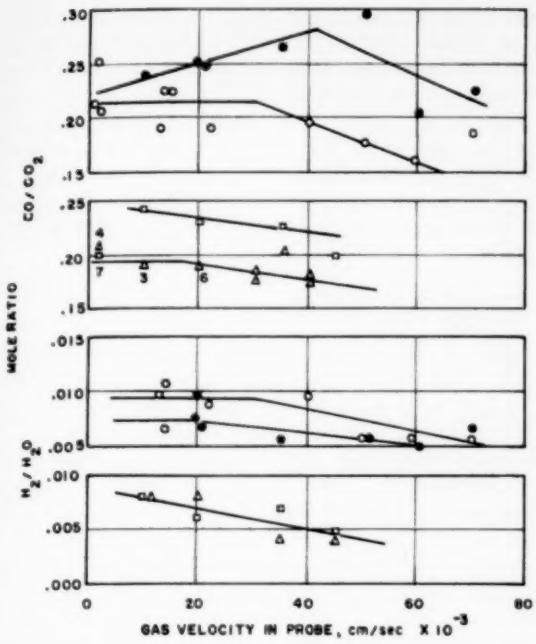

FIGURE 3. *Effect of rate of sampling on composition.*

○, 0.027-cm probe, design 1; ●, 0.027-cm probe, design 2; △, 0.035-cm probe, design 1; □, 0.035-cm probe, modified design 1. Numbers near points represent number of experiments averaged to find value plotted.

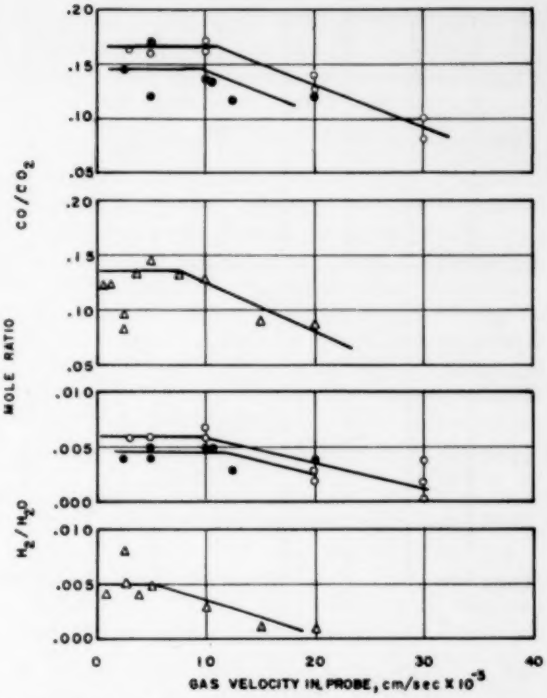

FIGURE 4. *Effect of rate of sampling on composition.*

○, 0.057-cm probe, design 1; ●, 0.061-cm probe, design 2; △, 0.070-cm probe, design 1.

It will be noted that the highest velocity of sampling in figures 3 and 4 is 70,000 cm/sec. If the velocity were calculated more accurately to take account of compressibility, the velocity would actually be about 92,000 cm/sec, the Mach number would be about 0.85, and the pressure at the entrance of the probe about ⅞ atm abs. Reynolds number of the flow formed from the internal diameter of the tube, density, velocity of sampling, and viscosity was always below 2,000, and hence if the flow were laminar in the flame, it would remain so in the entrance to the probe.

There was some indication with the 0.027-cm probe, at sampling velocities of 2,000 cm/sec and less, that poor quenching was caused by condensation of water in the gas passage. When the flow of cooling water in the probe was reduced until the exit water was about 37° C, quenching was improved. Tests with the larger steel probes at low sampling velocities were not so extensive, and it is possible that some of the low values obtained in the 0.061-cm and 0.070-cm probes could be due to the same cause.

TABLE 3.

Probe size	Carbon				Hydrogen			
	Maximum CO/CO_2	Maximum $(T_{eq})_{CO}$	Sampling velocity at point of inflection	Sampling rate [a] at point of inflection	Maximum H_2/H_2O	Maximum $(T_{eq})_{H_2}$	Sampling velocity at point of inflection	Sampling rate [a] at point of inflection
cm		*° K*	*cm/sec*	*cm³/sec*		*° K*	*cm/sec*	*cm³/sec*
0.027	0.220	2,450	30,000	2.3	0.010	2,100	30,000	2.3
.035	.195	2,420	17,000	2.2	.008	2,090	------	------
.057	.165	2,380	11,000	3.8	.005	2,040	10,000	3.5
.070	.135	2,335	7,500	4.1	.005	2,000	5,000	2.6

[a] At room temperature and pressure and wet.

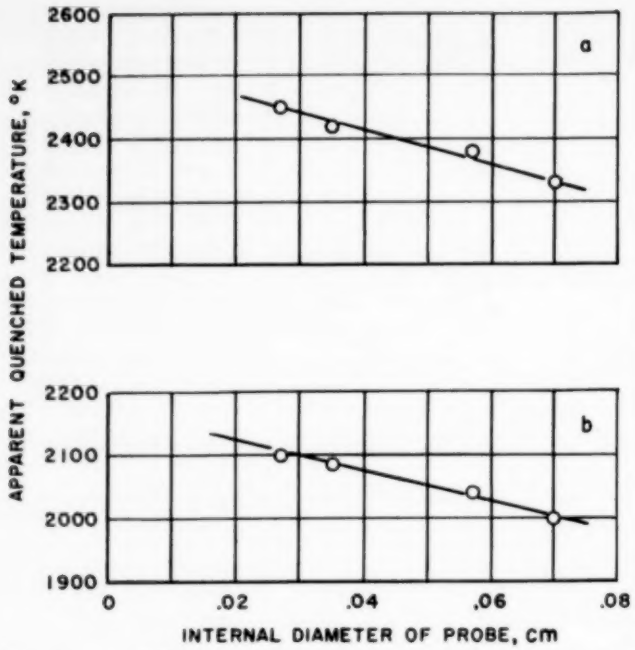

FIGURE 5. *Effect of size of probe on apparent quenched temperature.*

a, Based on CO/CO_2; b, based on H_2/H_2O.

The relation of apparent quenched temperature to the size of the probe is shown in figure 5. It is seen that, both for the data from the CO/CO_2 ratio and the H_2/H_2O ratio, apparent quenched temperature decreases linearly as the diameter of the probe increases. If we extrapolate to zero diameter, the apparent quenched temperature derived from the ratio CO/CO_2 is about 2,520° K, and from the ratio H_2/H_2O, about 2,175° K. These temperatures should be compared with a calculated flame temperature of 2,800° K. Apparently simple convective cooling in the probes is insufficient to preserve the gas sample unchanged, no matter how small the size of the probe. However, if the diameter of the probe is made very small, of the order of the mean free path of the gas molecules, it may be expected that processes other than convective cooling may begin to be effective.

3.2. Probe Materials

Probes with gas passages of stainless steel, platinum, and silver were tested. Effectiveness of quenching was little affected by the material of the probe. Values of the mole ratios of CO/CO_2 and H_2/H_2O obtained with probes of similar size but different materials were similar in magnitude.

Probes with stainless-steel gas passages proved particularly susceptible to corrosion and scaling, especially at the tip of the steel tube. It was suspected that interaction between the steel of the gas passage and the copper of the body was responsible. When the copper body was painted with an aluminum-silica heat-resistant paint, corrosion and scaling stopped. Before this paint was used, probes would clog by accumulation of scale in 10 min or less in some instances, and some probes were destroyed in less than 5 hr of use. After painting, one steel probe was used for 30 hr without any signs of deterioration. Silver probes proved undesirable because in each test the gas passage was constricted by formation of a loose black scale, possibly silver oxide. Platinum probes proved satisfactory; no failures were experienced with three different probes which were used for a total of 60 hr.

3.3. Probe Design

A probe with an internal diameter of 0.035 cm and a ratio of length of gas passage to diameter of 75 to 1 was built and tested. Results obtained with this probe were not significantly different from those obtained previously with a probe of the same diameter, but with a ratio of length of gas passage to diameter of 35 to 1. Therefore a ratio of lenght to diameter of about 35 to 1 is sufficient to cool the gas.

It was considered that conditions of flow in the entrance to the probe were among the factors that might influence the rate of cooling of the hot gas. In efforts to improve the mixing and rate of cooling, right-angle bends and 90° turns over a radius of 1/16 in. were introduced in the gas passages of two probes. Results obtained with a 0.027-cm probe having a 90° turn are illustrated in figure 3. Some improvement in performance over the straight probe is noted, but not enough to warrant adoption of this feature. Maximum apparent quenched temperature based on the carbon data was about 2,530°K. A 0.061-cm steel probe with a right-angle bend showed no improvement over the 0.057-cm steel probe. Maximum apparent quenched temperature was 2,350°K. Results obtained with the 0.061-cm probe are shown in figure 4.

An entrance nozzle, 0.060 cm in diameter, as illustrated in figure 1, was formed on the tip of a 0.035-cm platinum probe to prevent possible separation of flow and formation of a stagnant boundary layer. Results obtained with this probe are shown in figure 3. Some improvement was found over the plain 0.035-cm probe, but the gain was not outstanding. Maximum apparent quenched temperature was 2,470°K.

3.4. Effect of Temperature of Source of Exhaust Gas

The experimental work described previously was carried out on exhaust gas provided by burning a mixture of methane, air, and oxygen in mole proportions $CH_4:O_2:N_2=1:2:2$. Calculated adiabatic flame temperature was 2,800°K. The apparent quenched temperature based on the mole ratio CO/CO_2 was about 2,420°K when using a 0.035-cm platinum probe, and based on the mole ratio H_2/H_2O was about 2,090°K. It was decided to run a series of tests using flames of different temperatures as the gas sources to determine the variation of apparent quenched temperature with flame temperature. Mixtures with the following mole ratios were used to

provide flames with the indicated temperatures:

$CH_4:O_2=1:2$, 3,050°K;

$CH_4:O_2:N_2=1:2:4$, 2,600°K;

$CH_4:O_2:N_2=1:2:5.83$, 2,400°K; and

$CH_4:O_2:N_2=1:2:7.52$, 2,250°K.

All samples were analyzed gravimetrically using the combustion train. Sampling velocity ranged from 5,000 to 30,000 cm/sec, and the same 0.035-cm platinum probe was used.

In the case of the mixture $CH_4:O_2=1:2$, which was burned on a 0.315-cm nozzle, about 8 percent of the total burned gas, as determined from the tables of Hottel, Williams, and Satterfield, would remain after passage through the combustion train. This remainder if metered at the lowest indication of the flowmeter used would correspond to a sampling velocity of 45,000 cm/sec. As it was desired to collect samples at velocities lower than this for the purpose of comparison with previous work, the practice was adopted of bleeding air, dried and freed from CO_2, into the train after the probe but before the first absorption bottle. By holding a constant flow at the meter and varying the amount of air bled in, the flow in the probe could be changed and estimated.

At a sampling velocity of about 20,000 cm/sec, values of the mole ratio CO/CO_2 varied from 0.13 to 0.25 and the mole ratio H_2/H_2O varied from 0.0039 to 0.0085. Apparent quenched temperatures based on the carbon data ranged from 2,380° to 2,550°K, and based on hydrogen from 1,980° to 2,150°K. Average mole ratio CO/CO_2 was 0.240, which indicates an apparent quenched temperature of 2,530°K; average mole ratio H_2/H_2O was 0.007, which indicates an apparent quenched temperature of 2,090°K. The reason for this poor reproducibility is not known.

For the mixture $CH_4:O_2:N_2=1:2:4$, burned on the 0.475-cm nozzle, the apparent quenched temperature based on the CO/CO_2 ratio, 0.135, was 2,310°K, and that based on the H_2/H_2O ratio, 0.007 was 2,025°K.

For the mixture $CH_4:O_2:N_2=1:2:5.83$, also burned on the 0.475-cm nozzle, the apparent quenched temperature based on the CO/CO_2 mole ratio 0.110 was 2,250°K, and that based on the H_2/H_2O ratio 0.0043 was 1,920°K.

For the mixture $CH_4:O_2:N_2=1:2:7.52$, results were erratic and reproducibility was poor. For samples collected at the same conditions, mole ratio of CO/CO_2 ranged from 0.042 to 0.016 and mole ratio H_2/H_2O from 0.0005 to 0.006. Apparent quenched temperature based on CO/CO_2 ranged from 1,900° to 2,050° K and based on H_2/H_2O from 1,600° to 1,960° K. In these tests the gas velocity was 117 cm/sec at the port of the 1.27-cm nozzle, and the flame was irregular and unstable. The burner was mounted horizontally and the tip of the flame was displaced upward by convection currents. Under these conditions it was difficult to position the probe with respect to the flame. However, one group of tests that gave fairly consistent results indicated an apparent quenched temperature of 2,000° K based on carbon, and of 1,850° K based on hydrogen. The effects of convection were negligible when using burning mixtures with higher flame speeds in the smaller nozzles.

Apparent quenched temperatures based on hydrogen are uniformly lower than those based on carbon. This would indicate, perhaps, that reactions producing water are faster than those producing carbon dioxide and thus cannot be quenched as effectively.

In one series of tests, using the burning mixture $CH_4:O_2:N_2=1:2:2$, samples for volumetric analysis were collected simultaneously with the operation of the combustion train. Apparent quenched temperatures of the cooled gas were determined by the calculation of the mole ratios of CO/CO_2 and H_2/H_2O from both the gravimetric and volumetric analyses and by calculation of the equilibrium constants, from the volumetric analyses, for the reactions $CO_2 \rightleftharpoons CO+\frac{1}{2}O_2$ and $H_2O \rightleftharpoons H_2+\frac{1}{2}O_2$. Agreement was good for the carbon data. Temperatures derived from the equilibrium constants were about 40° C higher than those from the gravimetric mole ration CO/CO_2. For the hydrogen data, temperature based on the equilibrium constant was about 200° C higher than that based on the gravimetric mole ratio H_2/H_2O. Apparent quenched temperatures based on hydrogen data are always lower than those based on carbon regardless of the basis for determination of temperature.

Apparent quenched temperatures based on the gravimetric mole ratios are plotted against the calculted adiabatic flame temperatures in figure 6.

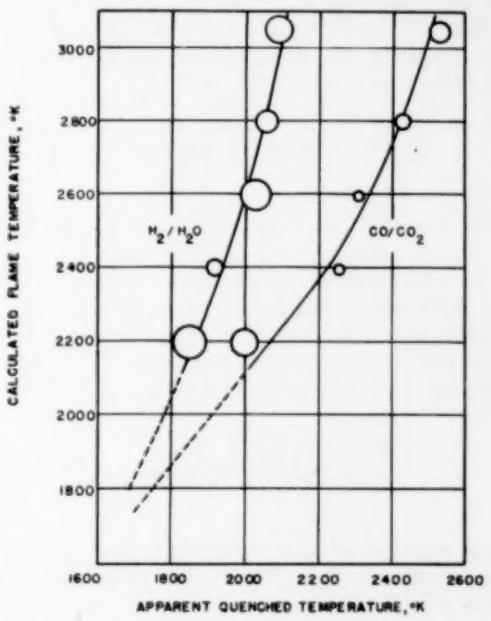

FIGURE 6. *Effect of temperature of gas source on apparent quenched temperature.*

Size of circles denote deviation.

The size of the points plotted represents the average deviation of the data. It is seen that the higher the temperature of the gas being sampled, the less effective is the quenching of reactions in a probe. For the gas mixture with a calculated flame temperature of 3,050° K, the apparent quenched temperature based on carbon data was 2,530° K, which is a drop of 520°; for the gas mixture with a calculated flame temperature of 2,250° K, the apparent quenched temperature based on carbon data was about 2,000° K, which is a drop of 200°. It is apparent also that as the temperature decreases, the difference between temperatures based on CO/CO_2 and H_2/H_2O also decreases. It appears that these two apparent quenched temperatures would become equal at about 1,600° K, and would coincide with the calculated flame temperature. Thus, apparently, a probe should function perfectly at this gas temperature and the composition of the cooled gas should be the same as the composition of the flame gas.

These experiments were made using various mixtures of fuel, oxygen, and nitrogen to change the temperature of the flame gas, and in doing so the composition as well as the temperature of the flame gas was changed. The effects observed may be due in part to this change of composition, but the magnitudes of such effects would be almost impossible to predict. A series of experiments designed to test the effects of concentration probably would give more reliable information, but time for this was not available, and this is left as a possibility for future endeavor. Effects of change of composition should be recognized, however, and an empirical correlation that includes the effects of composition on the sample may be of some value.

The complicated series of reactions that actually take place in the sample tube were simplified for the present purpose, in the case of reactions producing CO_2, to the reaction

$$2CO+O_2 \underset{k_2}{\overset{k_1}{\rightleftharpoons}} 2CO_2$$

and this was used as a basis of the empirical correlation. Correlations based on other reactions possibly could serve as well or better, but only a long series of experiments could indicate those that actually control over a wide range of conditions. Rates of reaction are designated by the letter k. The change of concentration (C) of CO_2 due to reaction is

$$\frac{dC_{CO_2}}{dt}=k_1C_{CO}^2C_{O_2}-k_2C_{CO_2}^2,$$

and the change of concentration due to change of sample temperature T in the tube at constant pressure p is

$$\frac{dC_{CO_2}}{dt}=-\frac{p_{CO_2}}{RT^2}\frac{dT}{dt}$$

from differentiation of the gas law, $p_{CO_2}=C_{CO_2}RT$. The total change is the sum of the individual changes, and this leads to

$$\frac{dp_{CO_2}}{p_{CO_2}}=\frac{k_1}{(RT)^2}\left[\frac{p_{CO}^2p_{O_2}}{p_{CO_2}}-\frac{p_{CO_2}}{K_p}\right]dt$$

after expressing concentration in terms of partial pressure p and using for this reaction the relations $K_c=K_pRT=k_1/k_2$. K is the equilibrium constant, expressed in terms of concentration or partial pressure. The rate of reaction is related to temperature by the empirical Arrhenius equation

$$k\sim e^{-\frac{A}{RT}}$$

where A is an apparent energy of activation. The time rate of change of gas temperature in small tubes under conditions of viscous flow is apparently nearly proportional to T^2 [17], and if this relation and the Arrhenius equation are substituted in the equation for dp/p, we get

$$\frac{dp_{CO_2}}{p_{CO_2}}\sim\frac{e^{-\frac{A}{RT}}}{(RT)^2}\left[\frac{p_{CO}^2p_{O_2}}{p_{CO_2}}-\frac{p_{CO_2}}{K_p}\right]\frac{dT}{T^2}.$$

This may be integrated to

$$\log\frac{p_2}{p_1}\sim\text{Eff}\left[\frac{p_{CO}^2p_{O_2}}{p_{CO_2}}-\frac{p_{CO_2}}{K_p}\right]\left[e^{-\frac{A}{RT}}\frac{A^2}{(RT)^2}+2\frac{A}{RT}+2\right]_{T_1}^{T_2},$$

where the term containing the partial pressures is an effective value over the limits of integration. Subscripts 1 and 2 refer to conditions before and after sampling, respectively. This was used as a basis for the correlation of the experimental data.

The value of A/R was arbitrarily chosen to be 20,000, and this makes $A^2/(RT)^2\sim A/RT+2$, and hence the latter term was neglected. Also, if the final temperature T_2 where reaction stops is about 1,600° K, then the terms containing T_2 are negligible with respect to those containing T_1. As a last simplification, the term p_{CO_2}/K_p was omitted, and initial values of partial pressures (from table 1) in the flame gas were used. These reduce the relation to

$$\log\frac{p_2}{p_1}\sim\text{eff}\left[\frac{p_{CO}^2p_{O_2}}{p_{CO_2}}\right]_1\left[\frac{e^{-\frac{20{,}000}{T_1}}}{T_1^2}\right],$$

and it was found that the relation is linear when the partial pressure term is raised to the 0.1 power. This is plotted in figure 7. It must be emphasized that the relative effects of concentration and temperature in this correlation are only estimated, and therefore the correlation must be used with caution in other situations.

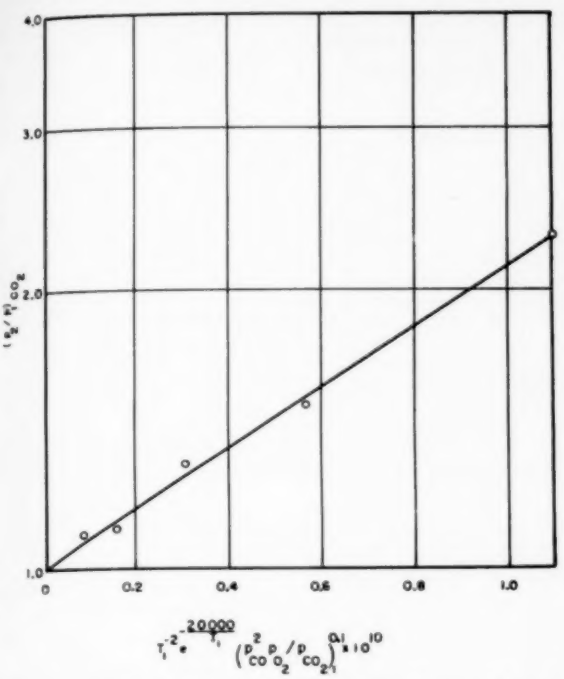

FIGURE 7. *Effect of initial conditions on change of carbon dioxide during sampling.*

p=atm; T=°K.

4. Conclusions

Apparent quenched temperatures derived from the observed compositions are always lower than the flame temperatures; this difference amounts to 500° when the flame is at 3,050° K. The difference between apparent quenched temperature and flame temperature becomes less as the flame temperature decreases. Below 2,250° K, the differences are small and composition of the gas sample is close to that of the flame gas.

Rate of sampling exerts little influence on the composition of samples, providing there are no fixed gradients of temperature and composition near the point of sampling.

Design of probes made little difference in the composition of the samples. A ratio of length to diameter of the gas passage of the probe of 35:1 is adequate for cooling. Apparent quenched temperature is affected by the size of the probe, decreasing as the diameter increases.

Effective quenching of reactions in probes in the range of sizes used in this investigation probably requires other means in addition to water-cooling. Sudden expansion to low pressure or dilution with cold inert gas might help to preserve the original composition.

5. References

[1] F. Haber and F. Richardt, Z. anorg. Chem. **38,** 5 (1904).
[2] F. Haber and F. Richardt, J. Gasbeleucht. **47,** 809 (1904).
[3] W. Allner, J. Gasbeleucht. **48,** 1035 (1905).
[4] F. Haber, Z. Elektrochem. **14,** 571 (1908).
[5] B. S. Lacy, Z. physik. Chem. **64,** 633 (1908).
[6] F. Haber and R. Le Rossignol, Z. physik. Chem. **66,** 181 (1908).
[7] F. Haber and H. J. Hodsman, Z. physik. Chem. **67,** 343 (1909).
[8] F. Haber, Z. physik. Chem. **68,** 727 (1909).
[9] F. Haber and J. E. Coates, Z. physik. Chem. **69,** 337 (1909).
[10] F. E. Carter, J. Gasbeleucht. **56,** 545 (1913).
[11] F. Hiller, Z. physik. Chem. **81,** 591 (1913).
[12] A. Reis, Z. physik. Chem. **88,** 513 (1914).
[13] N. Bubnoff, Z. physik. Chem. **88,** 641 (1914).
[14] L. Ubbelohde and O. Dommer, J. Gasbeleucht. **57,** 733 (1914).
[15] L. Ubbehohde and E. Koelliker, J. Gasbeleucht. **59,** 65 (1916).
[16] K. Bunte, H. Bruckner, and G. Choulat, Gas u. Wasserfach **82,** 763 (1939).
[17] P. E. Erbe, J. F. Grey, and J. L. Beal, Project Squid Tech. Mem. CAL–8 (Sept. 1, 1948).
[18] E. W. Hough, J. F. Valle-Riestra, and B. H. Sage, Jet Propulsion Laboratory, Calif. Inst. Tech. Progr. Rept. 9–40 (Aug. 12, 1944).
[19] H. C. Hottel, G. C. Williams, and C. N. Satterfield, Thermodynamic charts for combustion processes (John Wiley & Sons, Inc., New York, N. Y., 1949).
[20] B. Lewis and G. von Elbe, Combustion, flames and explosions of gases, (a) p. 690 and 766, (b) p. 258 (Academic Press, New York, N. Y., 1951).

WASHINGTON, July 5, 1957.

Journal of Research of the National Bureau of Standards Vol. 60, No. 1, January 1958 Research Paper 2819

Pyrolysis of Polyamides*

Sidney Straus and Leo A. Wall

Thermal decompositions of various nylon samples having different molecular weights and composition were investigated by several procedures: (1) The rate of volatilization at temperatures between 310° and 380° C; (2) the analysis of the volatile products by mass spectrometry; and (3) a direct measurement of volatilizing material obtained by carrying out the pyrolysis within the ionization chamber of a mass spectrometer.

Activation energies based on the rates of volatilization for the various samples varied from 15 to 42 kilocalories. The rate behavior, i. e., the observation of maxima in the rate-versus-conversion plots, is close to that given by theory for random decomposition. The different activation energies appear to be the result of a hydrolytic mechanism which is sensitive to trace polymerization catalysts. Increases in rates were obtained when sulfuric and phosphoric acids were added to nylon. The fluctuations found in activation energies, and the production of CO_2 indicates that a hydrolytic decomposition mechanism may be contributing to the over-all process. It appears evident that, compared to a pure hydrocarbon chain, the polyamides are much more susceptible to thermal decomposition.

1. Introduction

Although there has been considerable work done on the thermal decomposition of nylon and related substances [1 to 4],[1] relatively little attention has been paid to the kinetics of the process. In previous studies, product identification and structural changes in the polymer comprised the major portion of the work.

The purpose of this present investigation was first to establish a better understanding of the thermal decomposition of linear high polymers. Prior work [5] on linear and branched polyethylene showed a striking difference between rates of volatilization behavior for linear and for branched polyethylene. This difference has not yet been quantitatively accounted for in terms of any mechanism hitherto treated [6]. It was, therefore, considered desirable to investigate some linear polymers that from previous product-analysis were suspected of decomposing more or less randomly. A second purpose was to establish the energetics so that a comparison could be made with polyethylene and the thermal stability of the peptide linkage determined.

The effects on the process of moisture, traces of polymerization catalyst, i. e., acids, a free radical inhibitor, and surface area were also studied to some degree in order to cast further light on the details of the mechanism of decomposition.

2. Materials

Nylon samples 4406, 4408, and 4409, used in the present work for rate of volatilization determinations, have been described previously [3]. The first two were made from a mixture of hexamethylenediamine-adipic acid and caprolactam, whereas the last one contains, in addition, some hexamethylenediamine-sebacic acid. The other nylons under study were nylon-6 samples made from caprolactam. They were prepared by the National Aniline Co., Hopewell, Va.; one had a molecular weight of about 30,000 and the other about 60,000, as determined from viscosity measurements in formic acid. The relationship between the viscosity average of nylon in formic acid and the number average has been reported [7].

The Dacron sample used, a product of the E. I. du Pont de Nemours & Co., Inc., was in the form of bright threads with no delustrant added. The polyester had a 70-34 denier-filament structure.

3. Apparatus and Experimental Procedure

The experimental work consisted of (1) measuring rates of volatilization of the polymer in vacuum, and (2) identification of the various products of decomposition with the use of a mass spectrometer.

The apparatus and experimental procedure used in determining the rates of thermal degradation have been described previously [8, 9]. In brief, a 5- to 6-mg sample is placed in a glass crucible and suspended from a tungsten helical spring balance. It was determined that a Pyrex glass crucible gave a more accurate temperature measurement than a platinum crucible when the sample did not melt and flow freely on decomposition. This sample and weighing mechanism is enclosed in a Pyrex housing that could be evacuated to better than 10^{-5} mm of Hg. A preheated electric furnace is then placed in position around the glass portion containing the crucible in suspension. The furnace is controlled by means of an electronic thermostat which is able to hold the temperature constant to about $\pm 0.2°$ C.

There is a crossline on the tungsten spring that is observed during pyrolysis, and weight losses could be recorded at various time intervals. These data are then plotted as rate of volatilization in percent of original sample per minute versus percent volatilized. These curves exhibited very definite maxima in most cases. Activation energies were calculated from these maxima at 3 or 4 different temperatures.

The apparatus used to collect decomposition

* Presented in part before the 130th Meeting of the American Chemical Society, Atlantic City, N. J., Sept. 16, 1957.

[1] Figures in brackets indicate the literature references at the end of this paper.

products in the pyrolysis study is also described fully in a previous paper [10]. In brief, a 20 to 40-mg sample is placed in a small Pyrex tube enclosed in a larger glass housing. The system is evacuated and preheated at about 110° C to remove adsorbed gases and moisture. A tube furnace, preheated to the temperature of pyrolysis, is placed in position around the sample. Approximately 5 min are required for the sample to reach the temperature of pyrolysis and then the sample is heated for 30 min at 400° C. The heater is then removed from around the sample. During pyrolysis, some of the volatiles are condensed with liquid nitrogen.

There are four fractions collected:

(1) *Residue*, left in the small Pyrex tube. A brown crust.

(2) *Wax-like fraction*, volatile at the temperature of pyrolysis but not at room temperature. This tan deposit collects immediately outside of the heater in the apparatus. It is soluble in warm ethanol.

(3) *"Condensed" fraction*, volatile at room temperature. Collected by means of liquid nitrogen and sealed for mass spectrometer analysis.

The weights of fractions 1, 2, and 3 are measured directly on a semimicro balance.

(4) *Gas fraction*, volatile gases not condensable at liquid nitrogen temperature. Collected in a gas sample holder, and also analyzed in the mass spectrometer. The weight of this fraction is calculated from the volume, pressure, and composition of the gas.

4. Results

The rate data obtained in the volatilization of nylon samples 4406, 4408, and 4409 are shown in figures 1, 2, and 3. They all show maxima at about 30- to 40-percent volatilization. The temperatures in all three cases were at 310°, 315°, and 320° C. For nylon samples 4406 and 4408, the maxima in the curves are not too far apart for the three temperatures. This indicates a rather low activation energy.

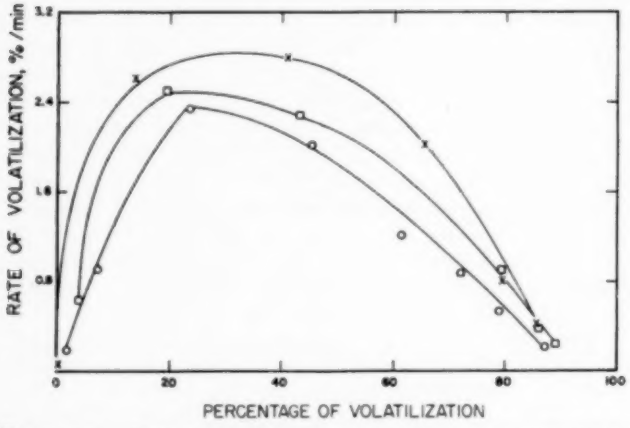

FIGURE 1. *Rate of volatilization versus percent volatilized for nylon 66–6, sample 4406.*

○, 310° C; □, 315° C; and ×, 320° C.

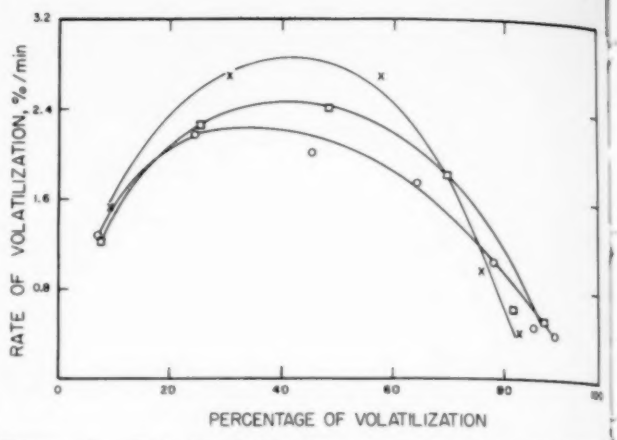

FIGURE 2. *Rate of volatilization versus percent volatilized for nylon 66–6, sample 4408.*

○, 310° C; □, 315° C; and ×, 320° C.

For nylon sample 4409, the rates at the maxima are further apart.

In figures 4 and 5, the rate of volatilization data were obtained on different molecular weights of the nylon-6 sample. The temperatures in all cases are higher than that used for the previous nylon copolymers. The lowest temperature is 340° C and the highest 380° C. Both figures show similar maxima curves, and the maximum volatilization rates are between 20 and 40 percent.

Finally, in figure 6, rate curves have been plotted for Dacron, a polyester of terephthalic acid and ethylene glycol. Four curves at temperatures 350°, 355°, 365°, and 370° C are shown; these have maxima somewhat different from the caprolactams with the maxima occurring at under 20-percent volatilization.

In order to determine the effect of catalysts on the volatilization rate, several catalysts that are commonly used for the polymerization of polyamides were added to the 60,000 molecular weight sample of the nylon-6 polymer. The effect of surface area on

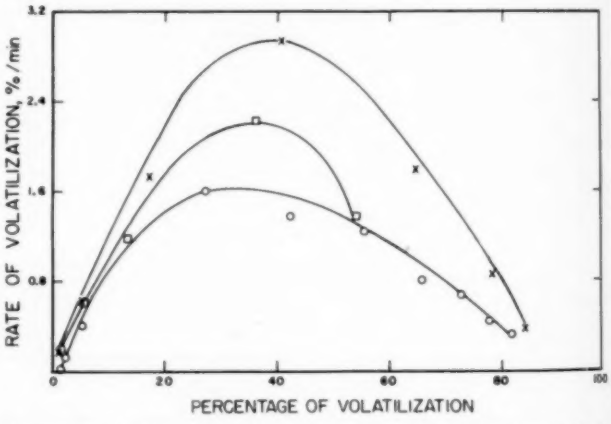

FIGURE 3. *Rate of volatilization versus percent volatilized for nylon 66–610–6, sample 4409.*

○, 310° C; □, 315° C; and ×, 320° C.

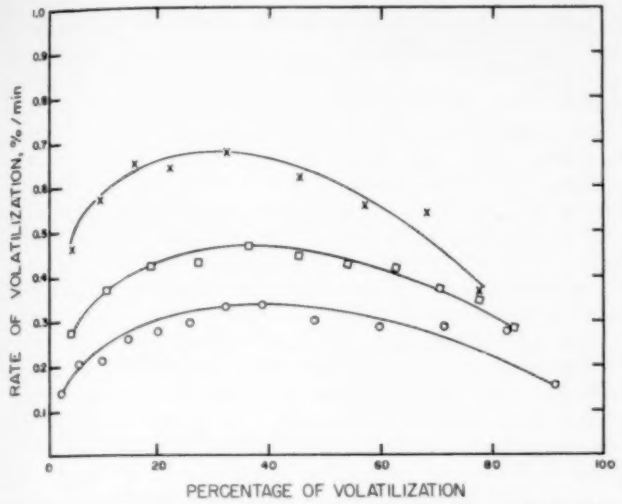

FIGURE 4. *Rate of volatilization versus percent volatilized for nylon–6, 30,000 molecular weight.*

○, 345° C; □, 355° C; and ×, 365° C.

degradation was also studied. The results are shown in the curves in figure 7.

Curve A is the normal curve for this polymer at 345° C. To obtain curve B, double the amount of sample, 10 mg instead of 5 mg, was used. The small white crystals formed a somewhat thicker layer, but when the crystals began to degrade they flattened out to some extent. The crystals did not actually melt but rather flowed slightly. In using double the amount of sample, the rate of volatilization is slower at the beginning, but at about 25-percent volatilization, the two curves become one. This would indicate some surface effect.

Curve C indicates the result obtained on a thicker sample. A nylon sample was dissolved in a 90-percent formic acid solution, a portion transferred to a weighing bottle, and the viscous solution evacuated

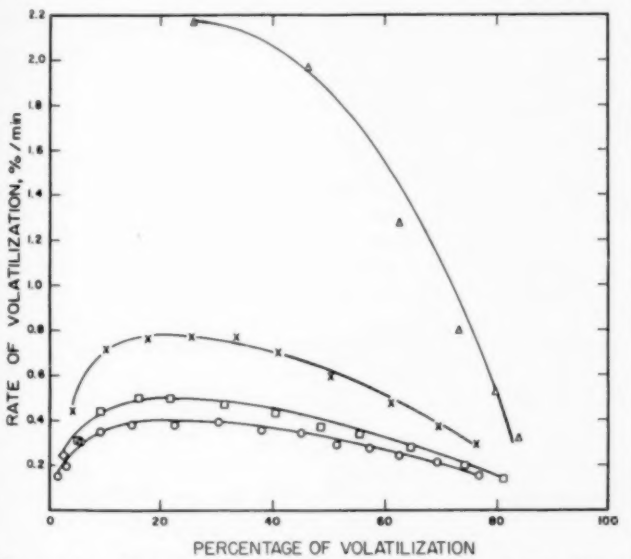

FIGURE 5. *Rate of volatilization versus percent volatilized for nylon–6, 60,000 molecular weight.*

○, 340° C; □, 345° C; ×, 355° C; and △, 380° C.

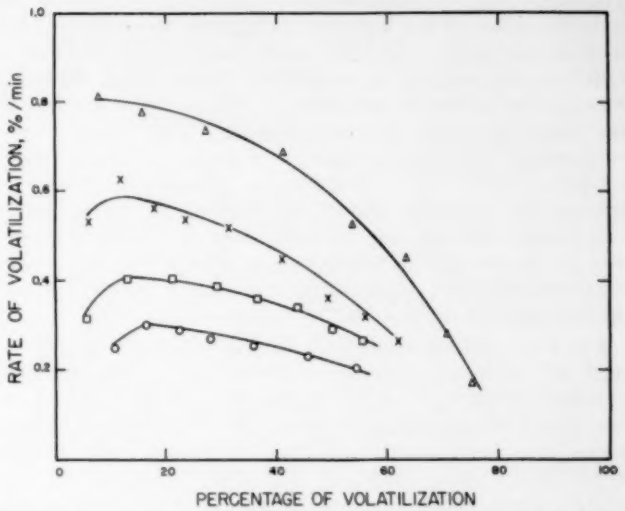

FIGURE 6. *Rate of volatilization versus percent volatilized for Dacron.*

○, 350° C; □, 355° C; ×, 365° C; and △, 370° C.

for several hours. A small portion was then placed in a pyrolysis apparatus and heated to 110° C for 1 hr in a vacuum of about 10^{-5} to 10^{-6} mm of Hg. The heating was continued until constant weight was obtained. The resulting particle mass, free of the formic acid, was approximately 2-mm thick and about 3 to 4 mm in length. The original sample used in a rate experiment consisted of approximately 25 to 30 crystals, each piece covering a smaller area and less than one-half as thick as the sample used to obtain curve C. As indicated from curve C, the maximum rate of thermal decomposition of the thicker particle mass was reduced by about one-half.

The addition of 5 percent of H_2SO_4 prior to

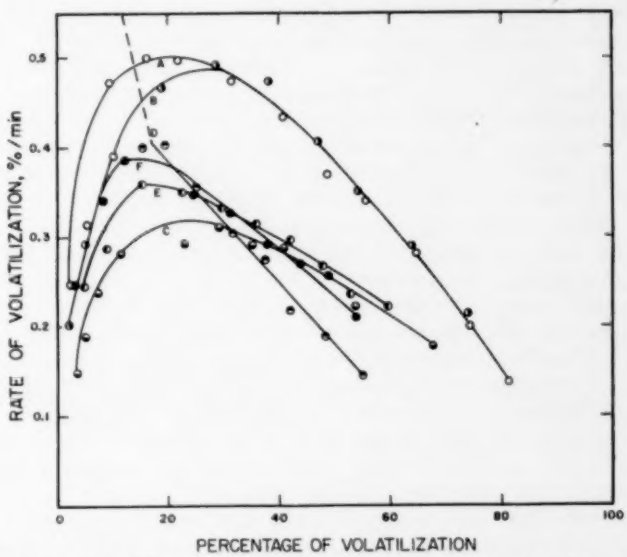

FIGURE 7. *Effect of trace substances on pyrolysis of nylon–6, 60,000 molecular weight.*

Temperature=345° C.

A–○, Original sample; B–◑, double amount of sample; C–◒, single thick specimen, specially prepared; D–◓, plus 5.0% H_2SO_4; E–◐, plus 1.0% 1,5-diaminoanthraquinone; F–●, plus 1.0% H_3PO_4; temperature=325° C.

pyrolysis had a considerable effect on the rate of volatilization of the nylon-6 sample at first, as can be seen in curve D. About 3 or 4 drops of dilute H_2SO_4 solution was added to a weighed amount of sample, enough to cover it completely; no more than 5 mg are used in rate determinations. The water was evaporated by heating gently in an oven to constant weight. After the furnace is placed in position around the sample, about 15 percent of the sample volatilizes during the 15 min that it takes for the sample to reach the temperature of the furnace. In other words, the degradation proceeds rapidly, even prior to attaining the 345° C temperature level.

Curve F shows the effect of the addition of 1 percent of orthophosphoric acid to the nylon before pyrolyzing at 325° C. As in the previous case, a few drops of acid solution were added to the polymer, which was then dried. At 325° C the maximum rate would have been about 0.125 in the absence of the acid. Thus, the presence of the acid increases the maximum rate by a factor of three.

To determine whether traces of acid catalysts used in the preparation of the polymer were also catalyzing its thermal decomposition, the original sample was leeched out. This was accomplished by soaking a small amount of nylon-6 sample in distilled H_2O for 5 days. The water was then decanted and fresh water added for 5 more days. At the end of this period, the water was removed and the sample preheated to 120° to 130° C for 2 hr in a vacuum of about 10^{-5} mm of Hg to constant weight.

The dried sample was treated in a rate experiment at 355° C, similar to the previous experiment at the same temperature. The maximum rate was reduced by a little more than one-half in the experiment. Apparently the leeching-out process with water is effective in increasing the thermal stability.

Finally, in curve E, we see the effect of the addition of 1 percent of 1,5-diaminoanthraquinone, an inhibitor, to the sample prior to pyrolysis. This, too, was added in the form of a water solution until the additive was well dispersed throughout the sample. The rate of volatilization of the nylon is slowed from 0.5 percent per minute at its maximum to about 0.35 percent per minute at 345° C, which is about a 6° C decrease for equivalent volatilization rate.

Prior to the decomposition of the nylons to obtain the volatile products, each of the various samples were preheated to 110° C for 1 hr in a vacuum of better than 10^{-5} mm of Hg. They each lost a small amount of volatile matter which was most probably H_2O. The losses were in the order of the following percentages: Nylon sample 4406—2.3 percent; sample 4408—2.5 percent; sample 4409—2.2 percent; nylon-6 (60,000 mol wt)—1.3 percent; nylon-6 (30,000 mol wt)—0.6 percent; and polypyrrolidone—4.8 percent. These percentages were subtracted from the weights of the original samples prior to calculations, both in the rate work and in the collection of the decomposition products. (Polypyrrolidone is a nylon-4 sample of low molecular weight having the following repeating unit [—NH-$(CH_2)_3$CO—].)

The mass spectrometer analysis of the fraction volatile at room temperature is shown in table 1, in mole percent. The amount of this fraction in percent of total pyrolyzed part is generally small for nylon breakdown and is shown on the bottom line. The analyses of the degradation products of nylon samples 4407 and 4409, shown in the first two columns, were determined about 5 yr ago at the Bureau in a somewhat similar pyrolysis apparatus [3]. Nylon sample 4407 is the same as the 4408 sample used in the present work for rate determinations. The compositions were the same; only the thickness of the samples was slightly different. This would make no difference in product determinations.

Previously [3] the water obtained in the mass spectrometer analysis was excluded from the volatile products. Water is unlikely as a product of the thermal decomposition unless hydroperoxides have been formed in the material; however, it is concluded in this work that it is very tightly adsorbed by nylons. Consequently, the previous data [3] have been recalculated to include water since it appears to have a significant effect on the rate of decomposition.

In nylon sample 4407 the major breakdown products in the fraction volatile at room temperature are CO_2 and H_2O in approximately equal amounts. The other constituents are small amounts of hydrocarbons, saturated, unsaturated, and cyclic compounds. Somewhat outstanding is the yield of cyclopentanone as compared to the other hydrocarbons. This is most probably a breakdown product of the adipic acid constituent. Hopff [11] also detected cyclopentanone on nylon decomposition.

TABLE 1. *Mass spectrometer analysis of fractions volatile at room temperature*

Components	Nylon 4407	Nylon 4409	Nylon-6, mol wt		Nylon-4
			30,000	60,000	
	Mole %	*Mole %*	*Mole %*	*Mole %*	*Mole %*
CO_2	43.7	92.3	55.8	59.4	64.3
H_2O	47.8	4.5	35.4	35.6	16.3
Ethylene	0.4	0.5	0.4	0.3	.....
Ethane	.3	.5	.....	.2	.....
Propadiene	.....	.....	.....	.1	.....
Propylene	.5	.....	.4	.7	.....
Propane	.2	.....	.....	.....	.....
Butadiene	.....	.....	.2	.4	.....
Butene	.2	.....	.2	.6	.....
Butane	.1	.....	.3	.5	.....
Isoprene	.....	.....	.3	.2	.....
Cyclopentene	.1	.....	.....	.....	.....
Cyclopentadiene	.....	.1	.....	.....	.....
Cyclopentanone	5.8	1.1	.....	.....	.....
Pentadiene	0.1	0.2	.....	.....	.....
Pentene	.2	.2	.1	.3	.....
Pentane	.....	.1	.1	.1	.....
Benzene	.4	.2	5.8	.1	13.3
Cyclohexene	.1	.1	.....	.....	.....
Hexadiene	.1	.2	0.3	.7	6.1
Hexene	.....	.....	.4	.2	.....
Hexane	.....	.....	.1	.2	.....
Toluene	.....	.....	.1	.1	.....
Dimethylbenzene	.....	.....	.....	.1	.....
Heptadiene	.....	.....	.1	.2	.....
Total	100.0	100.0	100.0	100.0	100.0
Fraction of pyrolyzed material, %	5	5	5	10	1 to 2

Nylon sample 4409 has considerably less H_2O in this fraction and more CO_2. The yield of cyclopentanone is also lower than in sample 4407. The former has the sebacic acid salt as part of its makeup in addition to the adipic acid salt, and this would certainly have the effect of decreasing cyclopentanone formation. The different amounts of water found in the 4407 and 4409 samples may be related to the lower peptide-link content of the 4409 material compared to the 4407.

Columns 3 and 4 indicate the mass spectra patterns of the two caprolactams of different molecular weight. The breakdown of the light volatile fractions are quite similar, mostly yielding CO_2 and H_2O. The high benzene figure in the 30,000-molecular weight nylon is most probably background in the mass spectrometer. The yield of monomer fraction for the nylon-4 sample is quite small, only 1 to 2 percent of the total volatilized part. The H_2O and CO_2 findings are actually very small.

The gas sample collected showed small amounts of H_2, CH_4, and CO. It was calculated that this fraction was less than 0.1 percent of the total volatilized part.

The heavier volatiles, which comprised approximately 95 percent of the total volatiles, were weighed after recovery from a warm ethanol solution. No attempt was made to analyze this waxlike fraction.

The products of decomposition were determined by mass spectrometry by another technique [12]. Small samples of nylons 4406, 4408, and 4409 were placed in a tube furnace and the degradation products evaporated directly into the ionization chamber of a Nier-type mass spectrometer. The samples began to degrade at about 240° C with the evolution of gases. Degradation was complete at 400° C.

Mass spectra were obtained from mass 28 to 452 in nylon sample 4406 and from 28 to 360, in nylons 4408 and 4409. The mass spectra were complicated with no recurring patterns. There were indications of cyclopentanone formation and also alkyl amines. The hexamethylenediamine-adipic acid salt has a molecular weight of 226, and this may explain a relatively large observed peak at 226. The molecular weight of the caprolactam is 113, and this also gave a relatively large peak. The 452 peak in nylon 4406 may be the dimer of the adipic acid salt. Quantitative data could not be accurately obtained for the actual amounts of the various molecules. In general, the pyrolysis products were of relatively low mass containing one basic unit or less. This is rather small compared with other polymers [13] such as polymethylene, polypropylene, polyisobutylene, etc., which have average molecular weights over 500 in the heavy waxlike fraction.

5. Discussion

On the basis of the rate curves and the product analysis, a random or nearly random type of breakdown is indicated for the nylon decomposition. There are really no outstanding individual volatile compounds with the possible exception of CO_2, but as the polymer decomposes, a large number of different compounds are produced.

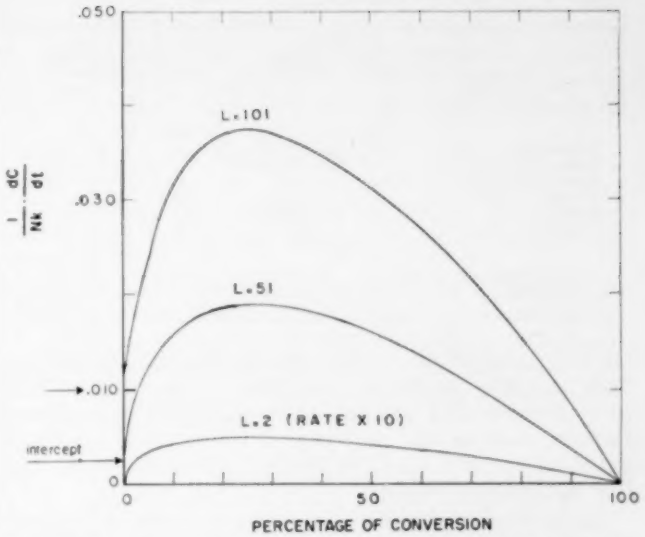

FIGURE 8. *Theoretical curves for random decomposition showing effect of critical size for evaporation, L, on rate of volatilization* [14].

Arrows indicate initial rates.

A set of typical theoretical curves for a decomposition in which scissions can occur with equal probability at any link in the chain is shown in figure 8 [14]. These curves show the effect of size of the volatilizing fragments on the rate of volatilization, L being the number of basic units in the smallest chain that does not evaporate without degradation. Thus, L–1 is the D. P. of the largest fragment that can vaporize without further decomposition. In these curves, the maximum occurs at about 26-percent conversion, at which point $dC/dt \simeq Lk/e$, where k is the over-all rate constant for the random decomposition, and e is the base of the natural logarithms, 2.7. The rate at zero time, i. e., the intercept at zero conversion in figure 8, is given by $dC/dt \simeq L^2k/N$. These relationships hold only when the initial degree of polymerization, N, is much larger than L. This condition is always fulfilled by the materials herein discussed. The curves in figure 8 show that the maximum rates are the more dependable quantities to use for the estimation of the rate constants because experimental initial rates would require very precise measurement at less than 1-percent conversion to be of any significance. Unfortunately, quantitative utilization of the maximum values also requires a determination of L. Nevertheless, an Arrhenius plot of the maximum rates should give dependable values for the activation energy.

The activation energies for the polymers studied are listed in table 2. The most striking aspect of the data is the large variation in the energies for the nylons. The low value of 14 kcal may be at least partially due to the low molecular weight of the first two materials. If the vaporization, and not the decomposition, process is rate determining,

TABLE 2. *Activation energies based on rates of decomposition*

Polymer	Molecular weight	Activation energy	Preexponential factor
		kcal	$L=5$
Nylon 4406	Low<10,000	14	3.6×10
Nylon 4408	Low<10,000	14	3.6×10
Nylon 4409	13,000	42	5.8×10^{11}
Nylon-6	30,000	27	1.03×10^{5}
Nylon-6	60,000	34	4.1×10^{7}
Dacron	~10^{5}	38	5.1×10^{8}
			$L=72$
Polymethylene (linear polyethylene)	5×10^{5}	68	1.9×10^{16}

then a value of 14 kcal is reasonable for the activation energy, provided the volatilizing compounds have a molecular weight in the region of 200. Other factors such as the presence of some trace catalysts may, of course, be a contributing influence to the low activation energy.

In figure 7, it is seen that various acids of the type often used in the preparation of polyamides and polyesters produce considerable effect on the rate of decomposition. It is also seen in table 1 that the amount of water found in the pyrolysis products is least for the material that gave the highest activation energy. These observations suggest that the decomposition is complicated by an ionic mechanism, the contribution of which to the overall decomposition is dependent on the amounts of trace catalysts, i. e., acid and adsorbed water. Ionic mechanisms are fairly rare in degradation processes; however, they have been suggested by other workers in the case of polyvinyl ethers [15]. The effect of the diaminoanthraquinone suggests free-radical intermediates. Evaporation or dehydration of both the catalysts and traces of water, as well as the inhibitor, at the pyrolytic temperature may explain the smallness of the observed effects. At these temperatures it would be expected that free-radical mechanisms are most important. It is of importance and somewhat surprising that lingering traces of moisture and acid appear to have pronounced effects, presumably by inducing, to a relatively small degree, ionic processes in the overall decomposition mechanism.

In general, the nylon materials showed a somewhat erratic behavior. From the data so far obtained (see table 2) the highest value of the activation energies, 42 kcal, is considered to be most representative for a free-radical mechanism of thermal decomposition.

The value of 38 kcal for the one sample of Dacron studied is seen to be quite close to the higher nylon values. Comparison with the result for polyethylene shows that the peptide and the ester linkage introduce, at least in the structures studied, a very large degree of thermal instability.

The free-radical chain mechanism for the decomposition of polyethylene [5] is most likely of the following type:

$$-CH_2-CH_2-CH_2-CH_2- \xrightarrow{k_1} 2-CH_2CH_2\cdot \qquad \text{(Initiation)}$$

$$-CH_2-CH_2\cdot + -CH_2-CH_2-CH_2-CH_2- \xrightarrow{k_3} -CH_2CH_3 + -CH=CH_2 + -CH_2CH_2\cdot \qquad \text{(Transfer)}$$

$$2-CH_2CH_2\cdot \xrightarrow{k_4} -CH=CH_2 + -CH_2CH_3 \qquad \text{(Termination)}$$

The step:

$$-CH_2CH_2CH_2CH_2\cdot \xrightarrow{k_2} -CH_2CH_2\cdot + CH_2=CH_2 \qquad \text{(Propagation)}$$

in polyethylene does not compete favorably with the transfer, k_3 [5]. Thus, the k_3 step, which is a composite of two elementary processes combined for the purpose of mathematical treatment [14, 16] of polymer decomposition, is the principal chain-carrying process. It would probably be more correct and descriptive to call this step, "propagation by transfer." The over-all constant for random decomposition by the above mechanisms is given by:

$$k=k_1+k_3R\approx k_3R=k_3\,(I/k_4)^{1/2}$$

where R is the total radical concentration and I is the rate of initiation of active centers. The term I includes k_1, a concentration term, and statistical factors depending on the exact mode of initiation. A considerable amount of further research would be required to determine the exact mode of initiation for the polymers discussed here. However, consideration of the structures shown below

Polyamides (nylon)

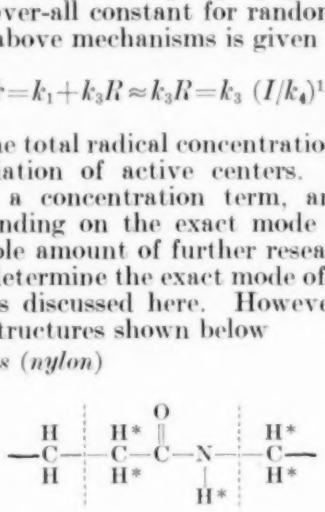

Polyester (Dacron)

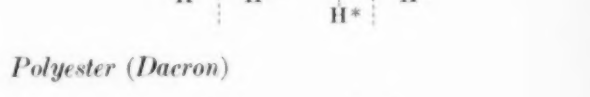

suggests that initiation by homolytic scission at the linkages indicated by the vertical dashed lines is more probable than at a carbon-carbon bond in polyethylene. The C—N bond is known to be weaker than a C—C bond, the strength of the former being about 66 kcal, whereas the latter is about 80 kcal, depending, of course, on the structure in which it is located. The C—N bond alpha to the carbonyl is certainly stronger than that beta to the carbonyl. Hydrolytic scission of the peptide links, which our experiments indicate, would account for both the amines reported in the pyrolysis of polyamides [1, 2] and the CO_2 found by all workers in the field, the latter arising from the decomposition of the acid groups produced by hydrolytic scission.

The starred hydrogen atoms are more likely to be abstracted by a radical and hence facilitate transfer in polymers with the above structures, again compared to a linear paraffin material. The products of the pyrolyses, in general, support the above hypotheses, although the products listed in table 1 certainly suggest also that decomposition does not proceed exclusively at the points depicted in the structures by a free-radical mechanism.

In polyethylene, approximately 98 percent of the products of pyrolysis was in the form of a high-boiling wax with an average molecular weight near 700. In the polyamides, about 90 to 95 percent of the products was nonvolatile, but of much lower average molecular weight. Mass spectrometer studies of polyamide pyrolysis indicate that maximum size of the fragment is about 400 mass units. A rough estimate of the critical size for evaporation, L, is then about 5 caprolactam units. In table 2, preexponential factors are given. Notwithstanding the difference in L values between the polyethylene and other materials, it is seen that these values are hardly constant for the polyamides and are very much lower.

No such behavior has been found in pyrolysis studies of addition polymers. The low and fluctuating values suggest the presence of a concentration factor, probably of water or acid, in the preexponential factors. With $L=5$, the rate constants for the nylons and Dacron refer to the apparent breaking of peptide or polyester bonds, while with $L=72$, the constant for polyethylene refers to the breaking of any C—C bond in the chain.

6. Conclusions

The pyrolysis of polyamides shows a behavior incompatible with a pure free-radical mechanism. It seems evident that even at the pyrolytic temperatures of 300° to 400° C and with prior exhaustive drying at 100° to 130° C in a vacuum, enough water remains to provide a complicating effect in the decomposition reaction. The hypothesis that traces of water and polymerization catalysts influence the pyrolysis provides the simplest explanation of the more puzzling aspects of polyamide decomposition, including the production of appreciable quantities of CO_2.

In the case of the 60,000 molecular weight nylon-6 material (see table 1), the amount of CO_2 produced would imply the hydrolytic scission of 15 percent of the original peptide bonds. This implies the presence of about 2 percent of water at the pyrolysis temperature, presumably tightly bound to the peptide group, and that the decompositions studied here were about half hydrolytic and half free radical.

It is also clear that the over-all process for nylon is typical of a random decomposition of linear chains similar to that for linear polyethylene. The Dacron rate behavior, however, does not exhibit as decisive a result.

The activation energies for nylon and Dacron are probably considerably lower than those to be expected if the suggested hydrolytic process was completely suppressed or eliminated. In any case, the activation energies would be unlikely to approach that for polyethylene.

The authors express their appreciation to F. L. Mohler and Paul Bradt, Mass Spectrometry Section, National Bureau of Standards, for making available their results on nylon decomposition in the mass spectrometer; to A. J. Sweet of the National Aniline Division, Allied Chemical and Dye Corp., Hopewell, Va., for samples of nylon-6; and to George B. Walker of Arthur D. Little, Inc., for the nylon-4 sample.

7. References

[1] I. Goodman, J. Polymer Sci. **13,** 175 (1954).
[2] I. Goodman, J. Polymer Sci. **17,** 587 (1955).
[3] B. G. Achhammer, F. W. Reinhart, and G. M. Kline, J. Research NBS **46,** 391 (1953) RP2210.
[4] T. Hasselstrom, H. W. Coles, C. E. Balmer, M. Hannigan, M. M. Keeler, and R. J. Brown, Textile Research J. **22,** 742 (1952).
[5] L. A. Wall, S. L. Madorsky, D. W. Brown, S. Straus, and R. Simha, J. Am. Chem. Soc. **76,** 3,430 (1954).
[6] R. Simha, J. Chem. Phys. **24,** 796 (1956).
[7] G. B. Taylor, J. Am. Chem. Soc. **69,** 635 (1947).
[8] S. L. Madorsky, J. Polymer Sci. **9,** 133 (1952).
[9] S. L. Madorsky, J. Polymer Sci. **11,** 491 (1953).
[10] S. Straus and S. L. Madorsky, Ind. Eng. Chem. **48,** 1,212 (1956).
[11] H. Hopff, Kunststoffe **42,** 423 (1952).
[12] P. Bradt and F. Mohler (NBS unpublished data).
[13] S. L. Madorsky and S. Straus, J. Research NBS **53,** 361 (1954) RP2553.
[14] R. Simha and L. A. Wall, J. Phys. Chem. **56,** 707 (1952).
[15] J. George, H. Mark, and H. Wechsler, J. Am. Chem. Soc. **72,** 3,896 (1950).
[16] R. Simha, L. A. Wall, and P. J. Blatz, J. Polymer Sci. **5,** 615 (1950).

Washington, June 27, 1957.

Journal of Research of the National Bureau of Standards Vol. 60, No. 1, January 1958 Research Paper 2820

Some Thermodynamic Properties of the Systems Polybutadiene-Benzene and Polyisobutene-Benzene*

R. S. Jessup

Experimental data are reported on densities at 26.9° C of solutions of polyisobutene in benzene covering the composition range from 0 to 10 percent by weight of polyisobutene, and on relative vapor pressures of solutions of polybutadiene and of polyisobutene in benzene covering the range from 0 to 50 percent of benzene. Values of apparent specific volume of polyisobutene in benzene were calculated from the densities of solvent and solutions. The results of the vapor pressure measurements were compared with the Flory-Huggins equation. The deviations from this equation for the polysiobutene-benzene system are much greater than for the polybutadiene-benzene system. The following equations represent the activities of the solvent for the polybutadiene-benzene and polysiobutene-benzene systems, respectively.

$$\ln a_1 = \ln v_1 + v_2 + 0.27v_2^2 + 0.06v_2^3,$$

$$\ln a_1 = \ln v_1 + \left(1 - \frac{1}{m}\right)v_2 + 0.50v_2^2 + 0.388v_2^3 + 0.184v_2^{12},$$

where a_1 represents activity of the solvent, v_1 and v_2 are volume fractions of solvent and polymer, respectively, and m is the ratio of molal volumes of polymer and solvent.

1. Introduction

Accurate measurements of thermodynamic properties of polymer solutions are of interest in connection with attempts to interpret the properties of such solutions in terms of statistical-mechanical treatments of various models. The present paper presents results of measurements of vapor pressures in the system polybutadiene-benzene, and of vapor pressures and solution densities in the system polyisobutene-benzene. Both polybutadiene and polyisobutene are of importance as constituents of synthetic rubbers. Polyisobutene should be of particular interest in connection with theoretical investigations of polymer solutions because of the relative simplicity of the structure of the polyisobutene molecule.

2. Materials

2.1. Polybutadiene

The sample of polybutadiene used has been described in a previous paper [1],[1] where it was designated as sample B. It was prepared by emulsion polymerization at 5° C, using a commercial *tert*-dodecyl mercaptan as the "modifier." It was purified in the Rubber Section of the Bureau by repeatedly dissolving it in benzene and then precipitating it by pouring the solution into methyl alcohol while stirring. After purification in this manner, the sample was again dissolved in benzene, a small amount (0.14 percent by weight of polymer) of phenyl-beta-naphthylamine was added as an antioxidant, the mixture was frozen, and the benzene removed by sublimation in vacuum to yield a product similar to foam rubber in appearance. The procedure described above removed soap, fatty acid, and stabilizer, as well as some of the low-molecular-weight polymer. After the measurements described in reference [1] the purified sample was kept in a refrigerator in an inert atmosphere.

In the present work, in order to remove traces of benzene and air, the sample was evacuated at room temperature to a pressure of less than 10^{-4} mm of mercury for about a month. It was found, however, that this did not completely remove either dissolved air (or other permanent gas) or benzene from the polymer. Permanent gases were reduced to a negligible amount by repeatedly adding benzene to the polymer and then pumping it off. Benzene was reduced to a negligible amount by evacuating to a pressure of less than 10^{-4} mm of mercury and heating to about 95° C. During this process most of the phenyl-beta-naphthylamine sublimed from the sample.

2.2. Polyisobutene

The polyisobutene sample was obtained by fractional precipitation[2] from solution of a low-molecular-weight commercial polyisobutene (Vistanex). The fraction used in the measurements had a viscosity-average molecular weight[3] of 76,000. This material was used without further purification except for removal of permanent gas and solvent. Permanent gas was removed by repeated addition of benzene to the polymer followed by removal of the benzene by evacuation. The final step in removal of benzene consisted in prolonged evacuation to a pressure of less than 10^{-4} mm of mercury while the temperature was gradually raised to about 140° C.

*The work described in this paper was done as part of a research project sponsored by the National Science Foundation, Polymer Research Group, in connection with the Government's synthetic rubber program.

[1] Figures in brackets indicate the literature references at the end of this paper.

[2] The fractionation of the polymer was done in the Polymer Structure Section of the Bureau.

[3] The molecular weight was determined by Miss H. V. Belcher of the Rheology Section of the Bureau.

Heating and evacuation were continued until the rate of removal of benzene was reduced to a few micrograms per day.

2.3. Benzene

Reagent grade benzene was purified by slow fractional freezing by a method described elsewhere [2], in which freezing proceeded upward along the length of a vertical tube containing the benzene while the liquid phase was stirred. This process was repeated twice, about 25 percent of the material being rejected each time. The resulting purified material had a density at 25° C of 0.87334 g/cm^3, as compared with the value 0.87368 g/cm^3 reported in the literature [3a]. This material was used without further purification for measurements of densities of solutions. It seems very improbable that the purity of the solvent has any appreciable effect on the values of apparent specific volume of solute derived from measurements of densities of solvent and solution.

For use in vapor-pressure measurements a portion of the benzene was transferred by vacuum distillation into a glass supply container which had been previously heated to 150° to 200° C while being evacuated to about 10^{-5} mm of mercury. Before entering the supply container the vapor passed through a drying tube containing magnesium perchlorate followed by phosphoric anhydride. The benzene in the supply container was then frozen in liquid air several times and evacuated to a pressure of about 10^{-5} mm of mercury, after which the sample was heated to room temperature and about 10 percent of the benzene was removed by evacuation. A fraction of the remaining benzene was then transferred by distillation to the previously evacuated vapor-pressure apparatus, and finally about 10 percent of the benzene in the vapor-pressure apparatus was removed by evacuation. The measured vapor pressure of the benzene so treated, in the liquid state at 0° C, agreed within 0.01 or 0.02 mm of mercury with an equation for the vapor pressure of the liquid based on the best available data [3b].

3. Apparatus and Methods

3.1. Density Measurements

The apparatus and methods used have been described previously [4], and only a brief description will be given here. Densities were measured with two bicapillary Pyrex pycnometers which were used previously [4], and which are of the type described by Heller and Thompson [5]. The capacity of each pycnometer was approximately 22 cm^3, and the diameter of the capillaries about 1 mm. The mass of solution in each pycnometer was determined by weighing on a semimicro balance on which readings could be repeated to about 0.02 mg. The volume of the solution in a pycnometer was determined by observing the positions of the menisci relative to those of reference marks on the capillaries to about 0.01 mm by means of a Wild cathetometer, while the pycnometer was immersed in a water bath whose temperature was maintained constant to about ±0.002° C. The observations were made through a plate glass window which formed one wall of the bath. Temperature was measured to 0.001° C by means of a platinum resistance thermometer and a Mueller bridge. The pycnometers were calibrated by weighing when empty and when filled with distilled water at temperatures near 27° C. All weights were corrected for air buoyancy, and for the masses of air and vapor above the liquid menisci in the capillaries.

In the previous work [4] the pycnometers were closed by glass caps fitted to the tops of the capillaries by standard-taper ground-glass joints. These could not be made to fit well enough to prevent loss of a small amount of solvent by evaporation. Also, because when the pycnometers were immersed in the water bath the caps projected out into the atmosphere which was at a lower temperature than the bath, it was suspected that some of the solvent in the capillaries might evaporate and condense in the caps. In the present work the glass caps were replaced by metal caps of the type shown in figure 1, in which a Monel metal cone is held by a brass nut against a brass sleeve, which in turn is soft-soldered to the top of the Pyrex capillary. This type of cap can be closed tightly enough to prevent any loss of solvent. It was found that when the pycnometers were weighed with the caps not tightened, subsequent tightening of one of the caps caused no appreciable change in weight. If a cap had once been tightened, then the subsequent removal of the nut apparently removed enough metal by abrasion to cause an appreciable change in weight. The procedure in filling the pycnometers and tightening the caps was such as to avoid such changes in weight. The pycnometers were first weighed empty with the nuts loosely in place. They were then filled with solution in the manner described previously [4] and placed in the thermoregulated bath with the nuts loosely in place and with the lower part of the caps, i. e., the brass sleeves, in contact with the water in the bath. After allowing sufficient time for the attain-

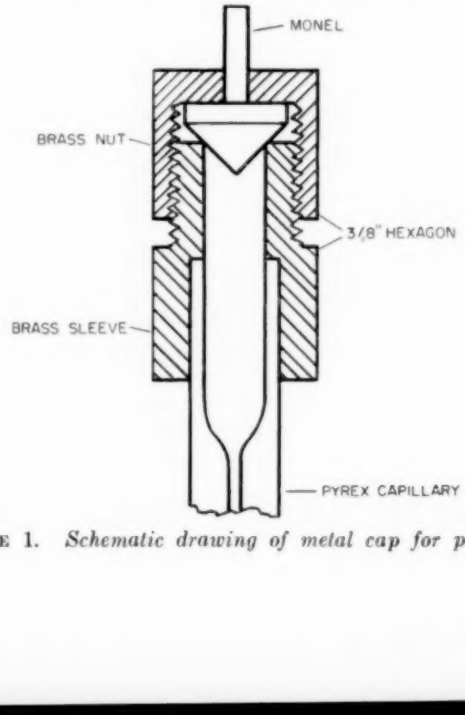

FIGURE 1. *Schematic drawing of metal cap for pycnometer.*

ment of thermal equilibrium the caps were tightened and the pycnometers were removed from the bath, cleaned, placed in the balance case, and weighed after allowing sufficient time for the attainment of temperature equilibrium.

The pycnometers were first weighed against a tare (a similar empty pycnometer) and then against each other. With the pycnometers empty the directly measured difference in weight (corrected for air buoyancy) usually checked the difference in the weights against the tare within 0.02 mg. With the pycnometers filled the check was not always this good, but was usually within 0.05 mg or less.

After the filled pycnometers were weighed they were immersed in the water bath to a point a little below the lower part of the metal cap. The caps themselves were heated to a temperature above that of the bath by means of electric heaters to insure against condensation of solvent in the caps. After sufficient time had elapsed to permit the system to come to temperature equilibrium, the heaters were removed and the pycnometers were lowered so as to be completely immersed in the water. After this a number of observations were made of the positions of the menisci in the capillaries relative to the reference marks etched on them.

Measurements of the heights of the menisci were facilitated by placing behind the capillaries a white Bakelite sheet with black lines about 0.3-mm wide drawn on its surface at an angle of 45° with the horizontal. This device has been described by Zeleny [6]. The menisci are sharply outlined by the apparent intersections of the black lines with their reflections in the surface of the liquid.

Measurements of the density of the sample of polyisobutene used were made to a precision of about 0.1 percent by the method of hydrostatic weighing.

3.2. Vapor-Pressure Measurements

Vapor pressures were determined from measurements of the difference between the vapor pressure of the purified benzene and the pressures over a weighed sample of polymer to which measured quantities of benzene had been added. The apparatus used is shown schematically in figure 2 (a). By means of the valve C, benzene could be transferred by distillation from the buret B to the polymer in the tube H. The amount of benzene so transferred was determined from the change in position of the benzene meniscus in the buret and the change in position of the mercury meniscus in the left arm of the manometer M, the diameter of which was known. In determining the mass of benzene transferred, great care was taken to insure that no liquid benzene was present in the left arm of the manometer or in the connecting tubing when the buret was being read. From the total amount of benzene transferred was subtracted the amount of vapor in the known volumes in the tube H, the right arm of the manometer, and the connecting tubing to obtain the benzene content of the polymer-solvent mixture. Benzene could also be transferred

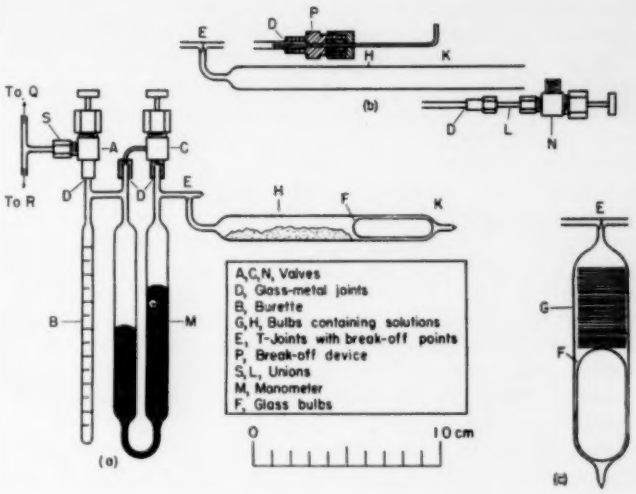

FIGURE 2. *Schematic diagram of vapor-pressure apparatus.*
(a) Assembled apparatus; (b) apparatus for introducing polybutadiene sample; (c) bulb for polyisobutene solutions.

from the polymer-solvent mixture to the buret B (fig. 2 (a)) by cooling the latter in liquid air and opening the valve C. Measurements of vapor pressure could thus be made both after increasing the benzene content of the mixture and after decreasing it.

The method of introducing the polybutadiene, mercury, and benzene into the apparatus will now be described. The tube H was initially open at one end, as shown in figure 2 (b), and was sealed at the other end to the smaller tube which contained a break-off point in the T-joint at E. The tube H was weighed empty, and again after introducing the desired amount of polybutadiene (about 1.0 g). The bulb F was inserted in H, which was then drawn down at the point K and sealed to a smaller tube which, in turn was joined to the brass union L by means of a glass-to metal soldered joint. The brass needle valve N was attached to the union and to a similar union leading to a vacuum system. After removal of air and benzene from the polymer sample as described in section 2.1, the valve N and union L were removed by sealing off the small tube connecting them to H.

To introduce mercury into the manometer, it was rotated 90° clockwise from the position shown in figure 2 (a) and a small flask containing the desired amount of mercury was sealed on in place of the tube H. The system was then evacuated, the valve A was closed and disconnected from the vacuum system, and the manometer was rotated so as to allow the mercury to flow into it. With the valve C open, air was then admitted slowly through the valve A, and the flask that had contained the mercury was disconnected from the manometer.

The tube H was then sealed to the manometer and to the breakoff device P (fig. 2 (b)). This consisted of a brass stuffing box connected to a short piece of glass tubing by a glass-to-metal soldered joint, and having a Teflon packing through which passed a heavy phosphor bronze wire. The system was then

evacuated through the valve A and a valve Q (not shown in figure) which was attached to the vacuum system. The connection to the vacuum system was sufficiently flexible so that the manometer could be tilted to liberate any air bubbles that might have been trapped below the mercury surfaces during the glassblowing operations. Then, with the manometer still connected to the vacuum system but with the vacuum pump shut off, the tube H was opened to the manometer by sliding the phosphor bronze wire through the stuffing box P so as to break off the glass point at E, and the breakoff device was removed by sealing off a short distance to the right of E. After this, a measurement of the pressure in the vacuum system always gave less than 10^{-4} mm of mercury, showing that no appreciable amount of air had leaked into the system.

The buret B was then immersed in an ice bath. The valve C and the valve Q (not shown in fig. 2) on the vacuum system were closed, and the valve R (not shown) on a bulb containing a supply of purified benzene was opened, allowing the benzene to distill into the buret. The buret was initially filled to a point above the highest graduation mark, the valve R was closed, and the excess benzene was removed by pumping it into the vacuum system. The valve A was then closed. The buret was then immersed in an ice bath and measurements of the vapor pressure of the supercooled liquid benzene at 0° C were made.

The temperature of the apparatus during measurements of the difference in pressure between solvent and polymer-solvent mixtures was controlled near 26.9° C by the same water bath used in the density measurements. The heights of the two menisci in the manometer were measured to 0.01 mm by means of a Wild cathetometer, the menisci being sharply outlined by the device of Zeleny [6] described in section 3.1.

The apparatus and procedure for measurement of the vapor pressures of polyisobutene-benzene mixtures differed from that described above only in that the sample bulb G (fig. 2 (c)) was used instead of H. In order to promote reasonably rapid attainment of equilibrium in the polymer-solvent mixture, the polymer was spread in layers approximately 0.2 mm thick on brass disks spaced about 1-mm apart in the tube G, the axis of which was kept vertical as shown in figure 2 (c).

4. Results

4.1. Densities of Polyisobutene Solutions

The experimental values of density at 26.900° C and the corresponding values of apparent specific volume of polymer, ϕ_2, are given in table 1. The values of ϕ_2 are also plotted as ordinate against mass fraction of polymer in figure 3. The values of ϕ_2 were calculated from the measured densities by means of the equation

$$\phi_2=\frac{1}{\rho_1}\left[1-\frac{\rho-\rho_1}{w_2\rho}\right],$$

where ρ_1 and ρ are the densities of solvent and solution, respectively, and w_2 is the mass fraction of polymer. The mean of the two experimental values of ρ_1 was used in this calculation.

The values of ϕ_2 in the lower concentration range are much less reliable than those at the higher concentrations, since, according to eq (1), the effect on the calculated value of ϕ_2 of a given error in ρ (or ρ_1) is approximately inversely proportional to w_2. Therefore the form of the curve cannot be determined accurately at the lower concentrations, and the curve in figure 3 is dotted in this region to emphasize this fact. The curve was drawn to fit the experimental points as well as possible and to have a horizontal tangent [4] at $w_2=0$. With one exception the points deviate from the curve as drawn by amounts corresponding to 5 ppm or less in density. It may be noted that if the value for the density of the solvent

TABLE 1. *Observed densities of polyisobutene-benzene solutions at 26.900° and calculated values of apparent specific volume of polymer*

Mass fraction of polymer, w_2	Density of solution	Apparent specific volume of polymer
	g/cm³	*cm³/g*
0	0.871311$_4$	
0	.871309$_0$	
0.005477	.871467$_3$	1.1098$_7$
.005477	.871471$_1$	1.1089$_6$
.010958	.871629$_2$	1.1093$_7$
.019323	.871889$_8$	1.1082$_1$
.019323	.871891$_7$	1.1080$_8$
.030266	.872211$_1$	1.1085$_2$
.040261	.872523$_1$	1.1080$_7$
.040261	.872517$_8$	1.1082$_4$
.050027	.872823$_2$	1.1079$_3$
.050677	.872834$_6$	1.1081$_4$
.050677	.872834$_6$	1.1081$_4$
.098313	.874305$_4$	1.1077$_0$
1.000	.913$_5$	1.094$_7$

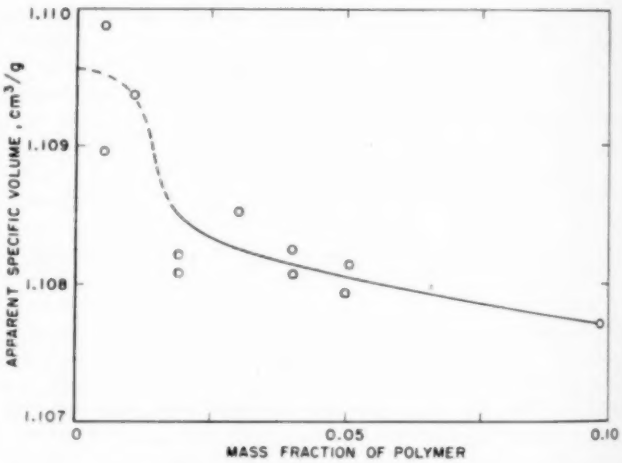

FIGURE 3. *Apparent specific volume of polyisobutene in benzene at 26.90° C.*

[4] This condition seems plausible from physical considerations, since in a sufficiently dilute solution the solute molecules are too far apart to interact appreciably.

were lower by 5 ppm the points representing the values of ϕ_2 would still show a slight downward trend with increasing w_2, and could be approximately represented by a straight line going from 1.1084 at $w_2=0$ to 1.1076 at $w_2=0.10$.

A decrease in ϕ_2 with increasing w_2 has been reported by Rosen [7] for polystyrene in cyclohexane, toluene, and chloroform. The decrease in ϕ_2 shown in figure 3 is much smaller in magnitude than that reported by Rosen, but the trend extends over a greater range of concentration. The density data of Streeter and Boyer [8] also lead to a decrease in apparent specific volume of polystyrene in *o*-dichlorobenzene with increasing polymer concentration in the range $w_2=0$ to 0.06. Horth and Rinfret [9] have reported discontinuities in curves of density versus polymer concentration for dilute solutions of polyvinyl acetate in chlorobenzene. These discontinuities correspond to *increases* in apparent specific volume with increasing polymer concentration. The data in reference [4] show no change in ϕ_2 with composition of solutions of polystyrene in benzene, toluene, ethylbenzene, and 2-butanone in the composition range $w_2=0.02$ to 0.10.

From the curve of figure 3 and the value given in table 1 for the density of the polyisobutene sample, the change in volume when a 1-g sample of polymer is dissolved in benzene varies from $+0.013$ to $+0.015$ cm^3. As shown previously [4], a change in volume upon mixing affects such thermodynamic properties as heat of mixing, free energy of mixing, etc. It has been calculated that the change in volume when a 1-g sample of polyisobutene is dissolved in a large amount of benzene will affect the heat of mixing by about -2 calories. Since ϕ_2 varies with composition as shown in figure 3, the partial specific volume of solvent will differ from the specific volume of the pure solvent by about 2×10^{-5} cm^3/g at $w_2=0.05$. This change in volume will affect the partial molal heat of dilution by about -0.25 calorie per mole of benzene. These thermal effects resulting from volume changes are approximately equal in magnitude, but opposite in sign, to the values of heat of mixing and heat of dilution calculated by Hildebrand's equation [10], the derivation of which implies no change in volume on mixing.

4.2. Vapor Pressures

a. Polybutadiene-Benzene

The results of vapor-pressure measurements on the system polybutadiene-benzene are given in table 2 in terms of the activity a_1 of the solvent, defined as the ratio f_1/f_1^0 of the fugacity[5] of the solvent in the mixture to that in the pure solvent. Also given in table 2 are the values calculated from the measured activities for the parameter μ in the Flory-Huggins [11] equation

$$\ln a_1=\ln v_1+\left(1-\frac{1}{m}\right)v_2+\mu v_2^2,$$

where m is the ratio of the molar volume of solute to that of solvent, and v_1 and v_2 represent volume fractions of solvent and solute respectively. In this calculation the term $1/m$ was neglected.

The results are also shown graphically in the lower curve of figure 4, where a_1 is plotted as ordinate against v_1 as abscissa, and in figure 5, where the calculated values of the parameter μ are plotted against v_1. Not all of the experimental points are plotted in figure 4, since in this plot they would lie so close together as to confuse the diagram. In

TABLE 2. *Results of vapor-pressure measurements in the system polybutadiene-benzene*

Experiment	Volume fraction solvent, v_1	Observed activity of solvent, a_1	μ
1*	0.0710	0.2392	0.330_9
2*	.1290	.3969	$.332_4$
3*	.2033	.5558	$.329_3$
4*	.2952	.6982	$.314_1$
5*	.3731	.7901	$.314_0$
6*	.4581	.8622	$.308_2$
7*	.5362	.9106	$.305_9$
8	.5367	.9079	$.290_8$
9	.4574	.8586	$.296_2$
10	.3722	.7872	$.307_5$
11	.2932	.6941	$.310_2$
12	.2051	.5560	$.320_3$
13	.1167	.3620	$.318_9$
14	.5381	.9074	$.284_0$
15	.4587	.8586	$.292_1$
16	.5369	.9068	$.284_8$
17	.4554	.8567	$.294_3$
18	.3794	.7926	$.301_7$
19	.2940	.6948	$.309_2$
20	.2051	.5562	$.320_9$
21	.1256	.3817	$.310_1$
22*	.1144	.3572	$.322_6$
23*	.1275	.3919	$.328_9$
24*	.2059	.5567	$.318_1$
25*	.2940	.6970	$.315_4$
26*	.3792	.7963	$.314_2$
27*	.4548	.8600	$.310_9$
28*	.5349	.9103	$.307_9$

*Experiments marked with an asterisk were made after increasing the benzene content of the mixture; all others were made after decreasing the benzene content.

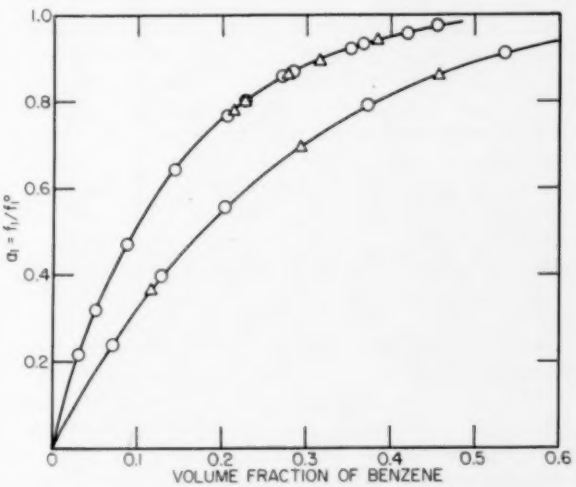

FIGURE 4. *Activity of benzene in mixtures with polyisobutene (upper curve) and with polybutadiene (lower curve).*

[5] Pressure ratios were converted to fugacity ratios in all cases, although difference was usually negligible.

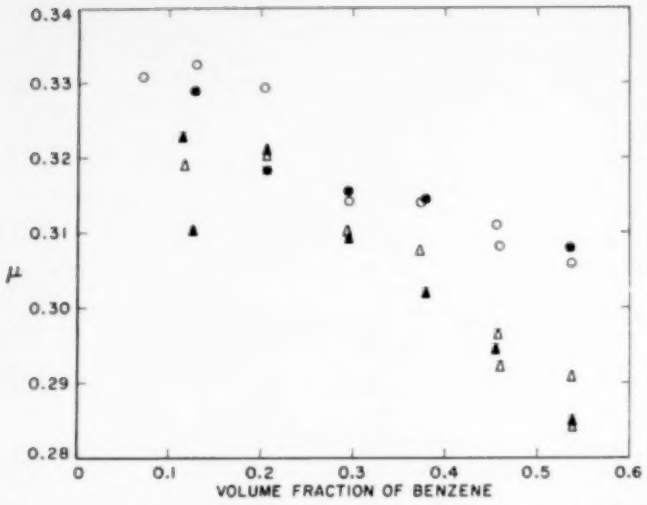

FIGURE 5. *Values of the parameter μ for the system polybutadiene-benzene.*

figure 5 the circles represent measurements made after increasing the benzene content of the mixture, while the triangles represent measurements taken after decreasing the benzene content. The open and solid symbols represent two different series of measurements.

After completing a preliminary series of measurements it was observed that when the benzene in the buret was frozen in liquid air, gas bubbles were liberated indicating the presence of permanent gas in the system. In view of the preliminary treatment of the polymer to remove dissolved gases it was at first thought that the presence of gas in the system indicated a leak in the apparatus. However, sensitive tests failed to show any such leak. It was finally concluded that the preliminary treatment of the polymer did not remove permanent gases completely. Therefore, before proceeding with the measurements, a series of experiments was performed in which benzene was added to and then removed from the polymer. It was found that each time this was done a small amount of gas was present in the benzene, and a small amount of benzene was pumped off to remove the gas. The amount of gas removed per experiment could not be determined quantitatively, but appeared to decrease as the number of experiments increased. After it was judged that only a negligible amount of gas remained, the vapor-pressure measurements were resumed. After the first series of measurements indicated by the open symbols in figure 5, a small amount of gas was found to be present in the system. The benzene was then transferred from the buret to the mixture and left for about a month, after which a second series of measurements of vapor pressure was made, the results of which are represented by the solid symbols in figure 5. Although the amount of gas in the system appeared to be considerably greater after the second series of measurements than after the first, it will be seen from figure 5 that there was little if any systematic difference between results obtained

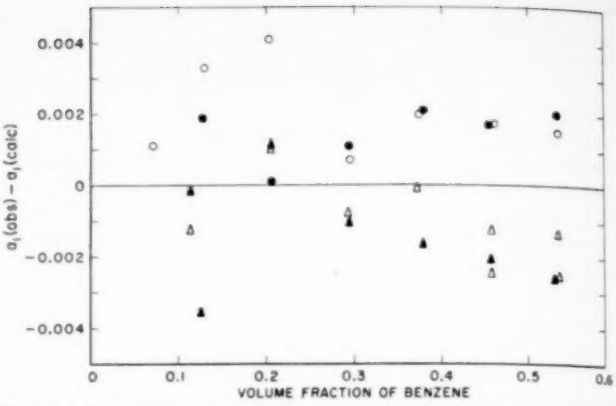

FIGURE 6. *Deviations of observed activities in benzene-polybutadiene system from equation (2).*

under the same conditions in the two series. This indicates that the amount of air present was not sufficient to affect the measured vapor pressures appreciably, and that the systematic difference between results obtained after increasing and after decreasing the benzene content of the mixture is due to hysteresis in the system polybutadiene-benzene.

The variation of μ with v_1 (fig. 5) shows that the vapor pressures in this system cannot be represented within the precision of the measurements by the Flory-Huggins equation. They can be represented, however, by adding a term in v_2^3 to this equation. Figure 6 shows deviations of the measured values of a_1 from

$$\ln a_1 = \ln v_1 + v_2 + 0.27v_2^2 + 0.06v_2^3. \qquad (2)$$

b. Polyisobutene-Benzene

The results of the vapor-pressure measurements in the system polyisobutene-benzene are given in table 3, and are shown graphically by the upper

TABLE 3. *Results of vapor-pressure measurements in the system polyisobutene-benzene*

Experiment	Volume fraction of solvent, v_1	Activity of solvent, a_1	μ
1*	0.0310	0.2162	1.037$_3$
2*	.0509	.3159	.975$_5$
3*	.0879	.4684	.916$_1$
4*	.1439	.6410	.871$_3$
5*	.2053	.7664	.929$_0$
6*	.2845	.8689	.784$_2$
7*	.3528	.9229	.752$_4$
8*	.4204	.9557	.721$_0$
9	.3844	.9398	.736$_4$
10	.3161	.8937	.761$_4$
11	.2283	.7989	.808$_9$
12*	.2283	.8021	.815$_0$
13*	.2858	.8717	.787$_7$
14*	.3683	.9325	.746$_9$
15	.2787	.8610	.783$_0$
16*	.2787	.8634	.788$_4$
17	.2140	.7766	.815$_5$
18*	.2140	.7806	.823$_7$
19*	.2719	.8586	.797$_0$
20*	.3563	.9306	.765$_4$
21*	.4567	.9745	.729$_0$
22	.4230	.9600	.730$_5$

*Experiments marked with an asterisk were made after increasing the benzene content of the mixture; all others were made after decreasing the benzene content.

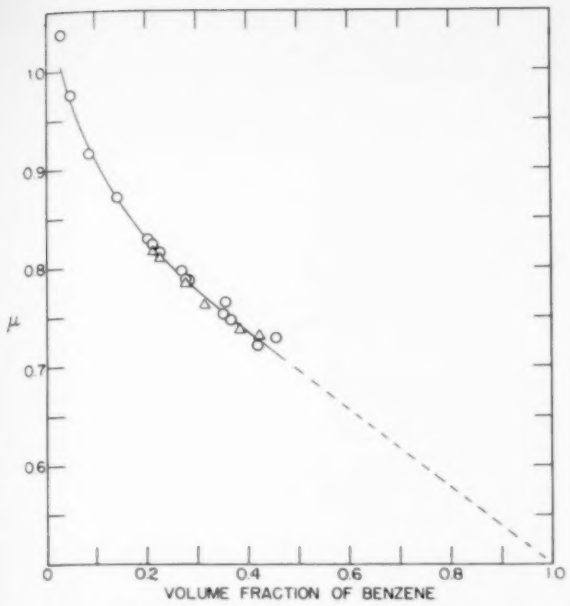

FIGURE 7. *Values of the parameter μ for the system polyisobutene-benzene.*

curve in figure 4. The values of the parameter μ given in table 3 are shown graphically in figure 7. The circles in this figure represent observations made after increasing the benzene content of the mixture, while the triangles represent observations made after decreasing the benzene content. The value of m used in this calculation was taken as the ratio of the molal volumes of polymer and solvent, namely 928. The dotted straight line in figure 7 which is tangent to the lower end of the experimental curve passes through the value $\mu=0.5$ at $v_1=1$. This value of μ has been reported [12] for dilute solutions of polyisobutene in benzene.

The same difficulties in removing air from the mixture were encountered with this system as with the system polybutadiene-benzene. It is not believed, however, that air in the system contributed appreciably to the hysteresis shown by the usually systematic deviations of circles and triangles from the curve in figure 7.

It is seen by comparison of figures 5 and 7 that the deviations from the Flory-Huggins equation and the variation of the parameter μ with composition are much greater for the polyisobutene-benzene system than for the polybutadiene-benzene system. It is not possible to represent the data on the polyisobutene-benzene system by as simple an equation as (2), but these data can be represented by

$$\ln a_1=\ln v_1+\left(1-\frac{1}{m}\right)v_2+0.5v_2^2+0.388v_2^3+0.184v_2^{12}. \tag{3}$$

Deviations of the experimental points from this equation are shown in figure 8. For this system the agreement between observations made under comparable conditions is generally less satisfactory, and the deviations of experimental from calculated

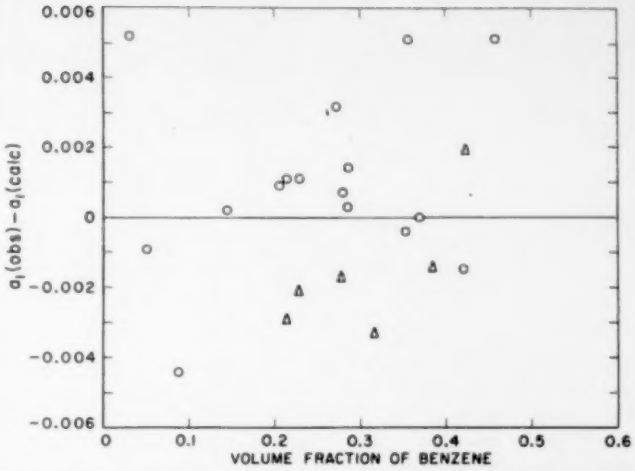

FIGURE 8. *Deviations of observed activities in the system polyisobutene-benzene from equation (3).*

activities are somewhat larger than for the system polybutadiene-benzene. This may be related to the fact that the time required for the attainment of equilibrium in the polyisobutene solutions is much greater than for the polybutadiene solutions, and therefore departures from equilibrium resulting from unavoidable fluctuations in temperature are likely to be larger in the polyisobutene solutions.

The vapor-pressure data reported here for the system polyisobutene-benzene at 26.9° C are in fair agreement with results at 25° C reported by Bawn and Patel [13] for solutions in benzene of a polyisobutene of molecular weight 45,000. Their curve representing values of the paramenter μ is somewhat lower at low values of v_1 than that shown in figure 7, and the two curves intersect at about $v_1=0.5$. The difference between the two curves at $v_1=0.1$ corresponds to about 3 percent in a_1.

5. References

[1] R. A. Nelson, R. S. Jessup, and D. E. Roberts, J. Research NBS **48,** 275 (1952) RP2313.
[2] F. W. Schwab and E. Wichers, J. Research NBS **25,** 747 (1940) RP1351.
[3] Selected values of properties of hydrocarbons, Am. Petroleum Inst. Research Proj. 44, Carnegie Inst. Technology, (a) table 5a (1950); (b) table 5k (1954).
[4] M. Griffel, R. S. Jessup, J. A. Cogliano, and Rita P. Park, J. Research NBS **52,** 217 (1954) RP2492.
[5] W. Heller and A. C. Thompson, J. Colloid Sci. **6,** 57 (1951).
[6] J. Zeleny, Rev. Sci. Instr. **7,** 289 (1936).
[7] B. Rosen, J. Polymer Sci. **17,** 559 (1955).
[8] D. J. Streeter and R. F. Boyer, Ind. Eng. Chem. **43,** 1790 (1951).
[9] A. Horth and M. Rinfret, J. Am. Chem. Soc. **77,** 503 (1955).
[10] J. H. Hildebrand and R. L. Scott, Solubility of nonelectrolytes, chap. VII, eq (34) and (35) (Rheinhold Publishing Co., Inc., New York, N. Y., 1950).
[11] See, for example, P. J. Flory, Principles of polymer chemistry, (Cornell Univ. Press, Ithaca, N. Y., 1953); M. L. Huggins, J. Polymer Sci. **16,** 209 (1955).
[12] Reference 10 p. 362, based on data by P. J. Flory, J. Am. Chem. Soc. **65,** 375 (1943).
[13] C. E. H. Bawn and R. D. Patel, Trans. Faraday Soc. **52,** 1665 (1956).

WASHINGTON, April 22, 1957.

Journal of Research of the National Bureau of Standards Vol. 60, No. 1, January 1958 Research Paper 2821

Infrared Measurements With a Small Grating From 100 to 300 Microns [1]

Earle K. Plyler and L. R. Blaine

Good resolution has been obtained with a small grating in the region from 100 to 300 microns. A high-pressure mercury lamp, having a quartz inner envelope, was used as a source and a Golay cell as a detector. The radiation was reflected from three filtering plates before passing through the entrance slit. This filtering served to reduce the stray radiation to about 5 percent.

1. Introduction

In the past several years small gratings have been used in spectrometers for the near-infrared region. It has also been shown that a small prism spectrometer could be converted, with only minor changes, into a far-infrared instrument.[2] Good resolution has been obtained in the region from 25 to 125 μ using a thermocouple as the detector. Further work has been done on the instrument, which increased the resolution and extended the wavelength range.

2. Experimental Procedure

In order to extend the measurements beyond 125 μ three changes were made in the instrument. A Golay cell with a crystal quartz window replaced the thermocouple, a high-pressure mercury lamp was substituted for the globar source, and a different arrangment of the filters replaced the previous three-filter arrangement described in footnote 2.

The Golay cell was found to have a greater sensitivity in the detection of the long-wavelength radiation than the thermocouple, making it possible to use narrower slits and to obtain better resolution.

High-pressure mercury lamps have much greater intensity in the far-infrared region than the globar source. It was found that an AH4 mercury lamp was adequate for the measurements made in the region from 100 to 300 μ. A section 1 by ½ in. was removed from the outer glass envelope which enclosed the quartz lamp. A small glass tube was introduced through the opening and nitrogen was circulated about the electrodes, which greatly added to the life of the lamp.

Ultraviolet and visible radiation are intense from the lamp, and the observers' eyes should be shielded. At first the lamp was housed in a black box with an aperture that permitted the radiation to fall upon the slit of the spectrometer. Later the lamp was coated with a layer of magnesium oxide. The MgO film absorbed only a small fraction of the radiation at 100 μ, but it was effective in scattering the short-wavelength region. A crystal of magnesium oxide 1-mm thick absorbed about 80 percent of the radiation at 100 μ, but with thinner layers the energy loss with the coating became negligible.

As measurements are carried out to longer wavelengths, increased filtering is required for the removal of the stray radiation. A new arrangement of the optical system has been made so that three reflection filters are employed in front of the entrance slit of the spectrometer. Figure 1 represents the system that was used. The filters that were placed in positions A, B, and C were reststrahlen plates of CsBr and CsI, gratings, and roughened silver scatter plates. In the measurements shown in figures 2 and 3, one filter of each type was used. For the region from 70 to 100 cm^{-1} the external filters as shown in figure 1 were a CsBr reststrahlen plate and two roughened silver plates, one of which was blackened. For the spectral region from 53 to 70 cm^{-1} a CsI reststrahlen plate was substituted for the CsBr plate. In some of the measurements a grating with 1,000 lines/in. was substituted for one of the silver plates.

Some spectra have been obtained in the region from 25 to 50 cm^{-1} by the use of small gratings with 60 lines/in. and 100 lines/in. In the measurements in this region it was necessary to use wider slits, and in the region of 400 μ the slitwidth was 4 mm. In order to obtain the wide slits, the regular slit jaws were removed and replaced by two metal jaws so that there was a separation of 2 mm when the slit drum read zero. This change enabled the observer to set the slits between 2 and 4.5 mm.

The strong water-vapor line at 26 cm^{-1} was observed, but it is estimated that the spectrum con-

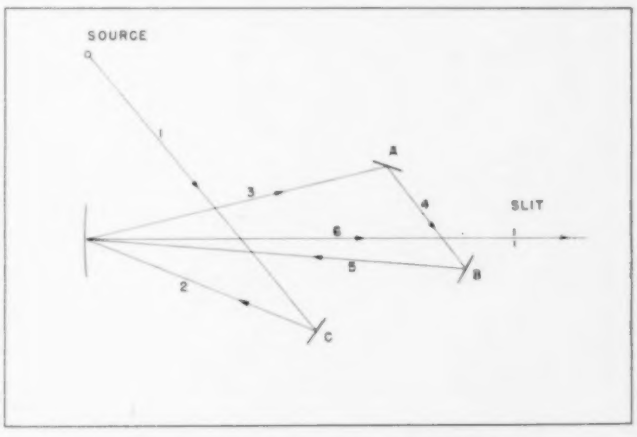

FIGURE 1. *Optical arrangement for the filters.*
The reflection filters are placed in positions A, B, and C.

[1] This work was supported by the U. S. Atomic Energy Commission.
[2] Earle K. Plyler and Nicolo Acquista, J. Research NBS **56**, 149 (1956) RP2660.

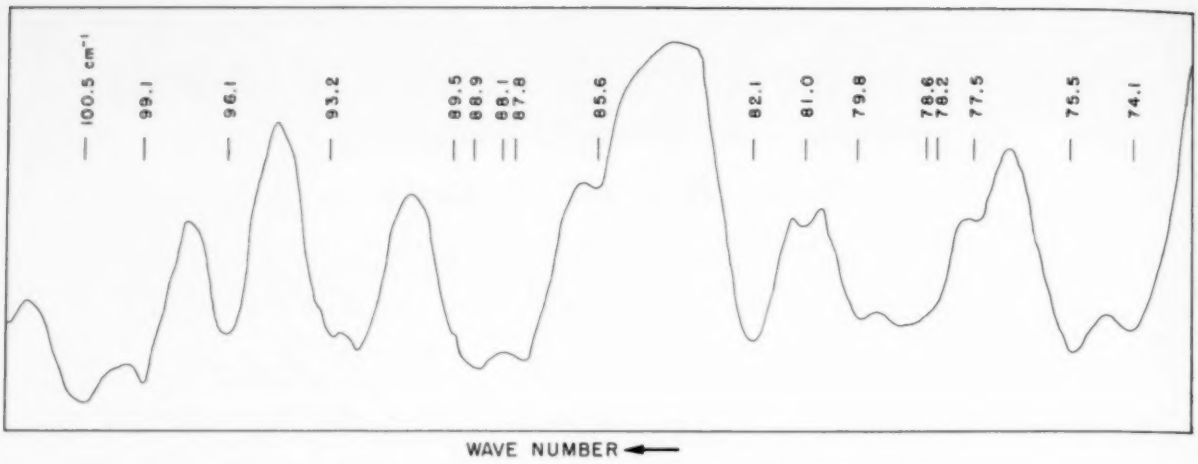

FIGURE 2. *Absorption spectrum of water vapor from 75 to 100 cm⁻¹.*

The slitwidths were 1.5 mm and a 180-lines/in. grating was used.

tained about 40 percent of stray radiation in this region. Before quantitative measurements can be made between 300 and 400 μ on the instrument a more efficient filtering system will be required.

3. Results

As the present investigation has been primarily concerned with the methods of measurements, only three examples of the results will be given. The absorption spectra of several molecules have been reported in other publications.[3]

Figure 2 represents the absorption spectrum of water from 73 to 100 cm^{-1} as measured with a 180-lines/in. grating. This region was included in the previous publication (see footnote 2), but now the stray radiation has been almost completely removed and the absorption lines of high intensity cause the deflection to approach the zero line. The wave numbers marked on the lines are the calculated values determined by Benedict.[4]

[3] D. E. Mann, J. H. Meal, and Earle K. Plyler, J. Chem. Phys. **24**, 1018-1022 (1956).

The amount of water vapor in the path was sufficient to produce nearly 100-percent absorption for the lines of moderate and high intensity; thus some of the weak lines could be observed. The observed wave numbers of some of the lines of low intensity agree closely with the calculated values. The wavelengths were determined experimentally by the measurement of the angle of the grating with reference to the central image.

Figure 3 represents the region from 53 to 70 μ. The more intense lines of the spectra have been identified and the wave numbers are marked on the chart. The two lines near 60 cm^{-1} are slightly distorted by second-order lines. The linewidths are about 0.6 cm^{-1}, which is a measure of the resolution obtained. The spectrum of water vapor recorded in figures 2 and 13 is for a path length of 2 m and relative humidity of 40 percent. The slitwidths were 1.5 mm for the region from 75 to 100 cm^{-1}, and 2.5 mm from 53 to 72 cm^{-1}.

[4] W. S. Benedict, private communication.

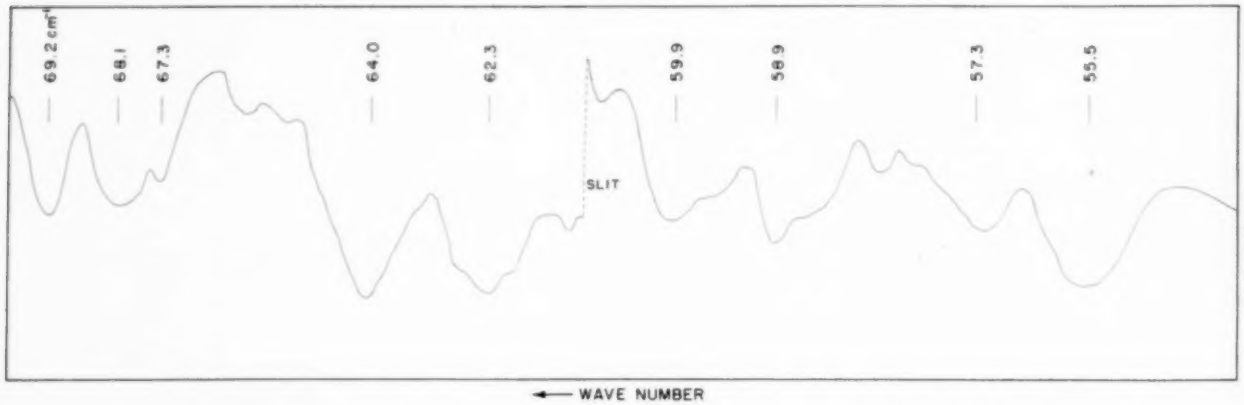

FIGURE 3. *Absorption spectrum of water from 55 to 70 cm⁻¹ as measured with a 180-lines/in. grating.*

The slitwidths were 1.5 mm to 62 cm^{-1} and 2.5 mm from 55 to 62 cm^{-1}.

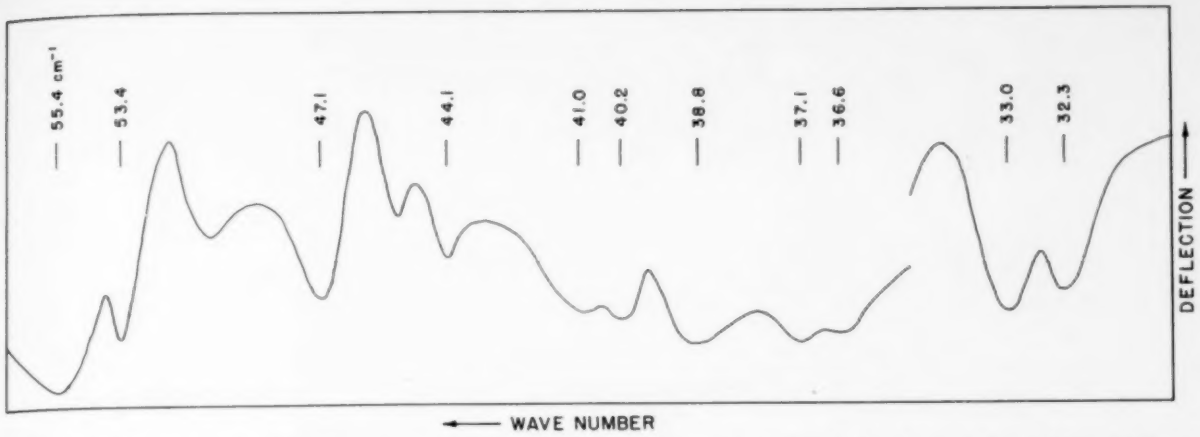

FIGURE 4. *Absorption spectrum of water vapor from 36 to 55 cm^{-1} as measured with a 100-lines/in. grating and from 30 to 36 cm^{-1} with a 60-lines/in. grating.*

The slitwidth was 4 mm for the entire region.

Figure 4 shows the absorption spectrum of water vapor from 30 to 55 cm^{-1}. The stray radiation was reduced to a small percentage by using a 0.2-mm window of LiF as a transmission filter. The slitwidths were 4 mm, and a 100-lines/in. grating was used from 36 to 55 cm^{-1} and a 60-lines/in. grating was used from 30 to 36 cm^{-1}. In observing the two lines at 32.3 and 33 cm^{-1} a window of KBr, 0.4-mm thick, was found effective in eliminating higher orders from the grating. The line at 47 cm^{-1} could be observed through the KBr window, but the energy in the higher wavelength region (47 to 100 cm^{-1}) was almost zero.

In conclusion it can be stated that a small grating is adequate for measuring spectra from 25 to 300 μ, and with further improvements in the filter system the measurements can be extended to 400 μ.

WASHINGTON, July 18, 1957.

Journal of Research of the National Bureau of Standards Vol. 60, No. 1, January 1958 Research Paper 2822

A Low-Frequency Annular-Slot Antenna

James R. Wait

The radiation characteristics of an annular slot cut in an ideally conducting ground plane are discussed. The voltage impressed between the concentric edges is assumed to be constant around the slot. The annular slot is backed by a hemispherical cavity which has imperfectly conducting walls. For a specified voltage, the power radiated in the upper half-space and the power absorbed by the hemispherical cavity are calculated. It is indicated that the power absorbed can be reduced greatly by lining the walls of the cavity with a wire mesh. A flush-mounted antenna of this type at low frequencies may have certain practical advantages over the more conventional monopole.

It is the purpose of this paper to examine the radiation characteristics of an annular slot cut in a thin perfectly conducting ground plane. The medium below the ground plane is taken to be a dissipative medium such as soil. A hemispherical bowl is hollowed out just beneath the annular slot. The problem is to calculate the power radiated into the upper half-space and the power absorbed by the walls of the hemispherical cavity.

The radiation into a half-space from an aperture or a slot cut in a perfectly conducting plane of infinite extent is derivable from a knowledge of the tangential electric field distribution $\vec{E}'$ over the aperture or slot. A general expression for the magnetic field $\vec{H}$ in the exterior region [1] [1] is (for a time factor exp $(i\omega t)$)

$$\vec{H}(\vec{r})=\frac{ik}{\eta_0}\iint_{\text{slot}}\vec{n}\times\vec{E}'\cdot\Gamma(\vec{r},\vec{r}')ds, \tag{1}$$

where $k=2\pi/\text{wavelength}$, $\eta_0=120\pi$, $\vec{n}$ is a unit vector which is pointing out and is normal to the slot aperture, $\vec{r}$ and $\vec{r}'$ are position vectors directed to a point in the aperture and to the field point respectively. $\Gamma(\vec{r},\vec{r}')$ is the dyadic Green's function and is given by the operator

$$\Gamma(\vec{r},\vec{r}')\cdot=\left(I+\frac{1}{k^2}\nabla\nabla\right)G(\vec{r},\vec{r}') \tag{2}$$

in terms of the scalar Green's function $G(\vec{r},\vec{r}')$ which, for a halfspace, is

$$G(\vec{r},\vec{r}')=\frac{1}{2\pi}\frac{e^{-ik|\vec{r}-\vec{r}'|}}{|\vec{r}-\vec{r}'|}. \tag{3}$$

Equation (1) can readily be applied to the case of an annular slot cut in a flat ground plane (see fig. 1). A spherical coordinate system (r, θ, ϕ) is chosen with the ground plane defined by $\theta=\pi/2$ and the inner and outer rim of the annular slot are $r=b-\Delta$ and $r=b+\Delta$, respectively. It is now assumed that the field in the slot aperture has only a radial component $E'(\rho')$ which does not vary in the ϕ direction. The resultant magnetic field in the exterior half-space has only a ϕ component and is given by

$$H_\phi=\frac{ik}{2\pi\eta_0}\int_{\phi=0}^{2\pi}\int_{\rho=b-\Delta}^{b+\Delta}\rho'\cos\phi'\frac{e^{-ik|\vec{r}-\vec{\rho}'|}}{|\vec{r}-\vec{\rho}'|}E(\rho')d\rho'd\phi' \tag{4}$$

[1] Figures in brackets indicate the literature references at the end of this paper.

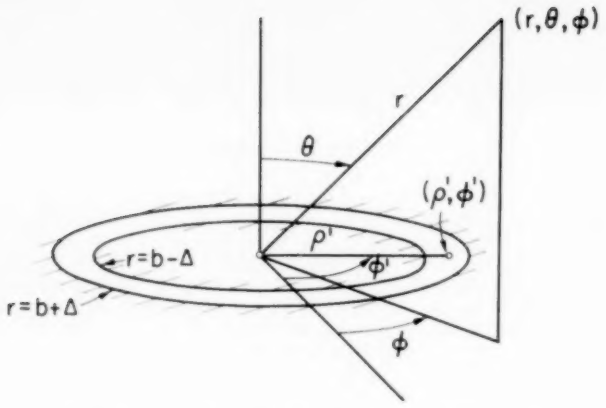

FIGURE 1. *Annular slot and upper half-space.*

where $\vec{\rho}$ is a position vector to a point in the slot. For a narrow slot such that Δ is small compared to b and to the wavelength, the above simplifies to

$$H_\phi \cong \frac{ikb}{2\pi\eta_0} V \int_0^{2\pi} \cos\phi' \frac{e^{-ikR}}{R} d\phi', \tag{5}$$

where $R=[r^2+b^2-2rb\sin\theta\cos\phi']^{1/2}$ and

$$V=\frac{1}{b}\int_{b-\Delta}^{b+\Delta} E(\rho')\rho' d\rho' \tag{6}$$

is the voltage across the slot.

In that far field, $kr>>1$ and therefore $kR\cong k[r-b\sin\theta\cos\phi']$ so that

$$H_\phi = \frac{ikbV}{2\pi\eta_0}\frac{e^{-ikr}}{r}\int_0^{2\pi}\cos\phi' e^{ikb\sin\theta\cos\phi'}d\phi' \tag{7}$$

$$= -\frac{kbV}{\eta_0}\frac{e^{-ikr}}{r} J_1(kb\sin\theta)$$

where $J_1(x)$ is the Bessel function of order one. For $kb<<1$,

$$H_\phi \cong -\frac{(kb)^2 V}{2\eta_0}\frac{e^{-ikr}}{r}\sin\theta \tag{8}$$

which has the same radiation pattern as a vertical electric dipole.

The power, P_r, radiated into the upper half-space is obtained by integrating the Poynting vector over an infinite hemisphere, therefore

$$P_r = \lim_{r\to\infty}\frac{\eta_0}{2}\int_0^{\pi/2}|H_\phi|^2(2\pi r\sin\theta)d\theta \tag{9}$$

and consequently the radiation conductance, g_r, for the upper half-space is [2]

[2] It may be of interest to note that g_r can be expressed in the alternate form

$$g_r = \frac{1}{4kb}\int_0^{2kb} J_2(2x)dx.$$

This integral has been tabulated by H. L. Knudsen in Antenna systems with rotational symmetry, D. Sc. thesis (Tech. Univ. of Denmark, Copenhagen, 1953).

$$g_r = \frac{2P_r}{V^2} = \frac{2\pi(kb)^2}{\eta_0}\int_0^{\pi/2} J_1^2(kb\sin\theta)\sin\theta\, d\theta. \tag{10}$$

This integral can be written in terms of a highly convergent series as was shown by Bailey [2]; consequently

$$g_r = \frac{2\pi kb}{\eta_0}\sum_{m=0,\,1,\,2\ldots}^{\infty} J_{3+2m}(2kb). \tag{11}$$

For $kb<<1$,

$$g_r \cong \frac{\pi}{\eta_0}\frac{(kb)^4}{6}. \tag{12}$$

In the preceding discussion, only the upper half-space has been considered. If the annular slot was cut in a metal plate located in free space, the total radiation conductance would be simply $2g_r$. In the present case, however, the annular slot is to be backed by a hemispherical cavity of radius a as indicated in figure 2. The magnetic field H_ϕ in the cavity consists of two parts, the primary field H_ϕ^p and the secondary field H_ϕ^s. The tangential fields at the walls of the cavity, which consist of "lossy" material, are assumed to satisfy the approximate boundary condition $E_\theta = ZH_\phi|_{r=a}$, where Z is the surface impedance.[3] The solution for the fields in the cavity can be obtained quite readily by using spherical wave functions.

The primary field is, of course,

$$H_\phi^p = \frac{ikbV}{2\pi\eta_0}\int_0^{2\pi}\cos\theta'\,\frac{e^{-ikR}}{R}\,d\phi'. \tag{13}$$

It is now noted that [3,p.1466]

$$\frac{e^{-ikR}}{R} = -ik\sum_{n=0}^{\infty}\sum_{m=0}^{n}(2n+1)\epsilon_m\frac{(n-m)!}{(n+m)!}\cos m(\phi-\phi')\, P_n^m(0)P_n^m(\cos\theta)\begin{cases} j_n(kb)h_n(kr); & r>b \\ j_n(kr)h_n(kb); & r<b \end{cases} \tag{14}$$

where $P_n^m(\cos\theta)$ is the associated Legendre polynomial and $j_n(x)$ and $h_n(x)$ are spherical Bessel and Hankel functions, respectively.[4] As a consequence of the orthogonality, the terms for

[3] The use of surface impedance is valid when the fields in the air-filled cavity vary slowly in a distance equal to the "skin depth" of the lossy material beyond the cavity walls. This is satisfied if $Z/\eta_0<<1$.

[4] The spherical Bessel and Hankel functions are defined by

$$j_n(x) = (-1)^n x^n\left(\frac{d}{x\,dx}\right)^n\left(\frac{\sin x}{x}\right)$$

$$h_n(x) = i(-1)^n x^n\left(\frac{d}{x\,dx}\right)^n\left(\frac{e^{-ix}}{x}\right).$$

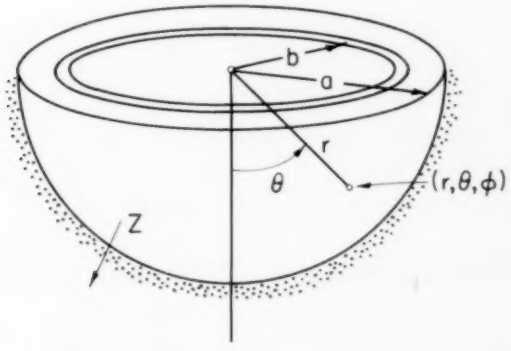

FIGURE 2. *Annular slot and lower hemisphere.*

$m \neq 1$ vanish in the integration with respect to ϕ', therefore

$$H_\phi^p = \sum_{n=1}^{\infty} A_n h_n(kr) P_n^1(\cos\theta) \tag{15}$$

for $r > b$, where

$$A_n = \frac{k^2 b V}{\eta_0} \frac{2n+1}{n(n+1)} P_n^1(0) j_n(kb). \tag{16}$$

The secondary field within the cavity is finite at $r=0$, is a solution of the wave equation, has azimuthal symmetry, and is therefore of the form

$$H_\phi^s = \sum_{n=1}^{\infty} B_n j_n(kr) P_n^1(\cos\theta). \tag{17}$$

The tangential electric field is obtained from

$$E_\theta = -\frac{1}{i\epsilon\omega r} \frac{\partial}{\partial r}(rH_\phi) \tag{18}$$

so that

$$E_\theta = \frac{i\eta_0}{kr} \sum_{n=1}^{\infty} \left\{ A_n \frac{\partial}{\partial r}[rh_n(kr)] + B_n \frac{\partial}{\partial r}[rj_n(kr)] \right\} P_n^1(\cos\theta). \tag{19}$$

Application of the boundary condition at $r=a$, leads to

$$\frac{B_n}{A_n} = -\frac{h_n' + (iZ/\eta_0)h_n}{j_n' + (iZ/\eta_0)j_n}, \tag{20}$$

where

$$h_n = h_n(ka),\ j_n = j_n(ka),$$

$$h_n' = \left\{ \frac{1}{x} \frac{\partial}{\partial x}[xh_n(x)] \right\}_{x=ka},$$

$$j_n' = \left\{ \frac{1}{x} \frac{\partial}{\partial x}[xj_n(x)] \right\}_{x=ka}.$$

Explicit expressions for the fields inside the cavity are thus available. The power absorbed, P_a, by the lossy walls can be obtained by integrating the Poynting flux crossing the hemisphere at $r=a$. Making use of the Wronskian relation [3, p. 1573],

$$h_n(x) \frac{dj_n(x)}{dx} - j_n(x) \frac{dh_n(x)}{dx} = \frac{i}{x^2},$$

it readily follows that

$$H_\phi \Big]_{r=a} = \sum_{n=1}^{\infty} S_n P_n^1(\cos\theta) \tag{21}$$

where

$$S_n = \frac{iA_n}{(ka)^2} \frac{1}{j_n' + (iZ/\eta) j_n}. \tag{22}$$

Therefore [5]

$$2P_a = \left[2\pi \operatorname{Re} Z \int_0^{\pi/2} |H_\phi|^2 \sin\theta r^2 d\theta \right]_{r=a} \tag{23}$$

and

$$\frac{2P_a}{\operatorname{Re} Z} = 2\pi a^2 \sum_{n=1}^{\infty} \sum_{n'=1}^{\infty} S_n S_{n'}^* \int_0^{\pi/2} P_n^1(\cos\theta) P_{n'}^1(\cos\theta) \sin\theta d\theta.$$

[5] Re indicates that the real part is to be taken.

Noting that [3, p. 783, part 1]

$$\int_{-1}^{+1} P_n^m(x)P_{n'}^m(x)dx=\frac{2}{2n+1}\frac{(n+m)!}{(n-m)!} \quad \text{for} \quad n=n'$$

$$=0 \quad \text{for} \quad n\neq n' \tag{24}$$

it follows that

$$\frac{2P_a}{ReZ}=2\pi a^2\sum_{n=1}^{\infty} S_nS_n^*\cdot\frac{n(n+1)}{2n+1} \tag{25}$$

where the asterisk denotes a complex conjugate. The conductance as seen by the annular slot, for the lower hemispherical bowl, is then given by [6]

$$g_a=\frac{2P_a}{V^2}$$

$$=\frac{2\pi \operatorname{Re} Z}{\eta_0^2}\left(\frac{b}{a}\right)^2\sum_{n=1}^{\infty}\frac{2n+1}{n(n+1)}\frac{[P_n^1(0)]^2[j_n(kb)]^2}{|j_n'+(iZ/\eta_0)j_n|^2}. \tag{26}$$

The total conductance at the annular slot is then g_a+g_r. The efficiency, ξ, of the annular slot can be defined as the ratio of the power radiated into the upper half-space to the total power, therefore,

$$\xi=\frac{P_r}{P_a+P_r}=\frac{1}{(g_a/g_r)+1}. \tag{27}$$

The preceding formulas could be employed to calculate the efficiency of the antenna for given values of the surface impedance Z, the radius of the annular ring, and the radius of the hemispherical cavity. Such an antenna might be feasible even at low radiofrequencies. In this case, the cavity could be a canyon, gorge, or ditch. Using a system of wires stretched between the canyon rims, a simulated annular aperture could be fabricated. In such an application, ka would be small compared to unity, and consequently,

$$j_n(ka)\cong\text{const.}\times(ka)^n$$

and

$$j_n'(ka)\cong\text{const.}\times(n+1)(ka)^{n-1}.$$

Therefore,

$$g_a\cong\frac{2\pi(kb)^2\operatorname{Re} Z}{\eta_0^2}\sum_{n=1,3,5\ldots}^{\infty}\frac{(2n+1)}{n(n+1)^3}\left(\frac{b}{a}\right)^{2n}[P_n^1(0)]^2 \tag{28}$$

$$\cong\frac{\pi(kb)^2\operatorname{Re} Z}{\eta_0^2}\frac{3}{4}\left(\frac{b}{a}\right)^2\left[1+\frac{7}{32}\left(\frac{b}{a}\right)^4+\frac{55}{576}\left(\frac{b}{a}\right)^8+\ldots\right].$$

The efficiency to this approximation is then given by

$$\xi=\frac{1}{1+(g_a/g_r)}, \tag{29}$$

where

$$g_a/g_r\cong\frac{\operatorname{Re} Z}{\eta_0(ka)^2}\frac{9}{2}\left[1+\frac{7}{32}\left(\frac{b}{a}\right)^4+\frac{55}{576}\left(\frac{b}{a}\right)^8+\ldots\right].$$

If the material lining the hemispherical cavity had a conductivity σ, then

$$\frac{\operatorname{Re} Z}{\eta_0}\cong\operatorname{Re}\left[\frac{i\epsilon_0\omega}{\sigma+i\epsilon\omega}\right]^{1/2}\cong\left(\frac{\epsilon_0\omega}{2\sigma}\right)^{1/2}. \tag{30}$$

For frequencies in the vicinity of 15 kc, with a typical ground conductivity of 5×10^{-3} mho/m,

$$\operatorname{Re} Z/\eta_0\cong0.01,$$

[6] It is also possible to obtain the conductance by integrating the Poynting vector over the area of the slot.

and, if the cavity radius was 500 ft, $ka \cong 1/20$. Therefore,

$$g_a/g_r \cong 18\left[1+\frac{7}{32}\left(\frac{b}{a}\right)^4+\ldots\right] \tag{31}$$

$$\cong 18 \qquad \text{if, say,} \qquad b \leq a/2.$$

For this case the efficiency, ξ, is 0.011 or about 5 percent. This could be improved by increasing the size of the cavity. For example, if the cavity radius was 1,000 ft, the efficiency would be about 20 percent for the same wall material.

A more promising approach is to line the cavity wall with a wire mesh. In this case, the surface impedance Z is the parallel combination of the impedance of the wire mesh and the intrinsic impedance of the cavity wall material. It is not difficult to show that [4]

$$\text{Re } Z/\eta_0 \cong \frac{GX^2}{(G+X)^2+G^2}, \tag{32}$$

where $G=\sqrt{\frac{\epsilon_0\omega}{2\sigma}}$ and $X=(d/\lambda)\log(d/2\pi c)$,

where d is the spacing between the wires, λ is the wavelength, and c is the wire radius. For a wire spacing of, say, 13 ft, $d/\lambda \sim 2\times10^{-4}$ at 15 kc, and for No. 8 wire $2c \cong 1/8$ in., and therefore $\log(d/2\pi c) \sim \log(400) \sim 6.0$. Since $G \cong 0.01$, it follows that

$$\text{Re } Z/\eta_0 \cong 6.4\times10^{-5},$$

which leads to

$$g_a/g_r \cong 0.115 \qquad \text{for} \qquad b \leq a/2 \qquad \text{and} \qquad a=500 \text{ ft}.$$

This corresponds to a radiation efficiency of 90 percent for the cavity-backed annular-slot antenna.

No attempt has been made here to estimate the over-all efficiency of the antenna. There is, of course, further absorption of energy radiated into the upper half-space. This loss is due to the finite conductivity of the adjacent ground plane. It could be calculated by representing the annular slot by an equivalent electric dipole and using the available data [4] for loss in radial wire ground systems. The efficiency ξ calculated here is a measure of the performance of the cavity-backed annular slot relative to a more conventional vertical monopole with the same electric moment.

The circular slot concentric to the hemispherical cavity is the simplest model and the most convenient for calculations. It is possible that other geometrical shapes such as elongated or flattened cavities would also be suitable.

The author would like to thank H. L. Knudsen for his helpful suggestions.

References

[1] H. Levine and J. Schwinger, On the theory of electromagnetic wave diffraction by an aperture in an infinite plane conducting screen, Comm. Pure Appl. Math. **3**, No. 4 (1950).

[2] A. Erdelyi, W. Magnus, F. Oberhettinger, and Tricomi, Higher transcendental functions, vol. 2, p. 91 (McGraw-Hill Book Co., Inc., New York, N. Y., 1953). [Note: In eq 21, the right-hand side should read $z^{-1}\sum_{m=0}^{\infty} J_{2\nu+2m+1}(2z)$.]

[3] P. M. Morse and H. Feshbach, Methods of theoretical physics, vol. 2 (McGraw-Hill Book Co., Inc., New York, N. Y., 1953).

[4] J. R. Wait and W. A. Pope, Input resistance of L. F. unipole aerials, Wireless Engineer (May 1955).

BOULDER, COLO., August 8, 1957.

Journal of Research of the National Bureau of Standards Vol. 60, No. 1, January 1958 Research Paper 2823

Relation Between the Absorption Spectra and the Chemical Constitution of Dyes: XXIX. Interaction of Direct Azo Dyes in Aqueous Solution [1]

May N. Inscoe, John H. Gould, Mary E. Corning, and Wallace R. Brode

Interaction of dyes in aqueous solution results in differences in the spectrum of the mixture when compared with the sum of the spectra of the individual dyes. A general survey, chiefly with azo dyes, was made to determine the effect of dye structure on this interaction.

The effect of other factors on the interaction of direct azo dyes was investigated. The addition of alcohol or non-ionic detergent prevents this interaction, while the presence of inorganic salts or an increase in dye concentration appears to increase the extent of interaction. The effect of acids and bases is dependent upon the nature of the dyes in the mixture.

The results obtained are consistent with the assumption that the forces involved in the interaction of direct azo dyes in mixtures are the same as those causing the aggregation of individual dyes and those binding these dyes to fibers.

1. Introduction

Dyes in aqueous solution often show a tendency toward association, and it is probable that the forces involved are closely related to those responsible for binding the dyes to fibers. This association may be between similar molecules or ions in solutions of individual dyes or between unlike molecules or ions in dye mixtures. In this paper the term "aggregation" is used to refer to the association of like molecules, while the association of unlike dye molecules in mixtures is designated as "interaction."

The association of like dye molecules or ions in aqueous solutions to form dimers or higher aggregates has been studied intensively and is so common a phenomenon that it has been considered a general property of dyes, closely related to the property of color [1].[2] Those cases in which aggregation is not observed may be regarded as exceptions in which steric [2] or electrical [3] influences prevent the close association of the molecules.

Striking changes in the absorption spectra of many basic dyes are produced by dimerization and further aggregation, and such association has been studied spectrophotometrically. In the case of azo dyes, changes in absorption spectra arising from aggregation are not as marked, and other physical measurements have more commonly been used to demonstrate the aggregation [4].

The nature of the forces involved in this aggregation of dyes is not yet clear. Some proposed explanations include hydrogen bonding, van der Waal's forces, the interaction of π-electrons, or the coupling of electron oscillators. It is very probable that more than one factor is operative in most cases.

The association of unlike ions or molecules in mixtures of dyes has not been as fully investigated as that of individual dyes, although the absorption spectra of dye mixtures in many cases suggest that such interaction occurs. Scheibe observed such behavior in mixtures of cyanine dyes [5], while Rabinowitch and Epstein found indications that mixed double ions were present in mixtures of thionine and methylene blue in water [1].

This interaction of dyes in mixtures has been most widely observed with direct cotton dyes, and the spectra of mixtures of substantive azo dyes in aqueous solution often differ from the spectra that would be predicted by the addition of the spectra of the individual components. The results obtained from the study of several such mixtures [6, 7] show that interaction to form a mixed dye complex often takes place, with equilibrium between the dyes and the complex, and suggest that the forces involved in this interaction are related to those operating in the dyeing of cotton.

In view of the apparent close relationship between the aggregation of dyes, the interaction of dyes in mixtures, and the binding of dyes to fibers, a wider survey of the interaction of azo dyes and the factors influencing this interaction was felt to be desirable. The results of this survey are described below.

2. Experimental Procedure

2.1. Dyes Used

The majority of the dyes used were commercial samples. When greater purity was desired, conventional methods for purification were employed. Some of the dyes had been prepared for other investigations by standard methods of synthesis and purification.

Stock solutions of dyes were prepared by dissolving weighed samples in distilled water and diluting to volume. In use, suitable aliquots of these stock solutions were diluted in volumetric flasks. For most measurements the final concentration used was chosen to give a maximum absorbance of the principal long-wavelength band between 0.5 and 1 when measured in a 2-cm cell; these concentrations ranged from 5 to 20 mg/liter.

[1] This research was supported by the United States Air Force through the Office of Scientific Research of the Air Research and Development Command.

[2] Figures in brackets indicate the literature references at the end of this paper.

The names used in this paper for the commercial dyes are those given by the Technical Manual and Year Book of the American Association of Textile Chemists and Colorists, Vol. XXXII, 1956, as representing the best-known prototype of the dye.

The dyes included in this survey are shown in table 1, where each dye has been assigned an arbitrary number for convenience of reference in this paper.

TABLE 1. *Dyes included in the survey*

Dye number	Name	Color index number [a]	Structure
			SUBSTANTIVE AZO DYES
1	Congo Red	370	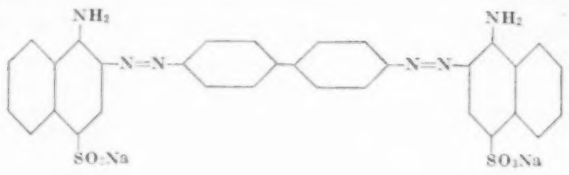
2	Diamine Violet N	394	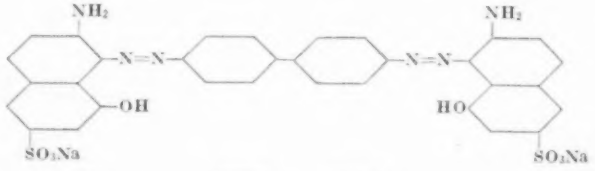
3	Chrysamine G	410	
4	Toluylene Orange R	446	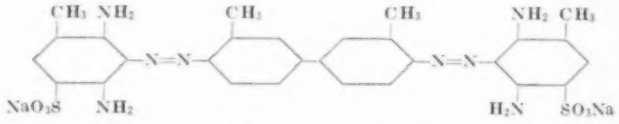
5	Benzopurpurine 4B	448	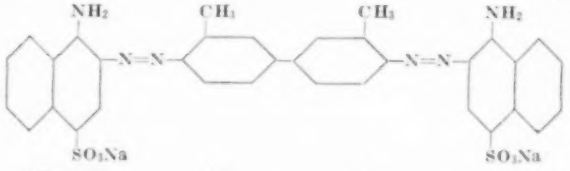
6	Benzo Blue 3B	477	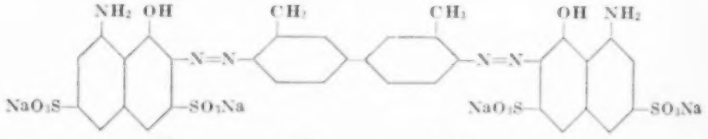
7	Benzopurpurine 10B	495	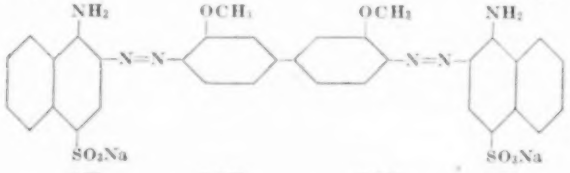
8	Benzo Azurine G	502	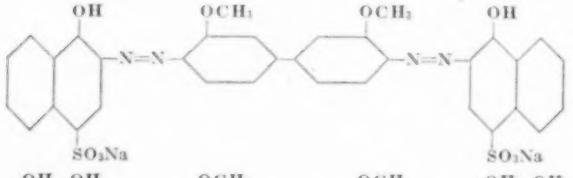
9	Dianil Blue G	508	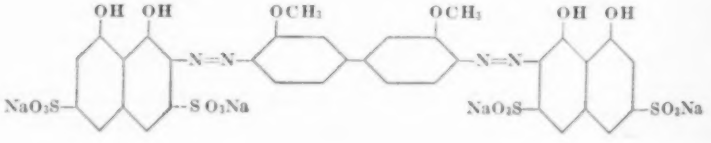

See footnotes at end of table.

TABLE 1. *Dyes included in the survey*—Continued

Dye number	Name	Color index number [a]	Structure
			SUBSTANTIVE AZO DYES—continued
10	Diamine Sky Blue FF	518	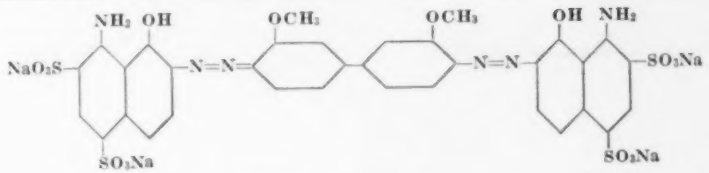
11	Brilliant Yellow	364	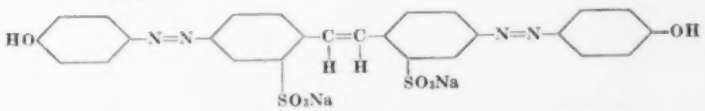
12	Chrysophenine G	365	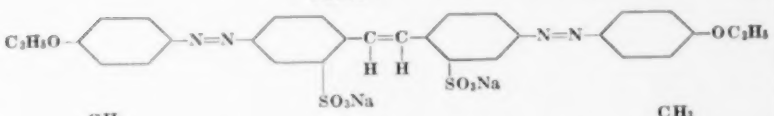
13			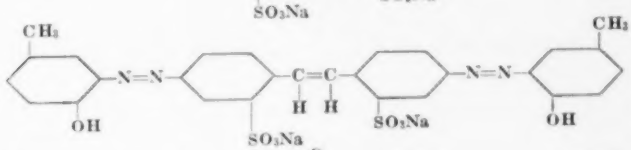
14	Benzo Fast Yellow 5GL	346	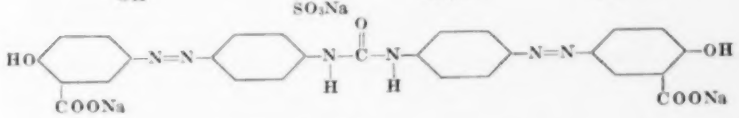
15	Benzo Fast Yellow 4GL	349	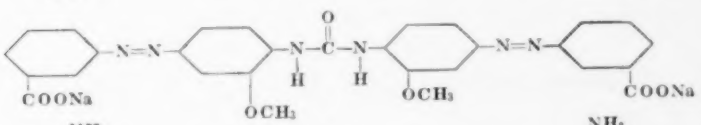
16	Benzo Fast Pink 2BL	353	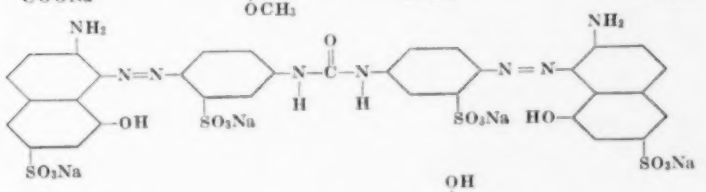
17	Benzo Fast Red 8BL	278	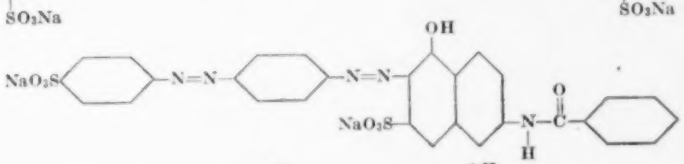
18	Diamine Fast Violet	325	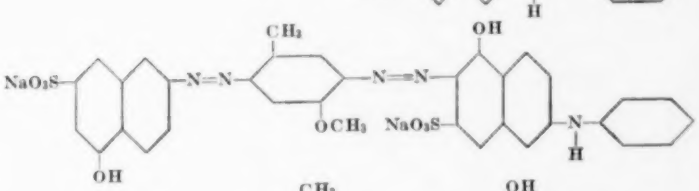
19	Zambesi Black D	Pr 201	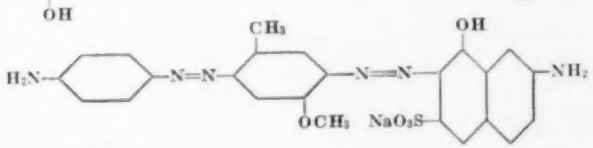
20	Benzo Fast Blue FR	533	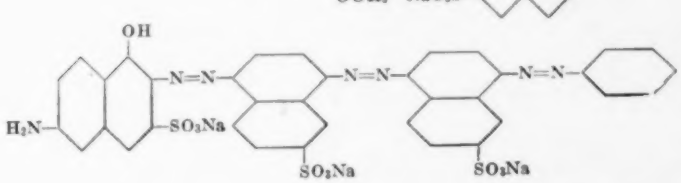

See footnotes at end of table.

TABLE 1. *Dyes included in the survey*—Continued

Dye number	Name	Color index number [a]	Structure
			SUBSTANTIVE AZO DYES—continued
21	Columbia Black FF Ex	539	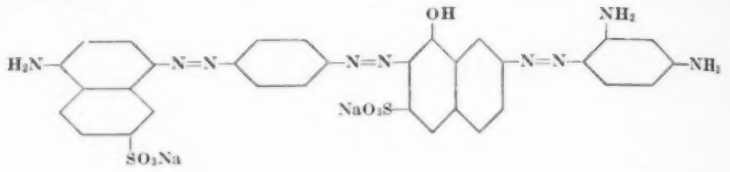
22	Diamine Bronze G	559	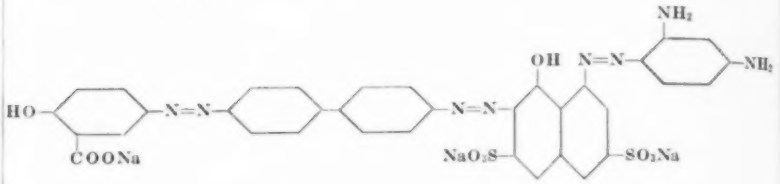
23	Direct Deep Black EW Ex	581	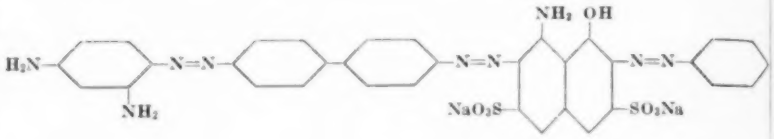
24	Chlorazol Dark Green	583	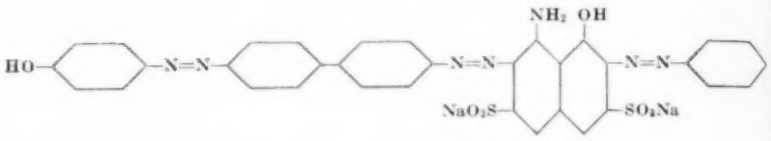
25	Diamine Green B	593	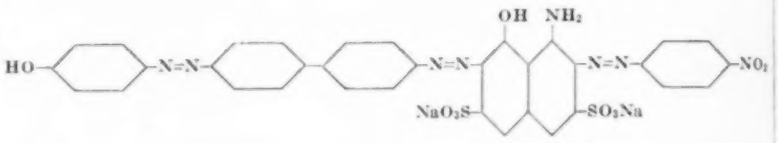
26	Diamine Green G	594	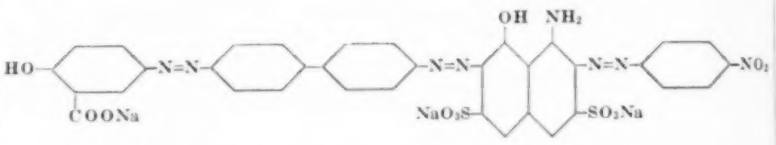
27	Congo Brown G	598	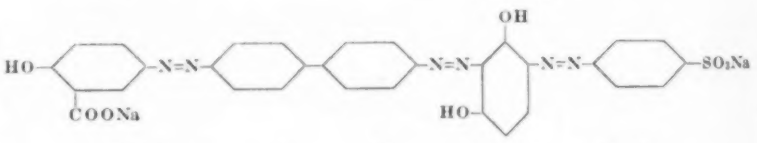
28	Benzo Brown G	696	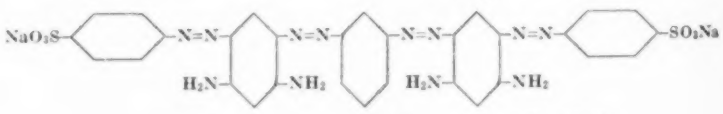
29	Erika B	139	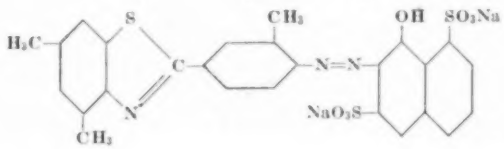
30	Chloramine Yellow	814	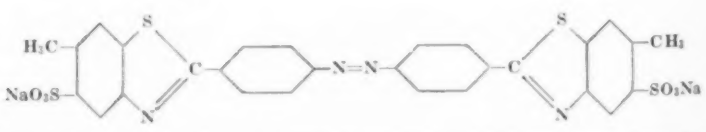

See footnotes at end of table.

TABLE 1. *Dyes included in the survey*—Continued

Dye number	Name	Color index number [a]	Structure
	MONOAZO ACID DYES		
31	Crocein Orange G	26	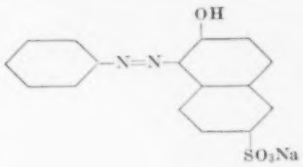
32	Orange G	27	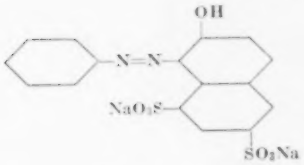
33	Azo Eosine G	114	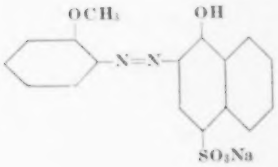
34	Orange II	151	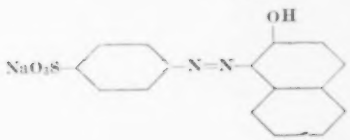
35	Amaranth	184	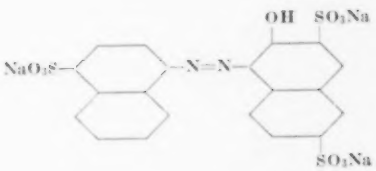
36	Cochineal Red A	185	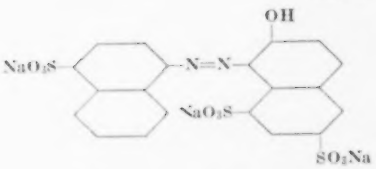
37	Eriochrome Blue Black B	201	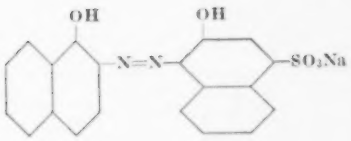
38	Eriochrome Blue Black R	202	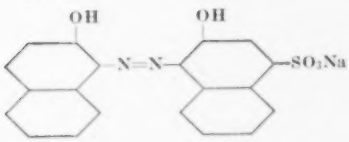
39	Sulphon Acid Blue B	209	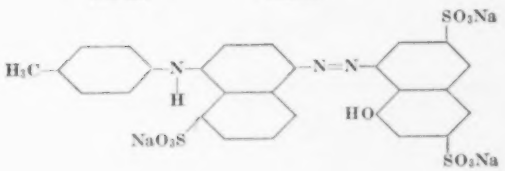

See footnotes at end of table.

TABLE 1. *Dyes included in the survey*—Continued

Dye number	Name	Color index number [a]	Structure
			MONOAZO ACID DYES—continued
40			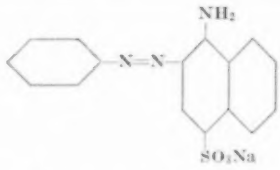
41			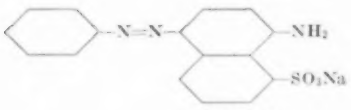
42			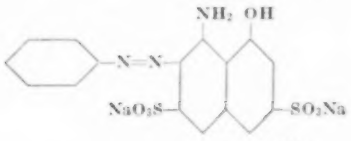
43			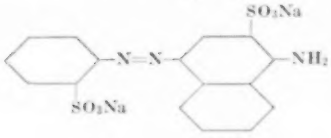
44			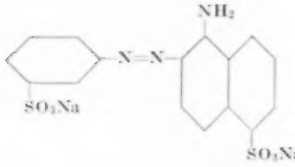
45			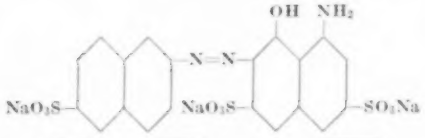
46			
			DISAZO ACID DYES
47	Naphthol Blue Black	246	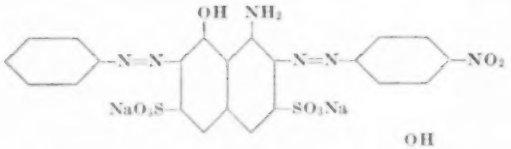
48	Cloth Red G	249	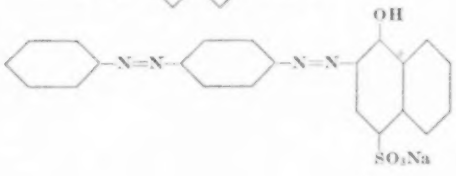
49	Brilliant Crocein M	252	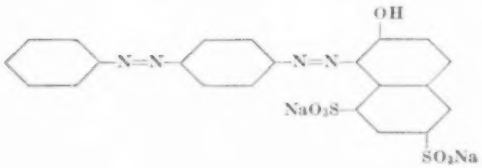

See footnotes at end of table.

TABLE 1. *Dyes included in the survey*—Continued

Dye number	Name	Color index number [a]	Structure
	DISAZO ACID DYES—continued		
50	Ponceau SS Ex	253	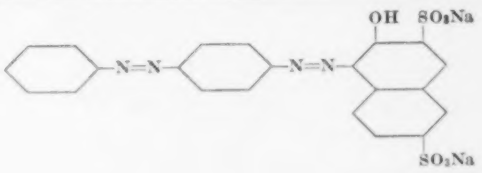
51	Acid Black N	294	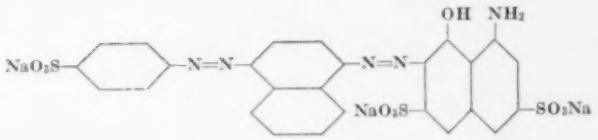
52	Nerol 2B	304	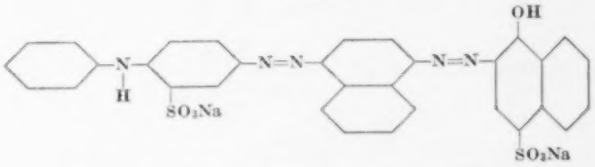
53	Sulphone Cyanine Black B	307	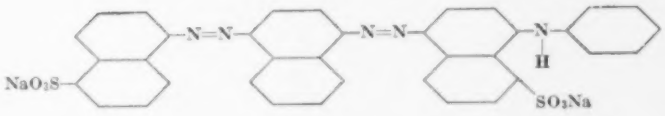
54	Naphthylamine Black D	308	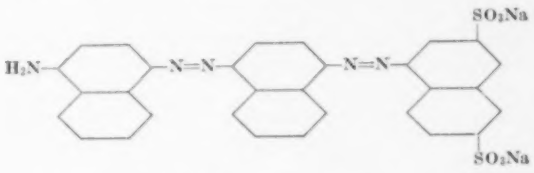
55	Acid Anthracene Red 3B [b]	487	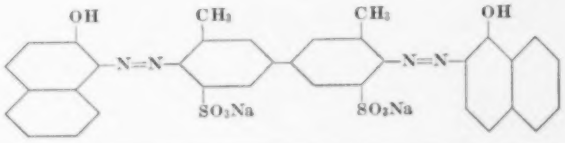
	MISCELLANEOUS DYES		
56	Guinea Green B	666	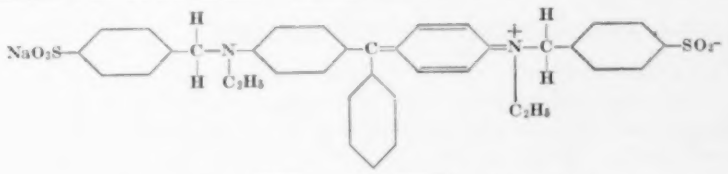
57	Methyl Violet	680	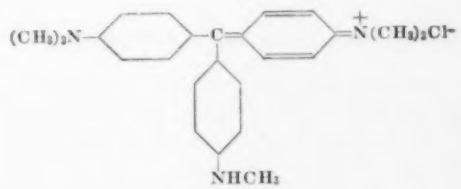
58	Methylene Blue	922	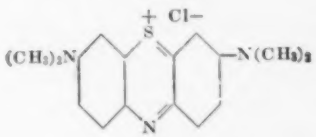

See footnotes at end of table.

TABLE 1. *Dyes included in the survey*—Continued

Dye number	Name	Color Index number [a]	Structure
	MISCELLANEOUS DYES—continued		
59	Genacryl Pink G		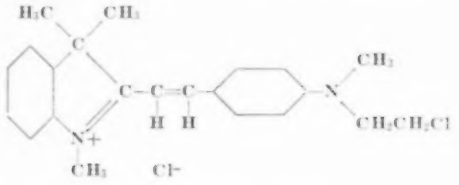
	OPTICAL BLEACHING AGENTS		
60			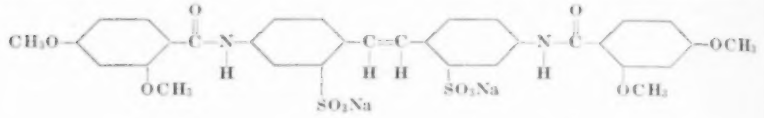
61			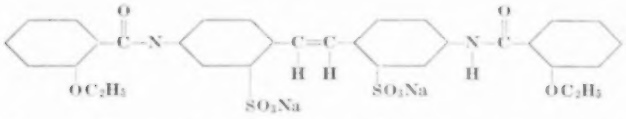
62			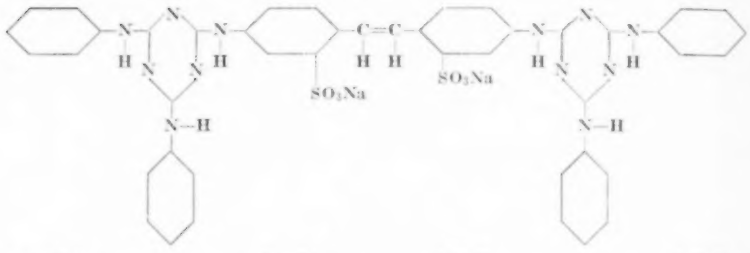
63			

[a] From Rowe, Colour Index, 1st ed., Society of Dyers and Colourists, Bradford, England, 1924.
[b] According to Ventkataraman (Synthetic Dyes, p. 519) it has been stated recently that the sulfonic acid groups are *ortho* to the biphenyl linkage.

2.2. Measurement of Absorption Spectra

The absorption spectra were determined by means of a Cary Recording Spectrophotometer (model 12) with matched fused quartz absorption cells, and with the solvent as the reference standard.

2.3. "Sum" and "Mixture" Curves

The existence of association effects may be demonstrated through changes in the absorption spectra of mixtures as compared with the summation of the separate curves of the two components. The "sum" curve can be obtained by the simple addition of the curves of each dye determined separately, but with the availability of a high-speed recording spectrophotometer, it is more easily produced by placing the dye solutions in two cells arranged one behind the other. To obtain the "mixture" curve, one of these cells was filled with solvent while the other contained a mixture of the two dyes, each at the same concentration as in the separate dye solutions. For purposes of comparison the spectrum of each individual dye was also determined, so that in all, four curves have been recorded for each pair of dyes studied.

When the sum and mixture curves were identical (that is, the spectra were additive) it was considered that there was no association (see fig. 1); while differences between the two curves (nonadditive spectra) were taken as evidence of interaction. Typical association effects are shown in figures 2 and 3.

Effects other than association, such as aging, precipitation, changes in *p*H, or phototropic changes, may also cause differences between the sum and mixture spectra. When aging, plating out, or precipitation was suspected, better results were obtained

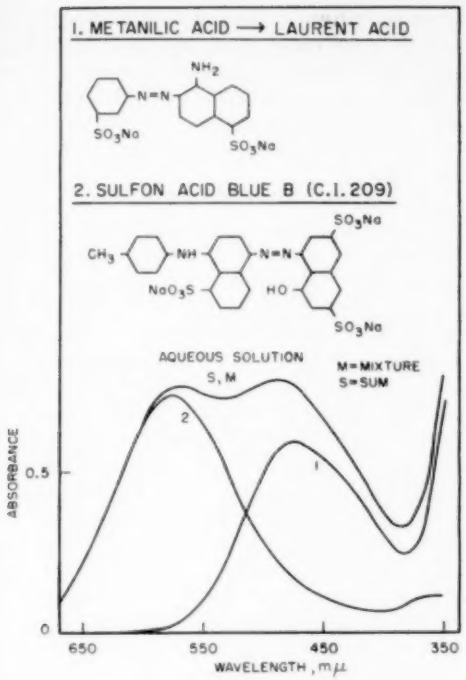

FIGURE 1. *Sum and mixture spectra for dye No. 44 (15 mg/liter) with Sulfon Acid Blue B (10 mg/liter).*

Length of cells equals 2 cm.

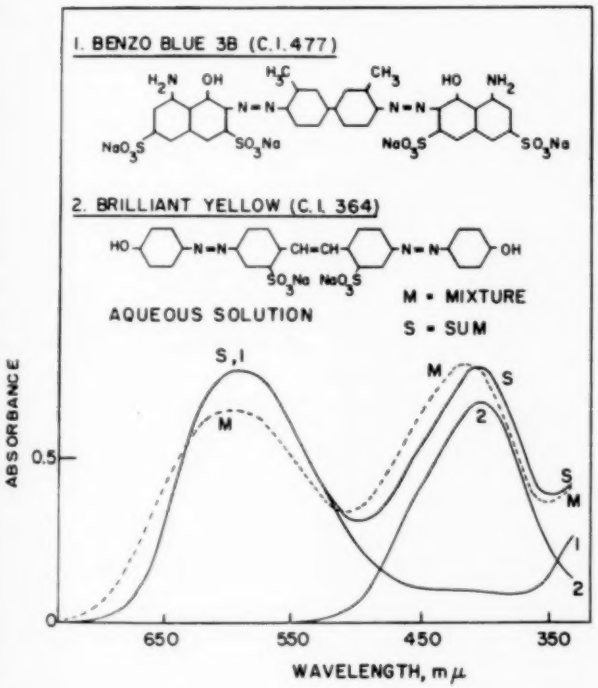

FIGURE 2. *Sum and mixture spectra for Benzo Blue 3B (10 mg/liter) with Brilliant Yellow (5 mg/liter).*

Length of cells equals 2 cm.

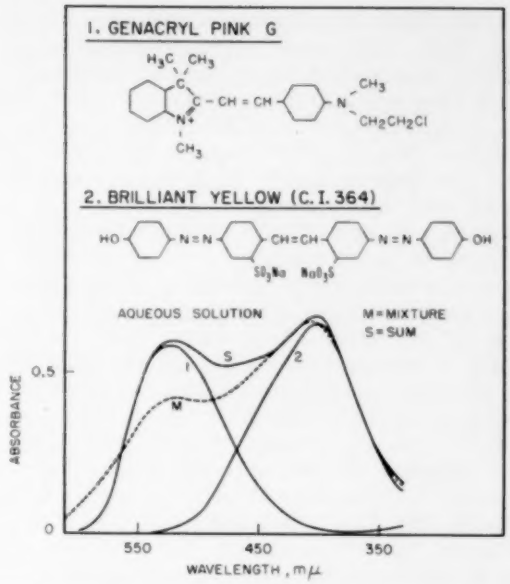

FIGURE 3. *Sum and mixture spectra for Genacryl Pink G (10 mg/liter) with Brilliant Yellow (5 mg/liter).*

Length of cells equals 2 cm.

by preparing the solutions immediately before measuring. For dyes sensitive to variations in *p*H, caused by dissolved carbon dioxide or by the presence of a second dye in the mixture, control by a buffer was necessary. Phototropic dyes were allowed to stand in controlled light conditions until equilibrium was established.

2.4. Irradiation of Solutions

In the study of the phototropism of dye mixtures, the solutions were irradiated during the measurement of the spectra in the manner described in an earlier paper [8].

3. Results

3.1. A General Survey of the Interaction of Dyes in Solution

The association of dyes in mixtures, as shown by the sum and mixture curves, is described for various groups of dyes.

a. Azo Dyes Substantive for Cotton

Thirty substantive azo dyes, representing different structural types, were studied in various combinations. In general, the results obtained with these dyes confirm the observations of earlier workers [6,7]. Mixtures of direct dyes usually give nonadditive spectra. As a rule, where the absorption bands are sufficiently well resolved, the absorption band occurring in the visible region and associated with the dye absorbing at shorter wavelengths increases in intensity, while that associated with the dye absorbing at longer wavelengths decreases. At the

same time, both absorption bands show a bathochromic shift. In cases where the bands overlap badly, the spectral changes cannot be classified as well, but they are still observable.

Disazo dyes derived from benzidine, *o*-dianisidine, or *o*-tolidine (Nos. 1 to 10) [3] appear to be most active in such dye interactions. Nonadditive spectra are observed with mixtures in which both dyes are of this type as well as with mixtures in which the second component is a direct azo dye of another type. Such dyes include disazo stilbene or urea derivatives, trisazo dyes, or disazo dyes of the type A→M→J-acid (or γ-acid) in which the substantivity is thought to be due to the presence of J-acid or γ-acid [9].

The changes in spectrum that are observed when one component of the mixture consists of a benzidine-type dye containing a naphthionic acid substituent (as for example Benzopurpurine 10B, No. 7) are often much less marked than the changes observed with benzidine dyes containing other groups. The substitution of NW-acid for the naphthionic acid groups of the Benzopurpurine 10B to produce Benzo Azurine G (No. 8) appears to increase the activity of the dye. It is possible that the amino group of the former is less favorable to dye interaction than the hydroxyl group.

Disazo derivatives of 4,4′-diaminostilbene-2,2′-disulfonic acid (Nos. 11 to 13) or 4,4′-diamino-N,N′-diphenylurea (Nos. 14 to 16) show a marked interaction with benzidine dyes, but the spectral differences observed with these dyes when the second component of the mixture is a J-acid or γ-acid derivative are much less pronounced. The stilbene dyes in particular show only slight interaction with dyes of this latter type.

The differences in sum and mixture curves obtained with mixtures in which one component is a trisazo dye (Nos. 20 to 27) are usually not as great as those observed when both components are disazo dyes.

Of the direct dyes considered, the type showing the least apparent interaction in most mixtures was the unsymmetrical type, A→M→J-acid (or γ-acid), where M is a phenyl derivative (Nos. 17 to 19).

Two direct monoazo dyes containing the benzothiazole group (Nos. 29 and 30) were investigated briefly. They behave in much the same manner as other direct dyes, although these dyes do not appear to have as great a tendency for interaction as do the benzidine dyes.

There are two general situations in which interaction of direct azo dyes might be expected to occur but where none is apparent from the spectra. One is the situation in which both components of a mixture have similar or identical terminal groups. Although each of these components may give nonadditive spectra with most other direct azo dyes of various types, the spectrum of the mixture is additive when the terminal groups are identical, or very nearly additive when the terminal groups are similar (see table 2). The additive spectra observed in these cases cannot be attributed to the proximity of the absorption bands of the dyes, for nonadditive spectra have often been observed with pairs of dyes whose absorption bands are even less widely separated. Nor can these additive spectra be taken as a positive indication that no interaction has occurred. Aggregation of some individual azo dyes with increasing dye concentration is known to take place, but this aggregation does not necessarily produce marked spectral anomalies [2], particularly at the concentrations used in these studies. Therefore, if the forces involved in the interaction of dyes in mixtures are related to those causing the aggregation of an individual dye, as well may be the case, it is possible that the interaction of two dyes possessing similar terminal groups may also occur without producing marked changes in the spectrum.

The second general situation in which additive spectra are obtained from mixtures of direct azo dyes is that in which both components of the mixture bear sulfonic acid groups on the central portion of the molecule (see table 2).

Chrysophenine G is a dye that is not appreciably aggregated in aqueous solutions, either by increased concentration or by added salts [10]. This has been explained as resulting from the mutual repulsion of

[3] The dye numbers refer to the dyes in table 1.

TABLE 2. *Mixtures of direct dyes giving additive spectra*

Components of mixture	Groupings involved
Dyes possessing similar terminal groupings	
Congo Red (No. 1) and Benzopurpurine 4B (No. 5)	
Benzopurpurine 4B (No. 5) and Benzopurpurine 10B (No. 7)	

TABLE 2. *Mixtures of direct dyes giving additive spectra*—Continued

Components of mixture	Groupings involved
Dyes possessing similar terminal groupings—Continued	
Diamine Violet N (No. 2) and Benzo Fast Pink 2BL (No. 16)	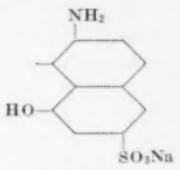
Chrysamine G (No. 3) and Benzo Fast Yellow 5GL (No. 14)	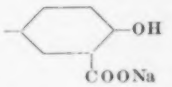
Benzo Blue 3B (No. 6) and Diamine Sky Blue FF (No. 10)	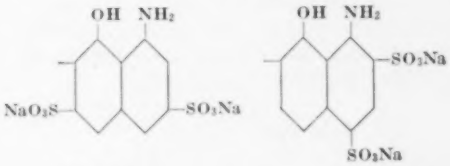
Benzo Blue 3B (No. 6) and Dianil Blue G (No. 9)[a]	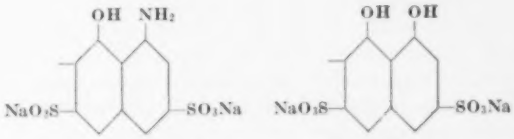
Dianil Blue G (No. 9) and Diamine Sky Blue FF (No. 10)[a]	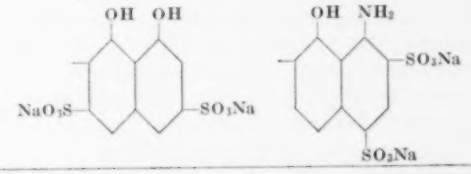
Dyes bearing sulfonic acid groups near the center of the molecule	
Brilliant Yellow (No. 11) and Chrysophenine G (No. 12)	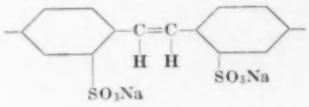
Brilliant Yellow (No. 11) and Dye Number 13	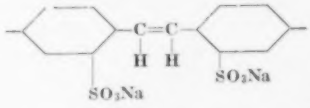
Brilliant Yellow (No. 11) and Benzo Fast Pink 2BL (No. 16)	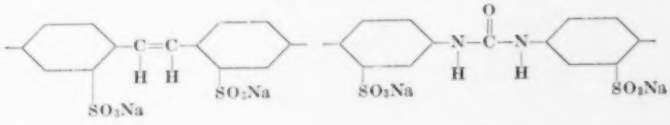
Chrysophenine G (No. 12) and Benzo Fast Pink 2BL (No. 16)	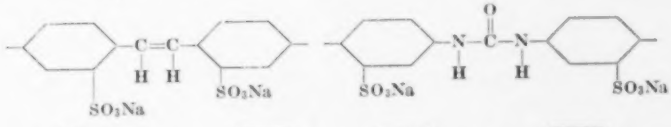
Brilliant Yellow (No. 11) and Benzo Fast Blue FR (No. 20)	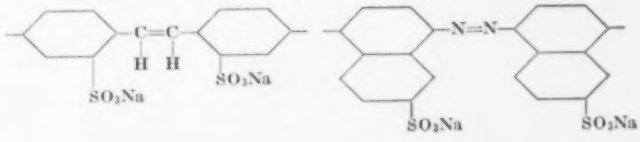

[a] The spectra of these mixtures are not completely additive but are very nearly so.

the sulfonic acid groups [11]. A steric effect may also be involved, with the bulky sulfonic acid groups interfering with the close approach of the dye molecules, thus preventing aggregation. The apparent lack of interaction in mixtures of dyes possessing sulfonic acid groups near the center of the molecule may very well arise from the same causes, for the electrical repulsion or the bulkiness of the sulfonic acid groups would be expected to interfere with the interaction of such dyes as well as with their aggregation. The slight apparent interaction observed in buffered mixtures of Chrysophenine G and Benzo Fast Pink 2BL suggests that the spacing of the sulfonic acid groups are sufficiently different in these two dyes to permit a slight interaction when the interference of the sulfonic acid groups is counteracted by the presence of salts. Inorganic salts appear to enhance interaction in the same way that they tend to increase the degree of aggregation of individual dyes.

b. Acid Dyes

Acid dyes in solution tend to be molecularly dispersed, although in some cases increasing salt concentration may bring about dimerization or slight aggregation [12]. It is therefore to be expected that such dyes also show little tendency for interaction with other dyes. Many mixtures containing acid dyes give additive spectra under all conditions, while in several other cases the spectra are additive unless the solutions contain added inorganic salts. In all cases where nonadditive spectra are observed with acid dyes, the spectral differences are not great.

Most of the 16 monoazo acid dyes studied (Nos. 31 to 46) show no interaction with each other, and the spectra obtained from mixtures of these monoazo dyes are generally additive.

One exception to this generalization is the dye Sulphon Acid Blue B (No. 39). Although this dye gives additive spectra with many monoazo dyes (see fig. 1), it gives nonadditive spectra with several 1-arylazo-2-naphthol derivatives. The presence of a sulfonic acid group in the 8 position of the naphthol portion apparently prevents this interaction. Since Sulphon Acid Blue B is also anomalous in its behavior with direct dyes, it seems that the nonadditive spectra observed with this dye are not related to the interactions being considered in this survey.

Several monoazo acid dyes give slightly nonadditive spectra with direct disazo dyes, particularly in buffered solutions, which increase the salt concentration. No interaction is observed when the disazo dye bears sulfonic acid groups near the center of the dye molecule or when the monoazo dye has sulfonic acid groups on both aryl nuclei. Additive spectra are also obtained in cases where both components contain similar groups; e. g., a mixture of Azo Eosine G (No. 33) and Benzo Azurine G (No. 8) gives an additive spectrum. The observation by Neale and Stringfellow [6] that the spectrum obtained from a mixture of Sky Blue FF and *o*-anisidine→Chicago acid is nonadditive is unexpected in the light of our observations. Monoazo dyes containing amino groups show less tendency toward interaction than do similar dyes containing hydroxyl groups, this being another case in which amino groups appear to be less active than hydroxyl groups in promoting interaction.

Monoazo dyes give no apparent interaction with trisazo dyes; and the interaction with dyes which owe their substantivity to the presence of J-acid groups is usually very slight.

These generalizations for the monoazo acid dyes also hold true for the nine disazo acid dyes investigated (Nos. 47 to 55). In those cases where nonadditive spectra are obtained with these dyes the spectral differences are usually more pronounced than those observed with the monoazo dyes, although they are still slight when compared to the differences observed with most direct dyes. This apparent greater tendency for interaction of disazo acid dyes as compared with monoazo acid dyes is to be expected in view of the increased molecular weights and the presence of more aromatic nuclei in the disazo acid dyes.

c. Miscellaneous Dyes

The study of the interaction of dyes in aqueous solution was extended briefly to other types of dyes.

Three basic dyes were considered—Methyl Violet (No. 57), Methylene Blue (No. 58), and Genacryl Pink G (No. 59). Mixtures of these dyes with each other give nonadditive spectra, but in acetate buffers (*p*H 4.7 and 5.7) the spectra of the mixtures are additive. Michaelis [3] has observed that various basic dyes that give evidence of aggregation in neutral solutions are not aggregated in solutions sufficiently acid to cause the dyes to exist as doubly charged cations. The *p*H of the acetate buffers used here is not sufficiently low to cause this change, and the lack of interaction in the buffered solutions cannot be explained by the presence of excess positive charges on the dye molecules.

The spectra of mixtures of these basic dyes with representative direct azo dyes give marked evidence of interaction, both with and without an acetate buffer (see figs. 3 and 4). The differences in the sum and mixture spectra are usually much greater in the absorption band associated with the basic dye than the region where the azo dye absorbs. In several cases the resulting changes in absorption are accompanied by hypsochromic shifts rather than the bathochromic shifts generally observed with mixtures containing only azo dyes. In the case of Methylene Blue, the interaction of the dyes is accompanied by the reduction of Methylene Blue by the azo dye.

The interaction of basic dyes with azo dyes is not limited to substantive dyes, since the acid dye aniline $\xrightarrow{\text{acid}}$H-acid (No. 42) also gives a nonadditive spectrum with Methyl Violet. In such cases the interaction of the dyes may be strengthened by the electrical attraction between the oppositely charged dye ions. A somewhat similar effect is observed when direct dyes on cotton are "topped" by small amounts of basic dyes [13]. The direct dye appears to act as a mordant for the basic dye, which would not otherwise adhere to the cotton.

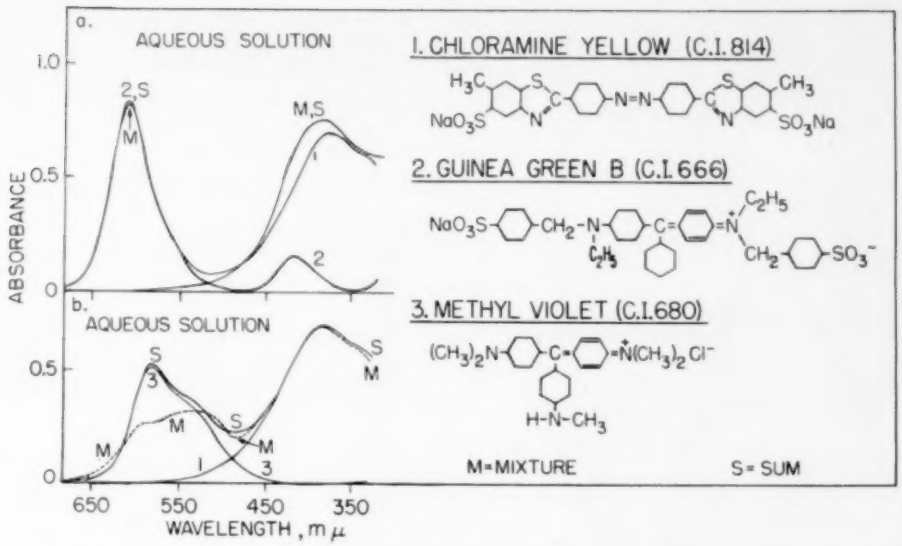

FIGURE 4. *Sum and mixture spectra for Chloramine Yellow (10 mg/liter) with (a) Guinea Green B (5 mg/liter) and (b) with Methyl Violet (2 mg/liter).*

Length of cells equals 2 cm.

The acid triphenylmethane dye, Guinea Green B (No. 56), containing only two amine groups, gives additive spectra with azo dyes (fig. 4a) and with Genacryl Pink G, while with Methylene Blue the spectrum is almost additive. With Methyl Violet, however, there is evidence of some interaction either with or without the use of an acetate buffer. Sheppard and Geddes, in discussing structural effects on the aggregation of dyes, mention that increasing concentration has little effect on the spectra of the diamino triphenylmethane dyes, indicating that these dyes have little or no tendency for aggregation, although the reason for this is not apparent [2]. The tendency of Guinea Green B to give additive spectra with most other dyes may well arise from the same cause.

d. Optical Bleaching Agents

These compounds are colorless fluorescent substances absorbing in the near ultraviolet and possessing substantivity for cotton. Many of them are aryl amido or substituted amino derivatives of 4,4′-diaminostilbene-2,2′-disulfonic acid [14]. Mixtures of four of these compounds (Nos. 60 to 63) with several substantive benzidine dyes give nonadditive spectra (see fig. 5b). The spectral changes observed in these mixtures are very similar to those observed in mixtures of two direct azo dyes, except that the absorption bands of both components usually decrease in intensity, whereas in mixtures containing only azo dyes there is commonly an increase in the absorption band associated with the dye that absorbs at shorter wavelengths. The spectral differences observed in mixtures containing a naphthionic acid derivative such as Congo Red are considerably less than those observed when other direct dyes are used, thus providing another instance in which amino groups do not appear to be as favorable to the interaction as do hydroxyl groups. Stilbene dyes such as Brilliant Yellow or Chrysophenine G and the nonsubstantive benzidine dye Acid Anthracene Red 3B give almost additive spectra with these colorless substances (see fig. 5a). This lack of interaction can probably be attributed to interference by the sulfonic acid groups in the molecules.

3.2. Other Factors and Their Effect on the Interaction of Direct Azo Dyes

After this general survey on the relationship between the constitution of dyes and their interaction in aqueous solution, the effects of other conditions on the interaction were investigated.

a. Alcohol

It has been clearly demonstrated that alcohol, like pyridine, inhibits the aggregation of azo dyes [15], as well as that of dyes of other types [1,16]. Pyridine (25% in aqueous solution) has also been shown to be useful for obtaining additive spectra with mixtures of dyes that normally show interaction in aqueous solution [6]. In view of the apparent relation between aggregation and interaction, it is not surprising that the interaction of direct azo dyes is also reduced by the presence of alcohol. For example, in a solution containing 4 percent of alcohol the spectrum of a mixture of Brilliant Yellow and Benzo Blue 3B is nonadditive, but the differences are much less than those observed in water alone. The spectrum of the mixture in 20 percent aqueous alcohol is almost additive, while in 40 percent alcohol no differences can be observed between the sum and mixture curves.

However, in absolute alcohol the spectra of mixtures of direct azo dyes or their diorthotolylguanidine salts again give some evidence of a slight interaction.

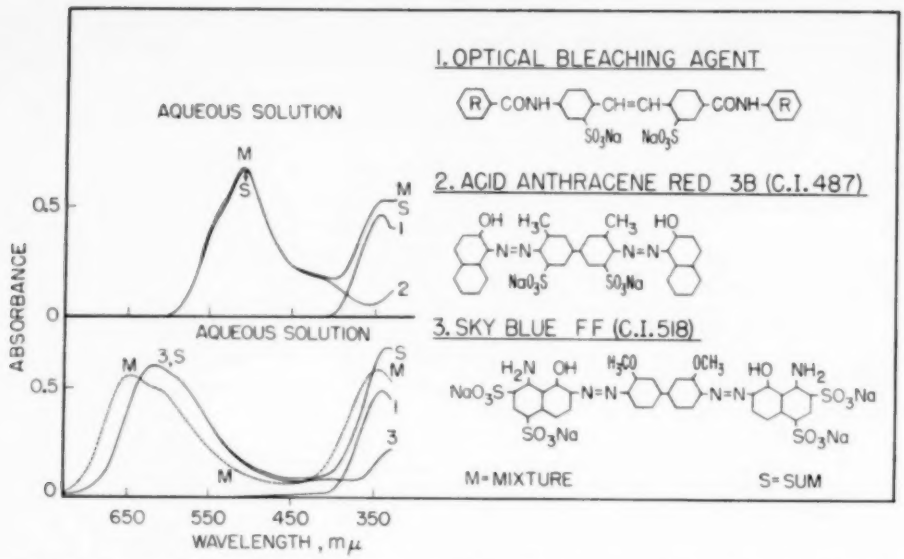

FIGURE 5. *Sum and mixture spectra for an optical bleaching agent (No. 61) (5 mg/liter) with (a) Acid Anthracene Red 3B (16 mg/liter) and with (b) Diamine Sky Blue FF (10 mg/liter).*

Length of cells equals 2 cm.

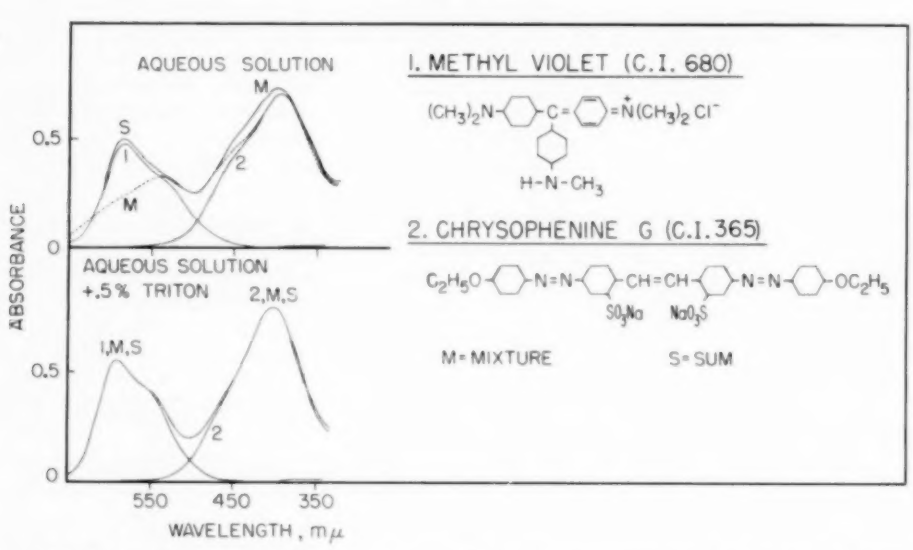

FIGURE 6. *Effect of a non-ionic detergent on the sum and mixture spectra for Methyl Violet (2 mg/liter) with Chrysophenine G (7.5 mg/liter).*

Length of cells equals 2 cm.

b. Non-Ionic Detergents

Non-ionic detergents such as polyethylene oxide condensates resemble pyridine, in that they prevent the aggregation of dyes, but are effective at much lower concentrations [17]. Such substances have also been reported [18] to give better results than pyridine when it is desired to obtain additive spectra with mixtures of dyes such as Chrysophenine G and Diamine Sky Blue FF which normally show interaction. These results are confirmed by the completely additive spectrum observed with a mixture of Brilliant Yellow and Benzo Blue 3B in aqueous solution containing 0.1 percent Triton X–100 (a condensate of ethylene oxide with an octylphenol). A mixture of Chrysophenine G and Methyl Violet requires slightly more detergent to prevent interaction, for a slight interaction is observed in 0.1 percent Triton X–100 solution, but the spectrum is strictly additive when the concentration of detergent is increased to 0.5 percent (see fig. 6).

The effect of the detergent concentration on these two mixtures is apparently related to the concentration effect that is observed with the individual dyes. At low concentrations Triton X–100 causes changes in the absorption spectra of the individual dyes which are dependent upon the detergent concentra-

tion. As the amount of detergent is increased, a concentration is reached beyond which no further change in spectrum is observed. With the direct azo dyes this limiting value occurs when the detergent concentration is between 0.03 and 0.05 percent, while the limiting value for Methyl Violet is close to 0.3 percent. In a dye mixture it appears necessary to have the detergent concentration above the limiting concentration for *both* components of the mixture in order to prevent the interaction of the dyes completely. It is of interest that, while solutions of Triton X–100 contain micelles even at very low concentrations, the monomer saturation concentration (the concentration above which essentially all detergent is in the form of micelles) is 0.3 percent [19].

c. Inorganic Salts

Since inorganic electrolytes are known to increase the aggregation of many direct dyes, their effect on the interaction of such dyes in mixtures is another factor of interest. Diamine Sky Blue FF (No. 10) and Brilliant Yellow (No. 11) can be taken as representative direct dyes giving nonadditive spectra. Brilliant Yellow is of more value in such studies than the classic example, Chrysophenine G; for it shows no phototropic changes to obscure the spectral effects of interaction, while its structure is similar and its association tendencies in mixtures appear to be identical with those of Chrysophenine G.

Diamine Sky Blue FF is reported to show increasing aggregation with increasing salt concentration [20]. This aggregation is reflected in changes in the absorption spectra (see fig. 7). As the concentration of potassium bromide is increased from 0 to 32 g/liter, the main absorption band of the dye becomes progressively lower and broader. Although there is no marked change in the position of the maximum, there is an apparent shift in the center of gravity of the band toward longer wavelengths. These changes do not appear to approach a limit at the maximum salt concentration used. Potassium sulfate produces similar changes in the spectrum of the dye. Both salts produce similar changes in the spectra of other related benzidine dyes (e. g., Benzo Azurine G, No. 8; Dianil Blue G, No. 9; and Benzo Blue 3B, No. 6), but with these dyes the maxima are shifted slightly to shorter wavelengths.

Since Brilliant Yellow is structurally similar to Chrysophenine G, which is not aggregated by salts [10], it would also be expected to be unaffected by salts. The spectrum of Brilliant Yellow is found to show no change as the concentration of potassium bromide is increased from 0 to 16 g/liter, indicating that probably no aggregation occurs.

When mixtures of Diamine Sky Blue FF and Brilliant Yellow are prepared in solutions containing increasing concentrations of potassium bromide or potassium sulfate, the absorption band associated with the Brilliant Yellow increases in intensity and is shifted to longer wavelengths (see fig. 8). As the salt concentration is increased, a limiting concentration is reached, beyond which no further changes are

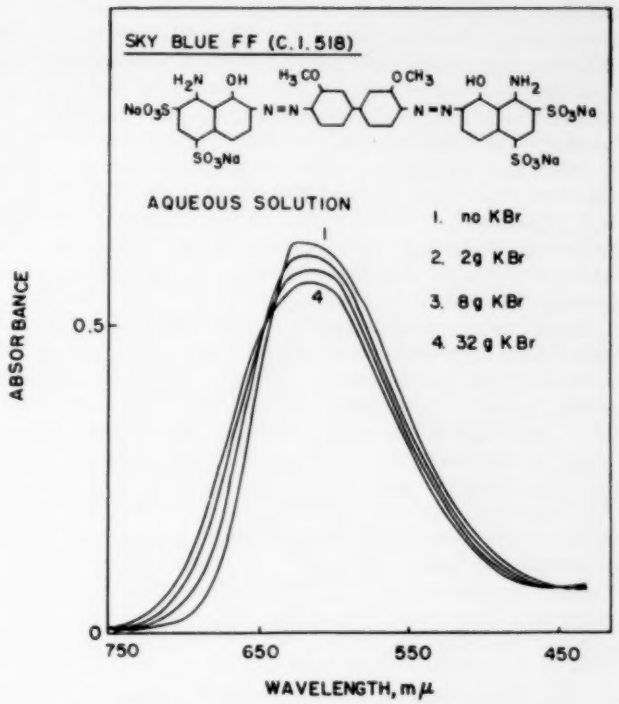

FIGURE 7. *Effect of potassium bromide on the absorption spectrum of Diamine Sky Blue FF (10 mg/liter).*

Length of cells equals 2 cm.

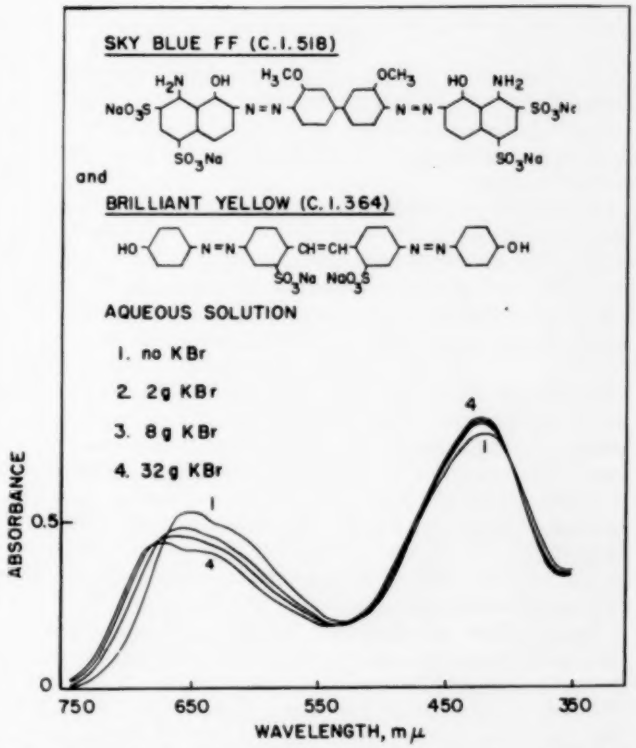

FIGURE 8. *Effect of potassium bromide on the absorption spectrum of a mixture of Diamine Sky Blue FF (10 mg/liter) and Brilliant Yellow (5 mg/liter).*

Length of cells equals 2 cm.

observed in this band. The spectrum of a mixture containing Diamine Sky Blue FF at a concentration of 10 mg/liter and Brilliant Yellow at a concentration of 5 mg/liter shows no further change in the 400-mμ region when the potassium bromide concentration is made greater than 4 g/liter, but 1 g/liter of the salt is sufficient to produce the maximum change when the concentration of Brilliant Yellow in the mixture is 2.5 mg/liter. The nature of the spectral changes observed in this band suggests that the addition of salts causes an increase in the interaction of the dyes in the mixture.

As the salt concentration is increased, the absorption band associated with the Diamine Sky Blue FF also changes in a manner suggesting increased interaction; that is, the band undergoes a bathochromic shift together with a decrease in intensity. However, these changes continue as the salt concentration is increased and a limit to the changes was not reached at a salt concentration of 32 g/liter. Similar results are obtained when different proportions of the blue and the yellow dye are used, even when Brilliant Yellow is present in sufficient excess to make it improbable that any free Diamine Sky Blue FF is present in the mixture. The progressive spectral changes observed with increasing salt concentration in this latter case resemble those produced by the action of salts on Diamine Sky Blue FF in the absence of Brilliant Yellow, and suggest an aggregation of the Brilliant Yellow-Diamine Sky Blue FF complex similar to that of the blue dye alone.

d. Concentration Changes

Another factor that can cause increased aggregation of dyes is increased concentration. This effect is particularly marked with certain basic dyes [2] but has also been demonstrated in the case of direct azo dyes [4].

A qualitative estimate of the effect of concentration on the spectrum of a dye can be obtained by making a series of measurements with dye solutions in both sample and reference cells. A fixed concentration difference is maintained between the solutions in the two cells while the total concentrations of the dye in both are increased. The spectral changes of Diamine Sky Blue FF observed in this manner, as the concentration in the sample cell is increased from 20 to 100 mg/liter while the concentration difference between the sample and reference cells is fixed at 20 mg/liter, are very similar to those observed with a fixed concentration of dye as the salt concentration is increased from 0 to 5 g/liter (see fig. 9). The effects of aggregation on the spectrum of the dye are thus similar in the two cases.

In the case of Brilliant Yellow, which is not appreciably aggregated, there is no noticeable change in spectrum as the concentration is increased.

With mixtures of Brilliant Yellow and Sky Blue FF, increasing the concentration of one component brings about changes in the absorption band associated with the other component very similar to the changes produced by increasing the salt concentration. When the concentration of Brilliant Yellow is

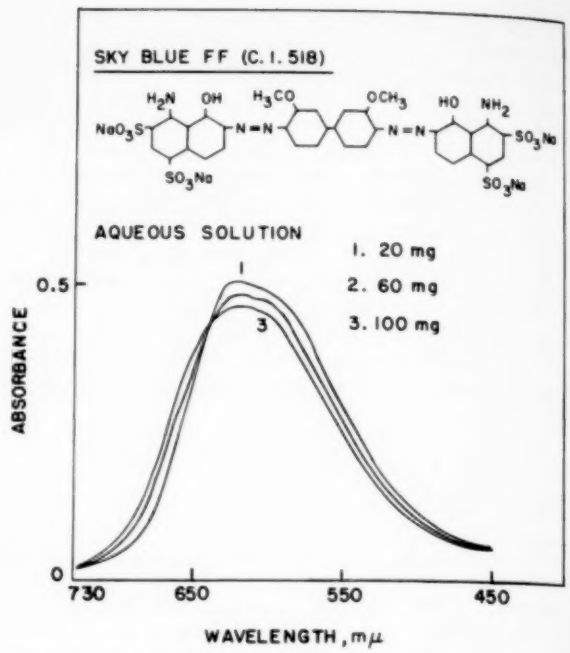

FIGURE 9. *Effect of concentration on the absorption spectrum of Diamine Sky Blue FF.*

1, Concentration of dye in sample cell equals 20 mg/liter. Reference cell contains water. 2, Concentration of dye in sample cell equals 60 mg/liter; in reference cell equals 40 mg/liter. 3, Concentration of dye sample cell equals 100 mg/liter; in reference cell equals 80 mg/liter. Length of cell equals 2 cm.

fixed at 5 mg/liter, its absorption band undergoes progressive bathochromic and hyperchromic shifts as the concentration of Diamine Sky Blue FF is increased from 0 to 20 mg/liter. For concentrations of the blue dye between 20 and 100 mg/liter, no further change is observed in this band.

When the concentration of Diamine Sky Blue FF is fixed at 4 mg/liter, an increase in the concentration of Brilliant Yellow brings about both a lowering and a bathochromic shift of the absorption band of the blue dye (see fig. 10). The curves obtained with small increments in the concentration of Brilliant Yellow show a single, well-defined isosbestic point until a concentration of 0.75 mg/liter is reached. Such an isosbestic point is to be expected if there is an equilibrium between the ions of the individual dyes and a single form of the Brilliant Yellow-Diamine Sky Blue FF complex, since Brilliant Yellow shows no absorption in this region. However, as the concentration of Brilliant Yellow is increased further, the isosbestic point is no longer observed, while the bathochromic, hypochromic shifts continue. The greatest changes are observed as the concentration of Brilliant Yellow is increased from 0 to 20 mg/liter, although concentrations of yellow dye up to 100 mg/liter are effective in producing marked changes, and no limit is observed with concentrations up to 500 mg/liter.

The absence of an isosbestic point, except at the lowest concentrations of Brilliant Yellow, indicates that the mixture contains more than two species absorbing in the region of the main absorption band of the blue dye, and the nature of the spectral changes

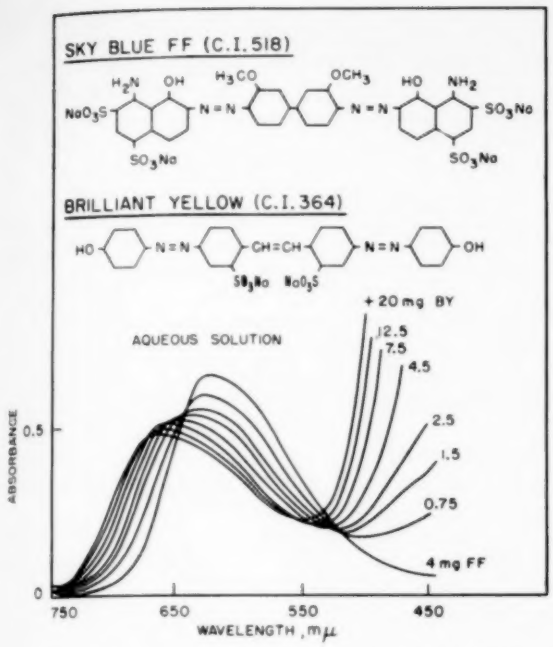

FIGURE 10. *Effect of increasing Brilliant Yellow concentration on the absorption spectrum of Diamine Sky Blue FF.*

Length of cell equals 2 cm.

observed suggests that the mixture is quite complex.

Similar series of curves, all showing progressive changes in absorption with isosbestic points observed only at the lowest concentrations of the yellow dye and with no indication of limits to the changes at higher concentrations, are also obtained when the concentration of Brilliant Yellow is gradually increased in mixtures containing fixed concentrations of Benzo Azurine G, Dianil Blue G, or Benzo Blue 3B.

e. Acids and Bases

In dilute acid solution (0.01 *N* or below) dyes such as Congo Red (No. 1) change color as a result of the addition of protons. The blue, acid forms of Congo Red and similar dyes give non-additive spectra with Chrysophenine G and with Brilliant Yellow, thus indicating that the presence of the positively charged groups does not prevent interaction of the dyes. This is to be expected, since the addition of positive charges to the dye molecule should reduce the repulsion by the sulfonic anions and facilitate the interaction of the dyes.

Azo dyes containing hydroxyl groups are not greatly affected by dilute acids, and the spectra obtained with mixtures of such dyes in acid solutions do not differ significantly from nonadditive spectra obtained in distilled water.

In dilute bases, dyes containing hydroxyl groups as the only auxochromes change color with the formation of phenolate ions. In this form such dyes give additive spectra in mixtures where interaction is normally observed in neutral solutions. For example, Brilliant Yellow (No. 11), Benzo Azurine G (No. 8), Dianil Blue G (No. 9), Chrysamine G (No. 3), and Benzo Fast Yellow 5GL (No. 15) give additive spectra with other direct dyes in 0.2 *N* sodium hydroxide solutions; while dyes such as Chrysophenine G, Congo Red, or Benzo Blue 3B, which contain either amino groups in addition to hydroxyl groups or else no hydroxyl groups, give nonadditive spectra with other direct dyes in basic solutions as well as in neutral solutions.

In order to obtain interaction of direct dyes, it is necessary that the forces acting to give interaction be large enough to overcome the repulsion of the negative charges localized on the sulfonic acid groups of the dye molecules. Additional negative charges added to the molecule of a hydroxyl-bearing dye by the formation of phenolate ions tend to be distributed over the whole molecule because of the conjugation of the oxygen with the rest of the molecule. The additive spectra obtained in basic solutions of such dyes suggest that the added repulsion resulting from the increased negative charges on the dye molecule is sufficient to prevent interaction with other dyes.

f. Phototropism and Dye Interaction

It was mentioned earlier that the phototropism of Chrysophenine G may give rise to misleading results in the study of the spectra of dye mixtures unless suitable precautions are taken. In some cases the phototropic property of this dye can be used to advantage in studying dye interaction.

A mixture of Chrysophenine G and the nonphototropic dye Diamine Sky Blue FF gives a nonadditive spectrum in aqueous solution by virtue of complex formation. When this mixture is irradiated with blue light, the spectral changes in the 400-mμ region (the region of maximum absorption for Chrysophenine G) resemble those observed with Chrysophenine G alone (see fig. 11a). The spectrum in the 600-mμ region (the region where Chrysophenine G shows no absorption but the absorption of Diamine Sky Blue FF is at a maximum) is also observed to change, although to a much smaller extent. The spectral changes produced in this region by illumination are of such a nature that they suggest a tendency toward less interaction of the two dyes on irradiation [21].

The effect of light on the spectrum of such mixtures leads to the conclusions that the complex itself is not phototropic and that only the more stable, "dark" form of Chrysophenine G is involved in complex formation. Irradiation of the mixture, particularly with blue light, leads to the formation of the less stable forms of Chrysophenine G with a resultant decrease in the concentration of the dark form. This then shifts the equilibrium between the free dyes and the complex, resulting in a decrease in the concentration of the complex and producing the observed spectral changes. This interpretation of the changes in spectrum is in agreement with that of Atherton and Peters [22].

If these conclusions are correct, it is evident that the effects of irradiation observed in the 600-mμ region should represent the extent to which the dye complex is broken up, while the changes in the 400-

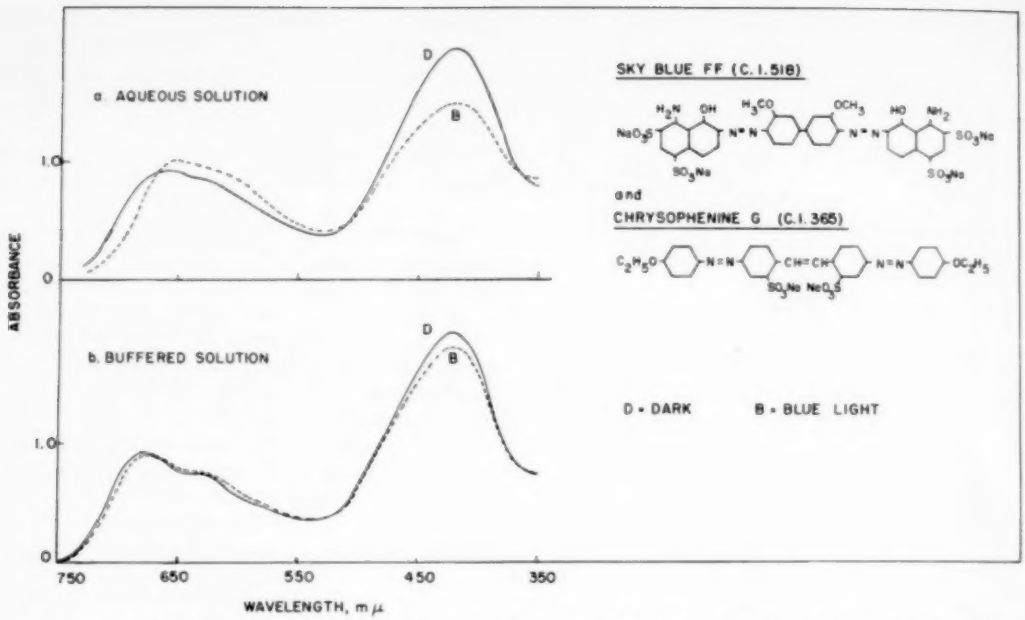

FIGURE 11. *Phototropic effect shown by a mixture of Diamine Sky Blue FF (20 mg/liter) and Chrysophenine G (10 mg/liter) in water and in a buffer solution (pH equals 5.7).*

Length of cell equals 2 cm.

mμ region should be related to the concentration of free Chrysophenine G in the mixture before irradiation, together with that released by the disruption of the complex. Unfortunately, heating of the mixture during irradiation also leads to dissociation of the complex, making the interpretation of the spectral effects more difficult and thus preventing a quantitative study of the effect at this time. In general, the changes observed are those which would be expected if an equilibrium exists between a complex, the dark form of Chrysophenine G, and free Diamine Sky Blue FF. An increase in the concentration of either dye or the addition of salts (or the use of an acetate buffer) results in increased interaction of the dyes, as shown by the relative decrease in the phototropic changes (see fig. 11b).

4. Conclusions

The results obtained in this general survey tend to confirm the idea that there is a fundamental relationship between the factors involved in dyeing cotton, in the aggregation of azo dyes, and in the interaction of azo dyes in mixtures. This relationship probably extends to dyes of other types as well.

The exact nature of the forces operative in the dyeing of cotton is still undetermined, as can be seen from the different opinions expressed in the symposium on the physical chemistry of dyeing [23]. It has been found empirically that several features in the structure of direct azo dyes tend to increase the substantivity of the dye, although the existence of substantive dyes that do not possess some of these features shows that many of these are not absolute requirements for substantivity and suggests that several types of interaction are responsible for the binding of dyes to cotton. Some of the features mentioned [24] as required or desirable for substantivity are linearity of the dye molecule, coplanarity of the molecule, the presence of hydrogen-bonding groups, the presence of a sufficiently long chain of conjugated double bonds, and the presence of a minimum number of solubilizing groups, the latter preferably arranged along one side of the molecule with hydrogen-bonding groups on the other side. The results of this survey indicate that these features also tend to favor the interaction of dyes in mixtures. Solubilizing groups such as the sulfonic acid group appear to be more effective in preventing interaction or the aggregation of individual dyes than in decreasing substantivity; this is apparent in the case of Chrysophenine G, which is substantive although the sulfonic acid groups prevent its aggregation, or its interaction with other dyes bearing suitably placed sulfonic acid groups.

One apparent contradiction can be noted. The presence of amino groups increases the substantivity of dyes, particularly on viscose [25], while the results given in this paper suggest a tendency for dyes containing amino groups as the only auxochromes to show less interaction in mixtures. Griffiths and Neale point out that the greater substantivity on viscose may result from the larger number of carboxyl groups on viscose than on cotton. If such is the case, the opposite effects of the amino group on the substantivity and on the interaction of dyes would not be surprising.

Other parallels may be drawn between dyeing, aggregation, and interaction. Increased dye concentration and increased salt concentration have been shown to cause increased aggregation of direct azo dyes as well as increased interaction in mixtures.

these changes also increase the rate and depth of dyeing of cotton. Similarly, stripping agents such as pyridine which remove dyes from fibers prevent the aggregation or the interaction of these dyes.

Probably the most significant similarity between these three phenomena is seen in the spectral changes they produce. The results given in this paper illustrate changes in spectrum brought about by aggregation due to increased salt concentration or increased dye concentration, as well as those resulting from the interaction of dyes. A comparison of these changes with those resulting from the dyeing of cellulose sheet by a number of substantive benzidine dyes [26] shows marked similarities, particularly in the direction of the spectral shifts as well as in the increased asymmetry on the long wavelength side of the absorption band.

Since work on this paper was completed and tentatively reported at the symposium of the Chemical Society of London in February 1956 [27], a paper by Derbyshire and Peters on the interaction between Chlorazol Sky Blue FF and Chrysophenine G has appeared [28]. From a study of the spectral changes caused by variations in the relative concentrations of the two dyes in aqueous solution, they conclude that a 1:1 complex is formed, provided that the Chrysophenine G is not in excess, and that complexes richer in the yellow dye are formed when higher concentrations of Chrysophenine G are used. Our results with Brilliant Yellow are consistent with the formation of such a 1:1 complex at low concentrations of yellow dye. However, the lack of a second isosbestic point as the concentration of the yellow dye is increased and the similarity between the effect of inorganic salts and the effect of increasing dye concentration on the spectrum of the mixture suggest a salting-out process rather than the formation of complexes richer in the yellow dye. From the heat of complex formation and from a study of the spectra of these dyes and dye mixtures on Cellophane, Derbyshire and Peters provide more evidence that the mechanism of complex formation is similar to that of dye adsorption by fibers.

WASHINGTON, August 5, 1957

5. References

[1] E. Rabinowitch and L. F. Epstein, J. Am. Chem. Soc. **63,** 69 (1941).
[2] S. E. Sheppard and A. L. Geddes, J. Am. Chem. Soc. **66,** 1995, 2003 (1944).
[3] L. Michaelis, J. Phys. Colloid Chem. **54,** 1 (1950).
[4] For a review of the literature, see H. A. Standing, Trans. Faraday Soc. **41,** 410 (1945).
[5] G. Scheibe, Kolloid Z. **82,** 1 (1938).
[6] S. M. Neale and W. A. Stringfellow, J. Soc. Dyers Colourists **59,** 241 (1943).
[7] D. R. Lemin and T. Vickerstaff, Trans. Faraday Soc. **43,** 491 (1947).
[8] W. R. Brode, J. H. Gould, and G. M. Wyman, J. Am. Chem. Soc. **74,** 4641 (1952).
[9] K. Ventkataraman, The chemistry of synthetic dyes, p. 499, 1288 (Academic Press, Inc., New York, N. Y., 1952).
[10] F. H. Holmes and H. A. Standing, Trans. Faraday Soc. **41,** 542, 568 (1945).
[11] T. Vickerstaff, The physical chemistry of dyeing, p. 187 (Interscience Publishers, New York, N. Y., 1950).
[12] E. Valko, J. Soc. Dyers Colourists **55,** 174 (1939); K. N. Davies and J. Whetstone, J. Chem. Soc., **1954,** 865; A. N. Derbyshire, Trans. Faraday Soc. **51,** 909 (1955).
[13] K. Ventkataraman, op. cit., [9] p. 277.
[14] D. W. Hein and E. S. Pierce, J. Am. Chem. Soc. **76,** 2725 (1954).
[15] J. T. Martin and H. A. Standing, J. Text. Inst. **40,** T671 (1949).
[16] S. E. Sheppard, Rev. Modern Phys. **14,** 303 (1940).
[17] J. T. Martin and H. A. Standing, J. Text. Inst. **40,** T689 (1949).
[18] H. H. Taylor and F. T. Simon, Am. Dyestuff Reptr. **34,** 319 (1945).
[19] L. M. Kushner and W. D. Hubbard, J. Phys. Chem. **58,** 1163 (1954).
[20] E. Valko, Trans. Faraday Soc. **31,** 230 (1935).
[21] W. R. Brode in The Roger Adams symposium, p. 50 (John Wiley & Sons, Inc., New York, N. Y., 1955).
[22] E. Atherton and R. H. Peters, Recent advances in the chemistry of colouring matters, Special Publication No. 4, London: The Chemical Society, p. 26 (1956).
[23] The physical chemistry of dyeing and tanning. Discussions Faraday Soc., No. 16 (1954).
[24] T. Vickerstaff, The physical chemistry of dyeing, 2d ed., p. 183 (Interscience Publishers, New York, N. Y., 1950).
[25] L. H. Griffiths and S. M. Neale, Trans. Faraday Soc. **30,** 3955 (1934).
[26] D. Krüger and H. Rudow, Ber. **71,** 707 (1938).
[27] W. R. Brode, Recent advances in the chemistry of colouring matters, Special Publication No. 4, London: The Chemical Society, p. 1 (1956).
[28] A. N. Derbyshire and R. H. Peters, J. Soc. Dyers Colourists, **72,** 268 (1956).

U. S. GOVERNMENT PRINTING OFFICE: 1958

THE NATIONAL BUREAU OF STANDARDS

The scope of activities of the National Bureau of Standards at its headquarters in Washington, D. C., and its major field laboratories in Boulder, Colorado, is suggested in the following listing of the divisions and sections engaged in technical work. In general, each section carries out specialized research, development, and engineering in the field indicated by its title. A brief description of the activities, and of the resultant publications, appears on the inside of the front cover.

WASHINGTON, D. C.

Electricity and Electronics. Resistance and Reactance. Electron Devices. Electrical Instruments. Magnetic Measurements. Dielectrics. Engineering Electronics. Electronic Instrumentation. Electrochemistry.

Optics and Metrology. Photometry and Colorimetry. Optical Instruments. Photographic Technology. Length. Engineering Metrology.

Heat. Temperature. Physics. Thermodynamics. Cryogenic Physics. Rheology. Engine Fuels. Free Radicals Research.

Atomic and Radiation Physics. Spectroscopy. Radiometry. Mass Spectrometry. Solid State Physics. Electron Physics. Atomic Physics. Neutron Physics. Nuclear Physics. Radioactivity. X-rays. Betatron. Nucleonic Instrumentation. Radiological Equipment. AEC Radiation Instruments.

Chemistry. Organic Coatings. Surface Chemistry. Organic Chemistry. Analytical Chemistry. Inorganic Chemistry. Electrodeposition. Molecular Structure and Properties of Gases. Physical Chemistry. Thermochemistry. Spectrochemistry. Pure Substances.

Mechanics. Sound. Mechanical Instruments. Fluid Mechanics. Engineering Mechanics. Mass and Scale. Capacity, Density, and Fluid Meters. Combustion Controls.

Organic and Fibrous Materials. Rubber. Textiles. Paper. Leather. Testing and Specifications. Polymer Structure. Plastics. Dental Research.

Metallurgy. Thermal Metallurgy. Chemical Metallurgy. Mechanical Metallurgy. Corrosion. Metal Physics.

Mineral Products. Engineering Ceramics. Glass. Refractories. Enameled Metals. Concreting Materials. Constitution and Microstructure.

Building Technology. Structural Engineering. Fire Protection. Air Conditioning, Heating, and Refrigeration. Floor, Roof, and Wall Coverings. Codes and Specifications. Heat Transfer.

Applied Mathematics. Numerical Analysis. Computation. Statistical Engineering. Mathematical Physics.

Data Processing Systems. SEAC Engineering Group. Components and Techniques. Digital Circuitry. Digital Systems. Analog Systems. Application Engineering.

•Office of Basic Instrumentation. •Office of Weights and Measures.

BOULDER, COLORADO

Cryogenic Engineering. Cryogenic Equipment. Cryogenic Processes. Properties of Materials. Gas Liquefaction.

Radio Propagation Physics. Upper Atmosphere Research. Ionospheric Research. Regular Propagation Services. Sun-Earth Relationships.

Radio Propagation Engineering. Data Reduction Instrumentation. Modulation Systems. Navigation Systems. Radio Noise. Tropospheric Measurements. Tropospheric Analysis. Radio Systems Application Engineering.

Radio Standards. High Frequency Electrical Standards. Radio Broadcast Service. High Frequency Impedance Standards. Calibration Center. Microwave Physics. Microwave Circuit Standards.

Recent Publications of the National Bureau of Standards

Journal of Research of the National Bureau of Standards, Volume 59, No. 5, November 1957 (RP2801 to RP2805 incl.). 60 cents. Annual subscription $4.00 ($5.25 foreign).

Technical News Bulletin, Volume 41, No. 11, November 1957. 10 cents. Annual subscription $1.00 ($1.35 foreign).

Basic Radio Propagation Predictions for February 1958. Three months in advance. CRPL–D 159. Issued November 1957. 10 cents. Annual subscription $1.00 ($1.25 foreign).

Circulars

C539, Volume 7. Standard X-ray diffraction powder patterns. 40 cents.*

C588. Determination and correlation of flow capacities of pneumatic components. 10 cents.*

Handbooks

H28, pt I. Screw-thread standards for federal services, 1957. $1.25.*

*Available from the Superintendent of Documents, U. S. Government Printing Office, Washington 25, D. C.**
(Foreign postage, one-fourth additional).

UNITED STATES
GOVERNMENT PRINTING OFFICE
DIVISION OF PUBLIC DOCUMENTS
WASHINGTON 25, D. C.

OFFICIAL BUSINESS

PENALTY FOR PRIVATE USE TO AVOID PAYMENT OF POSTAGE, $300 (GPO)

Journal of Research of the National Bureau of Standards Vol. 60, No. 1 January 1958

Contents

		Page
The condition of certain matrices, III. John Todd.	RP2815	1
Infrared study of some structural changes in natural rubber during vulcanization. Frederic J. Linnig and James E. Stewart.	RP2816	9
Crystal structure of barium hydrogen orthophosphate. Gordon Burley.	RP2817	23
A study of sampling of flame gases. C. Halpern and F. W. Ruegg.	RP2818	29
Pyrolysis of polyamides. Sidney Straus and Leo A. Wall.	RP2819	39
Some thermodynamic properties of the systems polybutadiene-benzene and polyisobutene-benzene. R. S. Jessup.	RP2820	47
Infrared measurements with a small grating from 100 to 300 microns. Earle K. Plyler and L. R. Blaine.	RP2821	55
A low-frequency annular-slot antenna. James R. Wait.	RP2822	59
Relation between the absorption spectra and the chemical constitution of dyes: XXIX. Interaction of direct azo dyes in aqueous solution. May N. Inscoe, John H. Gould, Mary E. Corning, and Wallace R. Brode.	RP2823	65

[A list of recent NBS publications is given on page 3 of the cover.]

For sale by the Superintendent of Documents, U. S. Government Printing Office, Washington 25, D. C. Price 60 cents (single copy). Subscription price: $4.00 a year; $1.25 additional for foreign mailing.

UNITED STATES GOVERNMENT PRINTING OFFICE, WASHINGTON : 1957